Institut für Biochemie und Biologie
Professur für Analytische Biochemie

Development of a Thermometric Sensor for Fructosyl Valine and Fructose using Molecularly Imprinted Polymers as a Recognition Element

Dissertation
zur Erlangung des akademischen Grades
"doctor rerum naturalium"
(Dr. rer. nat.)
in der Wissenschaftsdisziplin Analytische Biochemie

eingereicht an der
Mathematisch-Naturwissenschaftlichen Fakultät
der Universität Potsdam

von
Rajagopal Rajkumar

Potsdam, November 2007

Acknowledgements

My very special gratitude is directed to my supervisor Prof. Dr. Frieder W. Scheller for giving me this great opportunity to work in his internationally acclaimed group. Thank you for your continuous support during hard times, encouragement and fruitful discussions.

I thank Dr. Martin Katterle who guided me through my work and for all the good advice and creative suggestions concerning the project.

I would like to thank Dr. Axel Warsinke for helping me with the project, advice and being very kind to me.

I am grateful to Prof. Dr. Helmuth Möhwald, Max Planck Institute of Colloids and Interfaces for the physical chemist view of the project and valuable discussions and support.

I thank Prof. Günter Wulff, Heinrich-Heine University, Düsseldorf for his tips on making imprints. Thanks to Dr. Kristian Lettau for helping me to make my first imprints and introducing me to the thermistor.

My special thanks go to Prof. Ulla Wollenberger and Dr. Walter Stöcklein for the scientific discussions. I like to acknowledge Prof. Frank Bier for the support from Fraunhofer IBMT.

I thank Ms. Angelika Lehmann, Ms. Andrea Kühn, Mr. Joachim Jacob at Analytical Biochemistry, Uni-Potsdam for their friendly assistance in the lab. Further I would like to thank Ms. Annemarie Martins, Ms. Irena Shikova, Ms. Regina Rothe, Ms. Annegret Praast and Dr. Jürgen Hartmann at Max Planck Institute of Colloids and Interfaces for the technical help.

I am thankful to the Dr. Angelo Valleriani, the coordinator of IMPRS on biomimetic systems for the administrative and financial support. Further financial support from BMBF (InnoRegio 03i1314 and BioHySys 0311993) is acknowledged.

I like to thank moritz for nice little chats and for the help with the translation. Thanks roman for nice chats in the lab and for giving me company for long stays in the lab. I wish to thank roberto for nice jokes, for teaching me Italian ☺ and for friendship. Further I thank noya, carsten, katrin, merlin for a relaxed atmosphere in the lab and for the social activities. I also extend my thanks to the people at IBMT, soeren, umporn oliver, kai, & erika for the help and for social activities.

Special thanks to birgit for organising a pleasant trip to wöbbelin. It was a great time i had with your entire family. Thanks to Prof. Burkhard Micheel and Mrs Edith Micheel for the wonderful pinnow trip and showing me the interesting aspects of life at the countryside in germany.

Many thanks to buddy (lakshmanan) ☺, raveendra, sajini, bala, priya, sangita and saravana for all the fun I had in germany and who never let me feel alone, lifted my spirits up in the bad times and gave me a feeling of home away from home.

Further I thank my T3-friends atul, arun, tijo, amit, mishra, paruthi & robert for the funny evenings and parties. I wish to thank my friends sarath, sekhar, sridhar & ashoka for the nice moments i shared with them in india.

I admire the support given to me from all my teachers from my school days in SRSI, friends at the Anna University, Chennai and colleagues at CFTRI, Mysore who contributed one way or the other in fulfilling this task.

And last but certainly not least, I would like to thank my dad rajagopal, mom kanagam and my brother naveen for the moral support and love throughout these years.

I. Table of contents

II. List of figures

III. List of tables

IV. Abbreviations

2,4-D	2,4-dichlorophenoxyacetic acid
AIBN	Azobisisobutyronitrile
ARS	Alizarin Red
Au	Gold
BFA	boc-phenylalanine anilide
Boc	tert-Butyloxycarbonyl
BOD	Biological oxygen demand
CAP	Chloramphenicol
CCD	Charge couple device
CPG	Controlled pore glass
DMSO	Dimethyl sulfoxide
DSC	Differential scanning calorimetry
DVB	Divinylbenzene
EDMA	Ethyleneglycol dimethacrylate
Fru-Val	Fructosyl valine
GOD	Glucose oxidase
H_2O_2	Hydrogen peroxide
HbA1c	Glycated hemoglobin
HPLC	High performance liquid chromatography
ISE	Ion sensitive electrode
ISFET	Ion sensitive field effect transistor
ITC	Isothermal titration calorimetry
POD	Peroxidase
L	Litre
MS	Mass spectrometry
MeOH	Methanol
MIP	Molecularly imprinted polymer
MIP(Frc)	Molecularly imprinted polymer against fructose
MIP(Fru-Val)	Molecularly imprinted polymer against fructosyl valine
NBT	Nitrotetrazolium blue chloride
NMR	Nuclear magnetic resonance
OPA	ortho pthalic dialdehye
PBA	Phenylboronic acid

PDH	Phosphate dehydrogenase
QCM	Quart crystal microbalance
RIfS	Reflectometric interference spectroscopy
SPE	Solid phase extraction
SPR	Surface plasmon resonance
RT	Room temperature
TGA	Thermogravimetric analysis
TMB	Tetramethylbenzidine dihydrochloride hydrate
TNT	Trinitro toluene
TRIM	Trimethylolpropane trimethacrylate
XPS	X-ray photoelectron spectroscopy

ppt	parts per trillion
ppm	parts per million

Prefixes

m	milli	10^{-3}
µ	micro	10^{-6}
n	nano	10^{-9}
p	pico	10^{-12}
f	femto	10^{-15}
a	atto	10^{-18}

V. Thesis structure

Chapter 1 (***Introduction***) gives definition to biosensors together with descriptions of recognition elements and transducers of a biosensor. Later the historical development of molecular imprinting, synthetic approaches for MIP preparation and MIP formats in literature is described. MIP sensors with respect to different transducers are reviewed with few examples. Further a short overview of boronic acids is presented as they were used as a functional monomer in the present study. Finally the biological significance of template is described.

Chapter 2 (***Objectives***) describes the objectives of the thesis.

Chapter 3 (*Materials and Methods)* presents the details of the materials and instruments used in this work. Later it describes the synthetic strategies and the methods used for the characterisation of imprints.

Chapter 4 (*Results and Discussion)* is subdivided into four sections and presents the results of the work.

4.1 describes the development of MIP for fructosyl valine and the characterisation studies in batch

4.2 describes the development of thermometric MIP sensor for fructosyl valine

4.3 describe the detailed investigations on charactersiation of MIPs for fructose based on batch and thermometric method. A detailed investigation on interaction of fresh and equilibrated fructose with MIP is described.

4.4 describe the detailed investigation on interaction of fresh and equilibrated glucose with MIP followed by cross-reactivity studies with disaccharides.

Chapter 5 (***Summary***) looks into the holistic aspects of the work that was undertaken and a general summary is presented.

Chapter 6 (*References*) cites all the published papers and book articles that were referred in this thesis.

1 INTRODUCTION

Nature has always served as a model for mimicking and inspiration to humans in their efforts to improve their life. Its most important talent is the evolutionary development of systems capable of molecular recognition, i.e. distinguishing one molecule from another. Molecular recognition is the basis for most biological processes, such as ligand-receptor binding, substrate-enzyme reactions, and translation and transcription of the genetic code is therefore of universal interest. Researchers have been inspired by nature to produce smart biomimetic materials with molecular recognition properties by design rather than evolution. **Molecular imprinting** is one way to prepare such materials. Such smart materials with new functionalities are at the forefront of the development of a relevant number of ongoing and perspective applications ranging from consumer to space industry.

The concept behind molecular imprinting is to mold a material (with the desired chemical properties) around individual molecules. Upon removal of the molecular templates, one is left with regions in the molded material that fit the shape of the template molecules. Thus, molecular imprinting results in materials that can selectively bind to molecules of interest. Imprinted materials resulted in applications ranging from chemical separation to bioanalytics. In this work attempts were made particularly in the development of MIP based thermometric sensors. By mimicking the natural enzymes or antibodies molecularly imprinted polymers were developed that serve as host for binding guest molecules. These imprints were used as a recognition element to substitute natural biomolecules in biosensors.

1.1 Biosensors

Biosensors are defined by IUPAC as analytical devices incorporating a biological material (e.g. tissue, microorganisms, organelles, cell receptors, enzymes, antibodies, nucleic acids etc.), a biologically derived material or a biomimetic intimately associated with or integrated within a physiochemical transducer or transducing microsystem, which may be optical, electrochemical, thermometric, piezoelectric, magnetic or micromechanical.[1-3]

Biosensors usually yield a digital electronic signal which is proportional to the concentration of a specific analyte or group of analytes. While the signal may in principle be continuous, devices can be configured to yield single measurements to meet specific market requirements.

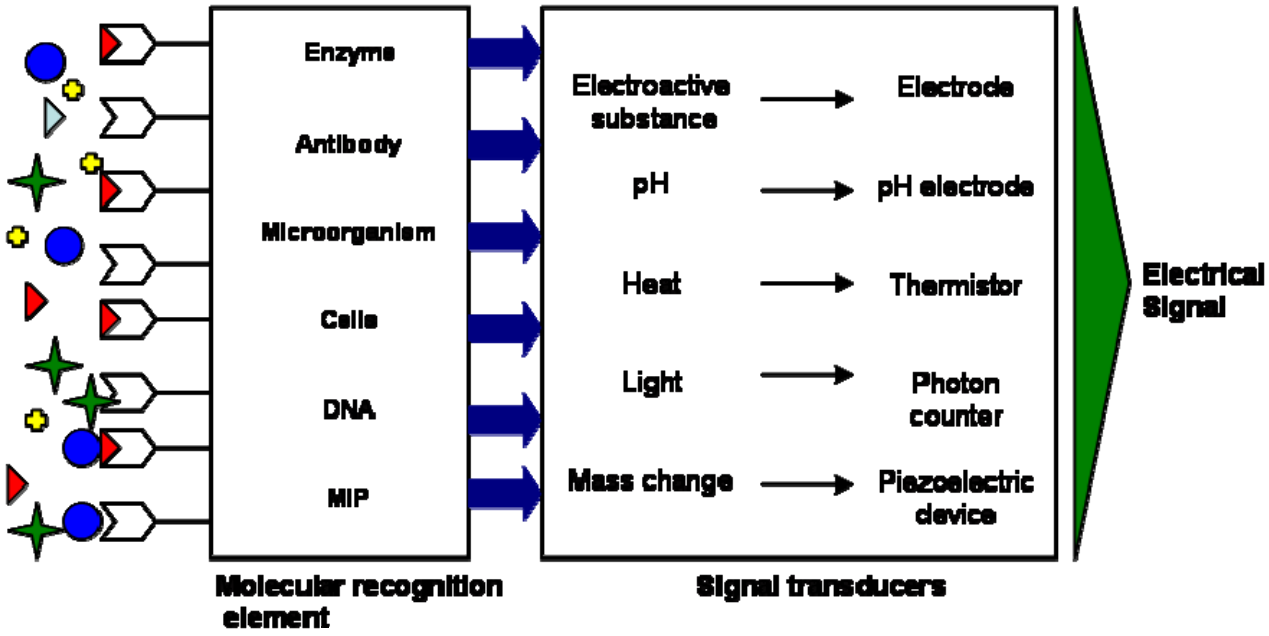

Figure 1. Scheme of a biosensor

1.2 Recognition Elements

The biological component of a biosensor can be enzymes, whole microbial cells, tissue slices, antibodies, natural and artificial receptors.[4]

1.2.1 Enzymes

A wide range of enzymes has been successfully used as a recognition element in biosensors owing to the combination of specificity and catalytic (amplification) properties. Enzymes allow a wide range of transduction technologies to be used and hence have found very wide applications in biosensors.[5] The most extensively studied and commercially developed one is a glucose biosensor. Glucose is oxidised by molecular oxygen catalysed by the enzyme glucose oxidase (GOD) to give gluconic acid and hydrogen peroxide. The reaction can be followed with a Clark oxygen electrode which monitors the decrease in oxygen concentration amperometrically.

GOD: $Glucose + O_2 \longrightarrow gluconic\ acid + H_2O_2$

The hydrolytic breakdown of urea is catalysed by the enzyme urease to give ammonia and carbon dioxide. This reaction can be followed potentiometrically with an ammonia ion sensitive electrode (ISE) which can detect 10^{-6} M ammonia.[6]

Urease: $(NH_2)_2CO + H_2O \rightarrow 2\ NH_3 + CO_2$

1.2.2 Microbial cells

Whole cells have been used in biosensors either in a viable or non-viable form. These are often used when the desired enzyme is unstable or difficult to purify. Use of whole microbial cells results in an increased stability but a decreased selectivity. The major limitation to the use of whole cells is the diffusion of substrate and products through the cell wall resulting in a slower response as compared to enzyme-based sensors. Usual practice is to preincubate the sensor with the analyte of interest before the measurement thus allowing enough time for induction of the necessary enzyme systems.

Microbial sensors are classified either as respiration activity measurement type or electrochemically active metabolite measurement type. In the former case changes in respiration activity of aerobic microorganisms caused by assimilation are detected by an oxygen electrode. In latter type the sensor detects electrochemically active metabolites such as H_2, CO_2, NH_3 and organic acids secreted from microorganisms. This type is not limited to aerobes but can also employ anaerobic microbes. Whole cell biosensors have been constructed to analyse, for example, alcohols, ammonia, antibiotics, biological oxygen demand (BOD), enzyme activities, mutagenicity, nitrates, organic acids, peptides, phosphate, sugars and vitamins.[7] *Pseudomonas fluorescens* was used to detect glucose in the range of 0.0125-0.125 mM and fructose was determined in the range of 0.1-10 mM using Bacillus lactofermentum.[8]

1.2.3 Antibodies

Antibody proteins are produced by the immune system of higher animals in response to the entry of ‘foreign’ materials into the body, for example, viruses and bacteria. In contrast to enzymes, antibodies do not (usually) catalyse chemical transformations, but rather undergo a physical

transformation. Antibodies are very specific in recognising and binding to the foreign substance. Binding leads to a variation in optical properties, electric charge, mass, or heat. This can be detected directly or indirectly by a variety of transducers. It is also possible to prepare and use monoclonal antibodies against virtually any desired analyte.

For example, antibodies were used for the determination of TNT using a photometric method. The TNT is incubated with the sepharose immobilised antibody to which it binds. TNT labelled with glucose-6-phosphate dehydrogenase is added to form G-6-PDH─TNT, then the assay is carried out with NAD, FMN and luciferase.

$$\text{G-6-PDH} + NAD^+ \longrightarrow \textit{glucono-6-lactone-6-phosphate acid} + NADH + H^+$$

Oxidoreductase/ Luciferase: $NADH + H^+ + FMN \longrightarrow NAD^+ + FMNH_2 \longrightarrow h\nu$

This is an extremely sensitive assay which can detect down to 10^{-18} mol/L (1 amol) of TNT.[9]

1.2.4 Receptors

Receptors are cellular, typically membrane proteins which bind ligands in a manner that results in a conformational change in the protein structure. The conformational change triggers an amplified physiological response such as ion channel opening or secreting an enzyme. Receptors were used as a recognition element principally for three reasons. Firstly, they possess high affinity and specificity refined by evolutionary processes. Secondly, they are natural targets for toxins and mediators for physiological processes and due to this they can be used for monitoring these compounds in clinical and environmental analyses. Thirdly, receptors can be used for real time elucidation of receptor-ligand interactions. A number of attempts have been made to detect toxins in environmental and clinical samples using receptor sensors.[10-12]

Receptors can be broadly classified into intact receptor-based biosensors and isolated receptor-based biosensors. In the former group the excised crustacean olfactory structures were used for neuronal sensing of chemoreceptor ligands such as amino acids, sex hormones and pyridine-based chemicals. The binding of ligand triggers the firing of an action potential in the nerve which can be determined using glass microelectrodes, outside the cell. A widely investigated isolated

receptor, nicotinic acetylcholine has been used with several transducers including ISFET and capacitance types used for the determination of toxins.[13]

1.2.5 Tissue materials and organelles

Plant and animal tissues may be used as a recognition element in a biosensors. The advantage of tissue based biosensors is an increased stability. Cells that could form the basis of tissue-based biosensors could be from a variety of sources including neurons, immune cells, endothelial cells, fibroblasts, myocytes, primordial and peripheral stem cells. This means that different tissue samples could generate different signals due to co-operative action. This could result in biosensors with a wide range of selectivities.

Arginine is broken down by bovine liver to urea and onithine. The urea is then determined with a urease enzyme based potentiometric biosensor.

Bovine liver: $arginine \longrightarrow urea + ornithine$

Urease: $(NH2)_2CO + H_2O \longrightarrow 2\,NH_3 + CO_2$

Banana tissue contains polyphenolases which catalyse the oxidation of molecules containing catechol groups to the corresponding o-quinone. A biosensor for dopamine with the detection limit of 1.3×10^{-6} M was developed using an oxygen electrode to follow the assay.[14]

Liver microsomes have a monoxygenase system with cytochrome P 450, which catalyses the hydroxylation of a large number of pharmaceutical derivatives, fatty acids and steroidal hormones. This oxidation can help to couple the organelle directly to an amperometric transducer.[15]

1.2.6 Nucleic acids

DNA biosensors, based on nucleic acid recognition processes, are being developed towards the goal of rapid, simple and inexpensive testing of genetic and infectious diseases and for the detection of DNA damage and interactions. The immobilisation of the nucleic acid probe onto the transducer surface plays an important role in the overall performance of DNA biosensors and

leads to a well-defined probe orientation, readily accessible to the target. DNA dendrimers can be used for imparting higher sensitivity onto DNA biosensors. These tree-like superstructures possess numerous single-stranded arms that can hybridise to their complementary DNA sequence. A greatly increased hybridisation capacity and hence a substantially amplified response is achieved by immobilising these dendritic nucleic acids onto the transducer.[16]

1.2.7 Molecularly imprinted polymers (MIPs)

Despite advantages which biosensors have in terms of specificity and selectivity, they suffer from the serious disadvantage of low stability of biological molecules, which makes their storage and operation in harsh chemical environments problematic. The search for possible solutions to this problem associated with the use of natural molecules in sensors has led to the development of stable synthetic analogues of natural receptors and antibodies. One of the most promising generic methods that, in theory, should be applicable for the design of affinity material for any type of analytes is ***molecular imprinting***. The more detailed aspects of molecular imprinting technology comprising synthesis and applications is described in section 1.4. Table 1 compares the advantages and limitations of molecularly imprinted polymers (MIPs) with that of biomolecules.

Table 1. Comparison between the advantages and limitations of MIPs with biomolecules

	MIPs	**Biomolecules**
Advantages	- medium to high affinity - stable under harsh conditions - inexpensive and easy to prepare, - can be reused - can work in organic solvents - compatible with micromachining	- high affinity and selectivity - solution assays possible - class-specificity possible
Limitations	- heterogeneous binding site - slow mass transfer - requires preparative amount of the - template/ template analogue in the pure form - affinity is strongly medium dependent	- low stability - poor performance in organic solvents - time-consuming preparation and purification - poor compatibility with micromachining

1.3 Transducer

The transducer is an important component through which the measurement of the target analyte is achieved by transforming the recognition element-analyte interaction into a quantifiable electrical signal. Several type of transducers were used in conjunction with the recognition element. Table 2 lists the general type of transducers used in biosensors.[3]

Table 2. General types of transducers used in sensor applications

Transducer system	Measurement mode	Type of biosensor
Electrochemical		
Enzyme electrode	Amperometric (current)	e^- from enzyme substrates / product
	Potentiometric (voltage)	H^+ from enzyme substrates/ product
Field effect transistors	Potentiometric (voltage)	Ions
Conductimetric	Conductance	Artificial cells
Impedimetric	Impedance	Enzyme based reactions
Gas electrode	Potentiometric (voltage)	Gases, enzymes, cell or tissue electrodes
Piezo-electric crystals	Mass change	Vapours, oil, immunological analysis
Optical	Absorbance, fluorescence	pH, enzyme substrates, immunological analytes
Surface plasmon and wave guide devices	Resonant signal (angle)	DNA, RNA, Proteins
Capacitive devices	Dielectric constant	Antibody sensors
Thermometric	Temperature	Enzyme thermistors

1.4 Molecular Imprinting

In nature, molecular recognition plays a decisive role in biological activity; for example in receptors, enzymes, and antibodies. Using a conceptually simple process, molecular recognition has been created in synthetic polymers using a technique analogous to what was formerly thought to be the mechanism of formation of antibodies. This process is called molecular imprinting and its origin can be traced to early theories on enzyme function and antibody formation. Basically, this process resembles Emil Fischer's idea of a "lock and key" fit to describe the specificity of enzymes.

In general, molecular imprinting is a methodology used to create the selective recognition sites in synthetic polymers. In this process, functional and cross-linking monomers are co-polymerised in the presence of the target analyte. This target analyte corresponds to the imprint molecule, which acts as a molecular template.

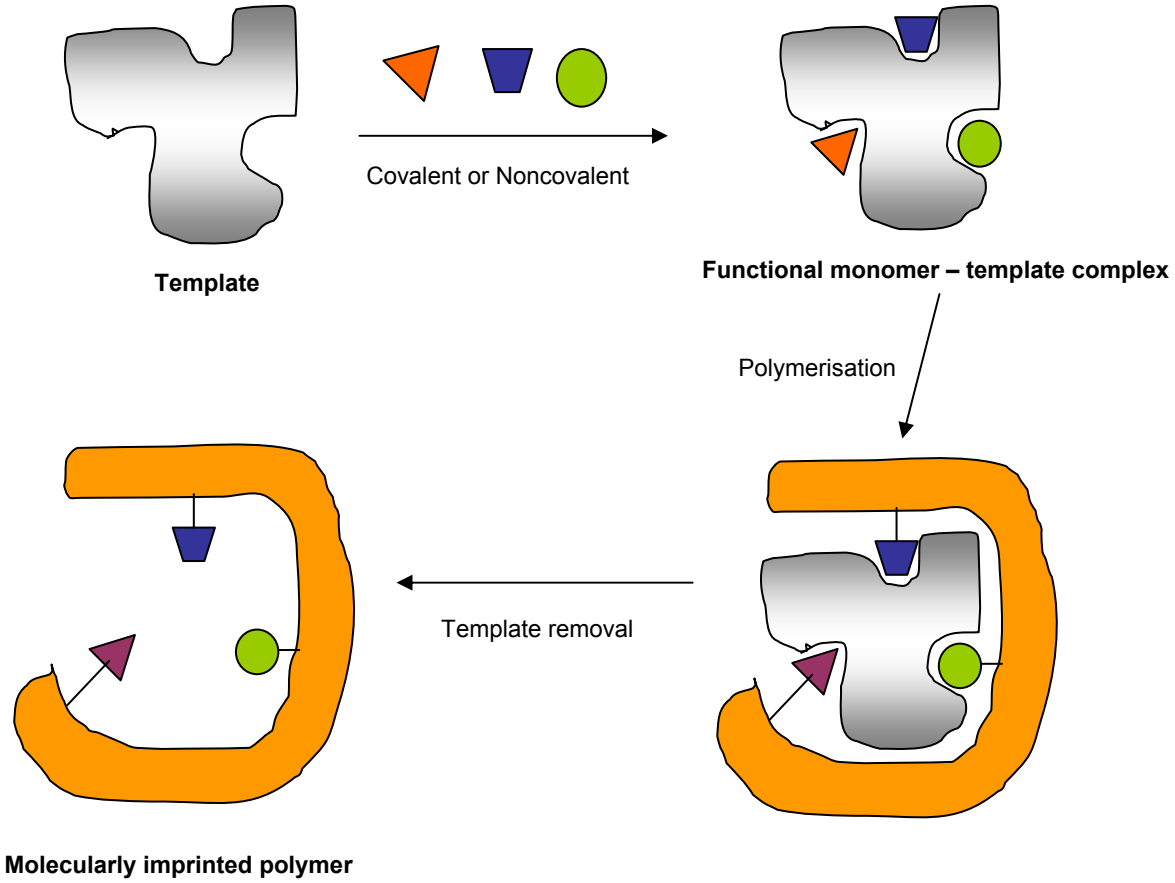

Figure 2. Scheme of molecular imprinting

1.4.1 Background

The discovery of molecular imprinting dates back to 1931 when Polyakov published an investigation on the effects of drying silica in the presence of different additives on its pore structure.[17] He reported a correlation between the structure of the additives used during the drying process and the extent of their rebinding to the silica. At the time of Polyakov´s first papers the origin of selectivity of the antibodies of the immune response was under debate. Mudd, Breinl Haurowitz and Pauling hypothesised the "instructional theory" for the formation of antibodies.[18-20] Pauling suggested that the antigens induce or otherwise imprint a binding site within the unfolded polypeptide chain of an antibody as illustrated schematically in Figure 3. Although this theory has later given way to clonal selection theory, these works represent the earliest example of imprinting.

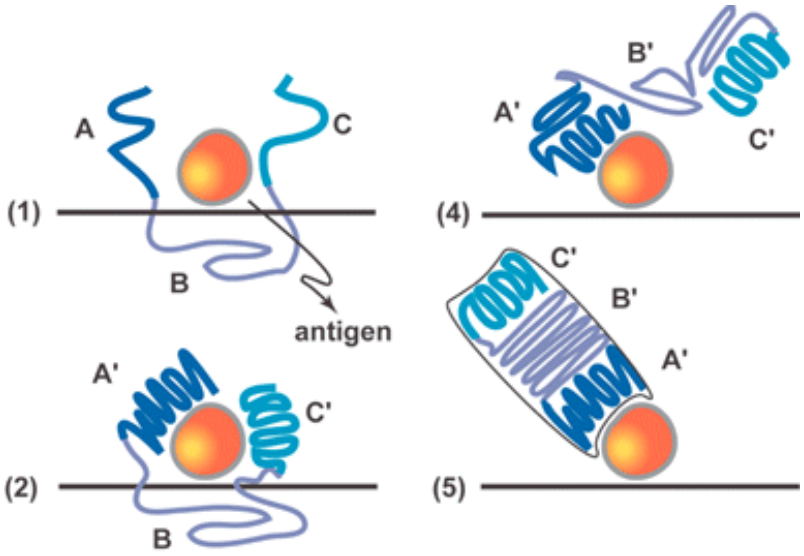

Figure 3. Scheme showing four steps of Pauling´s six step mechanism by which an antigen imprints structural information into an antibody molecule (adapted from reference [21]).

In a later study Franz Dickey, a student of Linus Pauling, in 1949 reported the polymerisation of sodium silicate using a dye as template. [22] In this method, the dye template was added prior to the polymerisation, which is the way that polymers are usually prepared today, and the adsorption power was compared with that of control gels, prepared in the absence of the template. Dickey observed that after template removal silica rebinds the same dye in preference to others.

The first works on imprinted organic polymers came from two different groups, independently, in 1972. One of these studies, presented by the Klotz group[23] involved the synthesis of binding sites from methyl orange in a polyethyleneimine cross-linked network. The other study, presented by Wulff et al., [24] involved an imprint that showed enantiomeric affinity for the D-form of glycerolic acid. Both of the cited studies involved a covalent linkage of the template molecule to the monomers before polymerisation. The most common approach today is to use non-covalent linkage of the monomers to the template molecule. This non-covalent approach for producing organic imprinted polymers was introduced in the early 1980s by the group of Mosbach.[25] Today MIPs are used in various applications like chromatography [26-31], sensing [32-36], catalysis [37-56] and solid phase extraction [57-61]. A large number of reviews describe the synthesis of MIP and its various applications. [30, 34, 62-83]

1.4.2 Molecular imprinting strategies and approaches

During molecular imprinting, polymerisable functional monomer–template complexes are formed by covalent or non-covalent interaction. The complexes were fixed by cross-linking polymerisation.

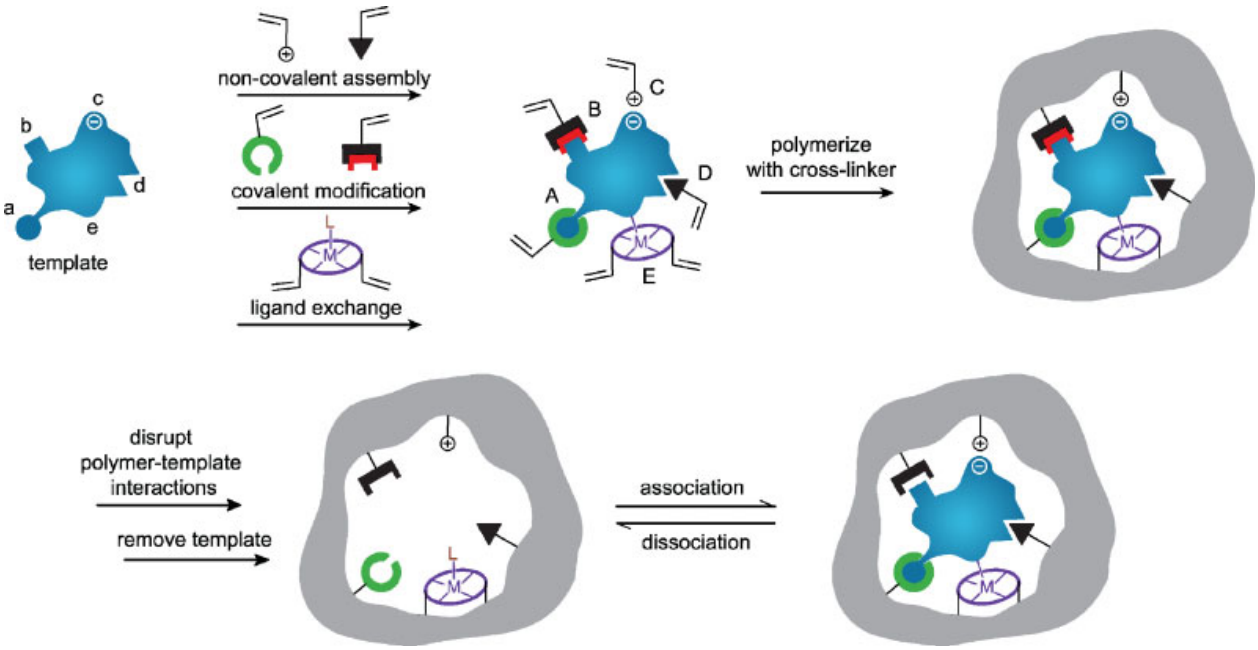

Figure 4. Schematic representation of the molecular imprinting process.(adapted from reference[84]).The formation of reversible interactions between the template and polymerisable functionality may involve one or more of the following interactions: (A) reversible covalent bond(s), (B) covalently attached binding groups that are activated for non-covalent interaction by template cleavage, (C) electrostatic interactions, (D) hydrophobic or van der Waals interactions or (E) co-ordination with a metal centre

The template molecules are then removed, providing binding sites ideally complementary in size, shape and functionality to the template. Upon re-introduction of the template preferential rebinding within the cavity should occur. In the pre-polymerisation mixture, the dissolved target interacts by covalent, non-covalent, or metal coordination interactions with the functional monomer responsible for localising the chemically active moieties of the target molecules during copolymerisation. Consequently, molecular imprinting is classified into covalent imprinting (pre-organised approach), non-covalent imprinting (self-assembly approach), and semi-covalent imprinting according to the type of interactions between functional monomer and target molecules in the pre-polymerisation mixture and during rebinding.[85, 86]

1.4.2.1 Covalent approach

Wulff and co-workers have made an intensive study of covalent molecular imprinting systems. This method involves the pre-formation of template-monomer complex, its polymerisation with an excess of cross-linker and the subsequent template removal. This approach to molecular imprinting promises the most homogeneous binding site distribution with largely identical binding pockets. The binding constants for the template molecule are higher thereby withstand the polymerisation conditions. A chemical synthesis step is necessary to bind the template to the functional monomer with bond types such as Schiff bases, boronates, ketals, carboxylic amides and esters. These relatively strong covalent interactions make it possible to use stoichiometric amounts of functional monomer with respect to the number of template molecules used. However, despite the high affinities of the polymeric material, the range of functional groups which can be targeted is restricted and the removal of the template molecules is tedious (chemical cleavage). This limits the application of covalently prepared MIPs. Figure 5 shows the covalent imprinting of phenyl-α-D-mannopyranoside via boronic ester linkages.

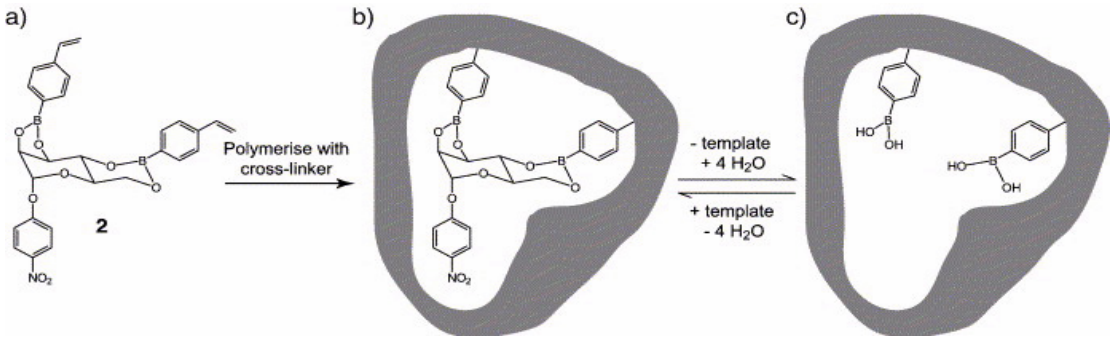

Figure 5. Covalent molecular imprinting of phenyl-α-D-mannopyranoside (adapted from [69])

1.4.2.2 Non-covalent approach

The non-covalent molecular imprinting approach was mainly developed by Mosbach and his co-workers. The types of interactions in non-covalent imprinting are ionic, hydrogen-bonding and hydrophobic effects, which are the types of interactions that rule our living world and therefore their use in molecular imprinting is inexhaustible. Complexation is achieved by mixing the template with an excess of functional monomer. As a consequence, even for those functional monomers that interact with the template molecule during self assembly, their final correct distribution and orientation are not perfectly ensured because of the molecular motion of the template with respect to the functional monomers during the polymerisation process. This results in a more heterogeneous binding site distribution. Nevertheless, owing to simple preparation procedures, the wide range of imprintable compounds, and reversible host-guest binding based on non-covalent interactions ('biomimetic binding') render the non-covalent imprinting approach the most widespread method for the synthesis of molecular imprints. Figure 6 illustrates the non-covalent imprinting of a dipeptide using methacrylic acid as a functional monomer.

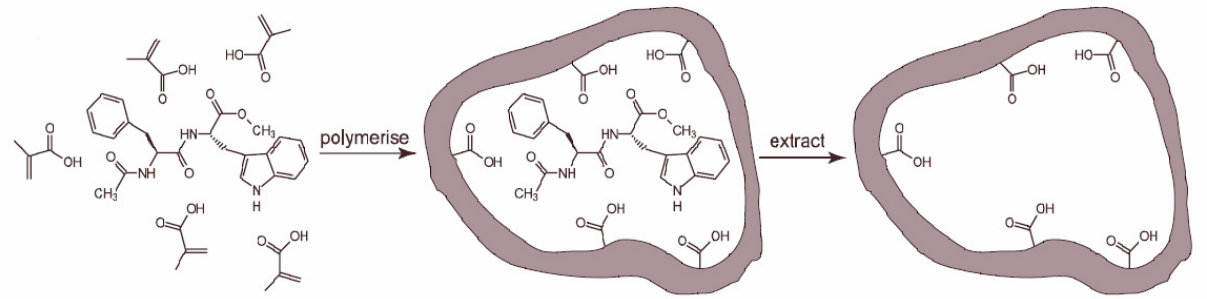

Figure 6. Non-covalent approach for molecuflar imprinting (adapted from [69])

1.4.2.3 Semi covalent approach

The semi covalent method or sacrificial spacer approach is a hybrid of covalent and non-covalent approach and was first introduced by Whitcombe et al.[87] In this method, a covalent template-functional monomer complex is used in imprinting process and after hydrolysis and template removal, the rebinding occur via non-covalent interactions. Figure 7 shows that the template cholesterol was esterified with 4-vinylphenol to give a 4-vinylphenyl carbonate ester. After co-polymerisation of the template construct with excess of cross-linker, the carbonate-bond was cleaved, releasing the template and a small, sacrificial molecule, carbonic acid. Following

extraction of the template, the imprinted recognition site contains a phenolic residue oriented in a manner that allows specific rebinding via non-covalent interaction with the hydroxyl group of cholesterol. Polymers synthesised by this method were shown to bind cholesterol from hexane solution with a single dissociation constant.

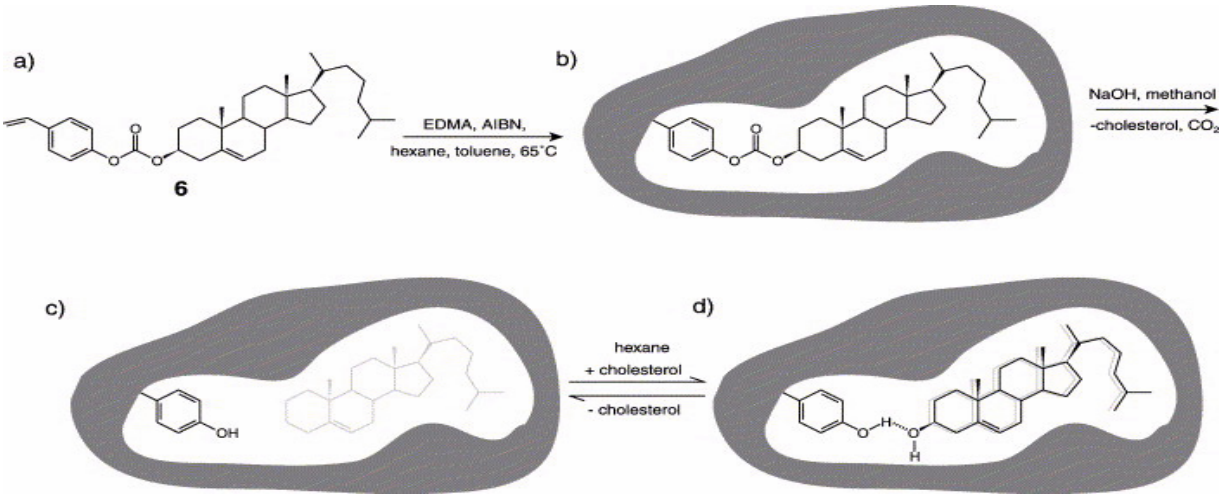

Figure 7. Semi-covalent approach for molecular imprinting (adapted from [69])

1.4.2.4 Metal coordinated systems

An important contribution to the development of metal-coordination interaction based MIPs was brought by Arnold and co-workers. In the first attempt to demonstrate the advantage of this binding interaction, the strong coordination between the iminodiacetic (IDA)-Cu^{2+} complex and imidazole was utilised to prepare MIPs. [88] Nearly quantitative desorption and reloading of the metal ions and substrates with these polymers suggested the high accessibility of the binding sites in these polymers.

1.4.3 MIP formats

The format in which the MIP is obtained is an important factor that determines the extent of application of MIPs. Sensor applications would require films or membranes to coat the transducers, binding assays would need colloidal suspensions whereas chromatographic columns or solid phase extraction cartridges would need beads.

Most MIPs were conventionally prepared by bulk polymerisation as a monolith. This is further grinded and sieved to obtain granular particles in the size of 25-50 μm for chromatographic applications. It is a simple and straightforward method which does not require any sophisticated equipment.

MIP particles, with uniform size can be synthesised by immobilising the template to the surface of amino functionalised silica. The prepolymersiation mixture was filled within the pores and polymersation was carried out. The dissolution of silica yields spherical MIP particles used for catalysis and chromatography.[89-92]

Silica particles containing surface-bound free radical initiators have been used as supports for grafting thin films of molecularly imprinted polymers (MIPs). This technique offers a means of fine-tuning the layer thickness for improved kinetic properties or enhanced capacity in chromatographic or sensor applications.[93]

Suspension polymerisation produces beads with a diameter between 5 and 50 μm depending on the stirring speed and the amount of surfactant. This technique based on the use of a liquid perfluorocarbon as the dispersing phase was described by Mayes and Mosbach.[94] In this method polymerisation occurs in droplets of the polymerisation mixture suspended in a continuous phase (often water containing a suspension stabiliser).

Precipitation polymerisation is another method that can provide particles in the submicron scale (0.3–10 μm). It is based on the precipitation of the polymeric chains out of the solvent in the form of particles as they grow more and more insoluble in an organic continuous medium. In this case,

particles are prevented from coalescence by the rigidity obtained from the cross-linking of the polymer, so there is no need of any extra stabiliser.[95, 96]

Two-step polymerisation produces monodisperse particles in the micron size range (2–50 μm) with good control of the final size and number of the particles. This was first described with MIP by Hosoya et al. in 1994.[97] It requires several swelling steps on the initial particles with the imprinting mixture before polymerisation proceeds. In this case, the continuous phase of the polymerisation medium is water.

Core-shell particles are monodisperse and can be obtained by emulsion polymerisation in the range of 0.05–2 μm.[98, 99] They have a structured morphology that allows the incorporation of any added property into the core of the particle without interfering with the imprinted shell. They are formed in a two-stage process from seed latex; however, unlike the two-step polymerisation (above) the seed particle (which may be cross-linked) is surrounded by a shell of new polymer in a second emulsion polymerisation. The continuous medium used during polymerisation is water.

Miniemulsion polymerisation was used to synthesise MIP nano spheres with particle diameter between 50 and 300 nm. These imprinted nano spheres were used to develop a MIP membrane.[100, 101] Zimmerman described the synthesis involving covalent attachment of dendrons to a porphyrin core, cross-linking of the end-groups of the dendrons, and removal of the porphyrin template by hydrolysis. This resulted in one recognition site per dendrimer molecule.[102]

Planar MIP structures such as films and membranes have been prepared either by polymerisation within a mould [103] or on a planar surface layer.[104] Grafting approaches have also been applied [105] and electropolymerisation has also been used to build up layers of acrylamide-based MIPs on ISFETs (ion-sensitive field effect transistors).[106, 107]

1.4.4 MIP sensors

The inherent specificity of molecularly imprinted materials has provided many opportunities for integration into sensing applications. The adaptability of the polymeric materials into different formats facilitates this integration. Table 3 summarises the different transducer types that have been used with MIPs and the following section describes the most prominent MIP sensors with selected examples.

Table 3. Transducers employed in MIP based sensors [108]

Transducer	Analyte	Range (μM)	Reference
General Formats			
Ellipsometry	Vitamin K1	qualitative	[109]
Capacitance	Theophylline	5000-33000	[110]
	Phenylalanine anilide	qualitative	[105]
	Phenylalanine	6000	[111]
Conductometry	Atrazine	0.005-0.05	[103]
Surface acoustic wave	Solvent vapours	(0.1μL/L)	[112]
Quartz crystal microbalance	Solvent vapours	(4 μL/L)	[112]
	Glucose	1000-20000	[113]
	S-Proporanolol	50-1300	[114]
Love-wave	2-methoxy3-methylpyrazine	n.c.	[115]
Infrared evanescent wave	2,4-D	4.5-1000	[116]
			[117]
Analytes generates signal			[118]
Fluorescence	Dansyl phenylalanine	25-250	[119]
Amperometry	PAH (Pyrene)	0.00015-0.2	
	Morphine	3.5-35	
Competitive binding formats			
Colorimetry	Chloramphenicol	10-3000	[120]
Voltametry	2,4-D	0.1-100	[121]
Polymer generates signal			
pH	Glucose	1000-25000	[122]
Fluorescence	cAMP	0.1-100	[123]

1.4.4.1 Quartz crystal microbalance based sensing

The method of mass-sensitive transduction of MIP/analyte binding events has been exploited most notably by the group of Dickert. Some of the earlier work performed in this area involved the use of polyurethanes as the imprintable matrix. [124-127] In this approach a stamp containing the microorganism is pressed into a prereacted polymer mixture.

Such imprints have been shown to be immediately useful in real-world applications, such as monitoring of engine-oil degradation [128] and the content of polyaromatic hydrocarbons in water.[129] The use of polyurethane to imprint larger chemical/biochemical entities has been detailed by the group, using combinations of QCM analyses with atomic force microscopy to examine MIP/cell interactions. [130-132]

Turner and co-workers described MIP synthesised against Microsystin-LR.[133] The polymer was used both as a material for solid-phase extraction (SPE) and as a recognition element in a piezoelectric sensor. Using the combination of SPE followed by QCM sensing, the minimum dectection amount of toxin was 0.35 nM which was more than sufficient for achieving the required detection limit for microcystin-LR in drinking water (1 nM). This work is the first example where the same MIP receptor has been used successfully for both SPE and the corresponding sensor.

A highly specific non-covalently imprinted polymer for L-menthol was casted in situ on to the surface of a gold-coated quartz crystal microbalance electrode as a thin permeable film. The detectability of L-menthol was 200 ppb with a response range of 0-1.0 ppm.[134]

Kugimiya and co-workers reported a piezoelectric sensor to detect indole-3-acetic acid, a plant hormone. The sensor showed a selective response and gave a linear relationship between frequency shift and amount of IAA in the range from 10 to 200 nmol. This technique requires an initial derivatisation of the QCM surface with vinyl-terminated thiols, to introduce polymerisable groups onto the surface to anchor the MIP layer.[135]

This first literature example of an integrated MIP–QCM sensing device capable of chiral discrimination was described by Haupt et al.[114] MIP imprinted with the chiral β-blocking drug S-propranolol was cast as a thin permeable film onto a gold electrode deposited on the quartz crystal vibrator. The mass increase of the polymer due to analyte binding was quantified by piezoelectric microgravimetry with the QCM. The sensor was able to discriminate between the R- and S- propranolol enantiomers in acidified acetonitrile solutions owing to the enantioselectivity of the imprinted sites with a detection limit of 50 μM.

Malitesta et al., utilised an electropolymerisation technique to imprint glucose based on poly(o- phenylenediamine).[113] The material is employed as the recognition element of a QCM biomimetic sensor for glucose. XPS was used to characterise the imprinting effect.

Piezoelectric quartz crystals coated with a 2-methylisoborneol (MIB) imprinted polymer gave responses which were consistently 5-10Hz (1.1-1.3 times) higher than those of sensors coated with a non-imprinted polymer. Geosmin, another tertiary alcohol odourant with an earthy odor resembling, and often accompanying MIB produced almost equal responses on either imprinted- or non-imprinted sensors. A number of other odourants were examined and their responses to the non-imprinted sensors were found to be similar to or greater than their responses to the imprinted sensors. The responses of MIB to the imprinted sensors were always the highest, while other odourants produced equal or higher responses using the non-imprinted sensor.[136]

MIP-QCM sensor for glucose was described by Ersöz et al., based on the ability of glucose to chelate copper (II) ion of methacrylamidohistidine (MAH) monomer to create a ligand exchange assembled monolayer which is suitable for glucose determination.[137] B_{max} (number of binding sites) and K_D (dissociation constant of the metal-chelate copolymer) were calculated using Scatchard plot and the detection limit was found as 0.07 mM.

The MIP film was fabricated onto a QCM chip using a pentadecapeptide, corresponding to the linear epitope of the dengue virus NS1 protein. Imprinting resulted in an increased polymer affinity not only towards the corresponding template but also to the virus protein. Direct detection of the dengue virus protein was achieved quantitatively. The QCM chip response to the NS1

protein was obtained using epitope-mediated imprinting demonstrating a comparable frequency shift in chips immobilised with monoclonal antibodies. The binding effect was further enhanced and confirmed using a monoclonal antibody to form a sandwich with the MIP-NS1 protein complex on the chip.[138]

The first experimental proof of concept of the combination of resonant MEMS with MIPs for the detection of 2,4-D was described by Ayela et al.[139]

1.4.4.2 Optical sensors

A practical optical sensing system for the determination of chloramphenicol (CAP) using MIP and HPLC was described from the group of Karube.[120] The method is based on competitive displacement of a chloramphenicol-methyl red (CAP-MR) dye conjugate from specific binding cavities in an imprinted polymer by the analyte resulting in a measurable change in absorbance at 460 nm. The sensor shows a linear response in the concentration range 3–1000 mg/ml and effectively detected CAP extracted from serum.

A new optical polymer-based sensor was developed, which is able to recognise amines in organic solvents with high sensitivity. Thin polymer membranes were prepared and investigated, which contain a chromogenic functional dye (reactant) that shows a significant colour change during a reversible chemical reaction with the analyte.[140]

Fluorescence-based sensing

Fluorescence sensing represents an attractive means of creating an effective chemosensor, due to ease of use and detection of sub-micromolar concentrations. As MIP materials are inherently versatile, a variety of methods have been employed to attain optical transduction of specific binding events via fluorimetry.

A new type of a fluorescent receptor system specific for sialic acid has been prepared by Piletsky et al. [141] The MIP was synthesised using allylamine, vinylphenylboronic acid and ethylene glycol dimethacrylate in the presence of sialic acid as template. After template

removal, the MIP suspension was used in reaction with o-pthalic dialdehyde (OPA) reagents, both in the presence and absence of sugars. It was found, that sialic acid promoted the fluorescence development in this system, probably as a result of the so-called "gate effect", resembling natural occurring receptors. Rapid detection of sialic acid in the concentration range of 0.5-10 μM was shown possible within 40 minutes. The MIP was able to discriminate sialic acid from other sugars such as glucose and mannose.

The same group reported a MIP sensor for creatine. Highly cross-linked MIP was prepared using methylated creatine, allyl mercaptan and OPA using EDMA as cross-linker and DMSO as porogen. The background fluorescence of MIP suspension was low, but increased dramatically in the presence of creatine. The sensor shows a linear response between 20-100 μM for creatine. Creatinine, the molecule with less similar structure gave half of the signal obtained for creatine. Surprisingly ammonia, which is small enough to fit into the MIP cavity did not produce a response of comparable magnitude to creatine.[142, 143]

A system for the detection of triazine herbicide was described by the Piletsky et al.[144] This method is based on the competition between fluorescent-labelled and the unlabelled analyte for the specific binding sites, that were produced in polymer by imprinting of the template. After grinding of the polymer block and splitting off the template molecules a suspension of the polymer was used for the herbicide-specific sensor system. Selective detection of triazine in the concentration range of 0.01-100 mM was achieved.

Ye and Mosbach reported a new type of scintillation assay for (S)-propranalol. During imprinting a scintillating monomer was incorporated into the MIP. When a tritium labelled template is bound the monomer transforms the β–radiation into a fluorescent signal.[145]

A commonly used method of introducing fluorescence transduction of binding events to a MIP is derivatisation of functional monomers to include a fluorescent moiety. When rebinding occurs the resultant changes in the electronic properties of the monomers produce a fluorescent signal. Rathbone and co-workers [146] synthesised a selection of monomers bearing fluorescent

substituents (such as coumarin and acrylamidopyridine), which effectively detected the template rebinding. A similar approach yielded MIPs for the biologically important compound cyclic guanosine monophosphate.[147]

A D-fructose specific sensor was described by Gao et al. [148, 149] They designed and synthesised an anthracene-boronic acid conjugate with a methacrylate moiety attached allow for incorporation into MIPs. With the addition of D-fructose, the fluorescence intensity was enhanced significantly in a concentration-dependent manner in the range of 0.01 mM – 100 mM. The selectivity studies indicated that the fluorescence intensity changes due to the addition of glucose and mannose at the same concentrations were far smaller than that of D-fructose.

MIPs were prepared against cAMP that contain a fluorescent dye, trans-4-[p-(N,N-dimethylamino)styryl]-N-vinylbenzylpyridinium chloride, as an integral part of the recognition cavity, thus serving as both the recognition element and the measuring element for the fluorescence detection of cAMP in aqueous media. This fluorescent molecularly imprinted polymer displays a quenching of fluorescence in the presence of aqueous cAMP, whereas almost no effect is observed in the presence of the structurally similar molecule, cGMP. [123]

Luminescence based sensing

A flow injection competitive assay analogous to enzyme immunoassays has been developed for 2,4-dichlorophenoxyacetic acid (2,4-D) using a MIP instead of the antibody. A glass capillary was modified by covalently attaching an imprinted polymer to the inner capillary wall. The herbicide 2,4-D was labeled with tobacco peroxidase, and chemiluminescence was used for detection in combination with a photomultiplier tube or a CCD camera. In a competitive mode, the analyte-peroxidase conjugate was passed together with the free analyte through the polymer-coated capillary mounted in a flow system. After a washing step, the chemiluminescent substrate was injected and the bound fraction of the conjugate was quantified by measuring the intensity of the emitted light. Calibration curves corresponding to analyte concentrations ranging from 2.25 nM- 225 nM were obtained. [150-152]

The techniques of imprinting and sensitised lanthanide luminescence have been combined to create the basis for a sensor that can selectively measure the hydrolysis product of the nerve agent Soman in water. The sensor functions by selectively and reversibly binding the phosphonate hydrolysis product of this agent to a functionality-imprinted copolymer possessing a coordinatively bound luminescent lanthanide ion, Eu^{3+}. Instrumental support for this device is designed to monitor the appearance of a narrow luminescence band in the 610-nm region of the Eu^{3+} spectrum that results when the analyte is coordinated to the copolymer. For this configuration, the limit of detection for the hydrolysis product is 7 ppt (parts per trillion) in solution with a linear range from 10 ppt to 10 ppm. Chemically analogous organophosphorus pesticides tested against the sensor have been shown not to interfere with determination.[153-155]

Surface plasmon resonance based sensing

In surface plasmon resonance spectroscopy (SPR) the measurement of slight shifts in the resonant angle of incidence, induced by changes in the dielectric properties of the sample medium (in this case, an imprinted polymer matrix) in contact with the silver film, can be used to track events such as MIP-template molecule interactions.

In 1998 Lai et al., developed a sensory system based on the optical phenomenon of surface plasmon resonance (SPR), which employs either photothermal deflection spectroscopy (PDS) or a photodiode array (PDA) for detection.[110] MIP against theophylline was used as the sensing element. The linear range of the assay was found to extend up to 6 mg/mL, with a detection limit estimated at 0.4 mg/mL for theophylline in aqueous solution. A cross-reactivity study of the anti-theophylline and anti-caffeine polymers, using eight other drugs structurally similar to theophylline and caffeine, showed none or very slight affinity for the other drug molecules. Similar molecular recognition characteristics were observed for the anti-xanthine polymer.

A MIP–SPR sensor selective for sialic acid was developed by Takeuchi and co-workers.[156] A mixture of covalent and non-covalent interactions was used to create binding sites for sialic acid. The sensor showed a selective response in aqueous media to ganglioside on which sialic acid is located at the non-reducing end. The sensor shows a linear response for 0.1 to 1.0 mg of

ganglioside. Recently the same group described MIPs selective for lysozyme which were prepared on SPR sensor chips.[157]

Cross-linked films consisting of the acrylamide-acrylamidophenylboronic acid copolymer that are imprinted with recognition sites for β-nicotinamide adenine dinucleotide (NAD^+), β-nicotinamide adenine dinucleotide phosphate $NADP^+$, and their reduced forms (NAD(P)H), are assembled on

Au-coated glass supports. The binding of the oxidized cofactors NAD^+ or $NADP^+$ or the reduced cofactors NADH or NADPH to the respective imprinted sites results in the swelling of the polymer films through the uptake of water.[158]

Reflectometric interference spectroscopy (RIfS) was used to study the interaction of MIP (imprinted with either (R,R)- or (S,S)-2,3-di-O-benzoyltartraric acid) with the corresponding templates. With these sensors chiral separation with a separation factor of 1.2 could be achieved whereas a reference polymer resulted in no separation.[159]

1.4.4.3 Electrochemical sensing

Kriz and Mosbach in 1995 described a competitive amperometric sensor specific for morphine as one of the earliest reported MIP-based electrochemical sensors.[119] Their method of morphine detection involves two steps. In the first step, morphine binds selectively to the MIP in the sensor. In the second step, an electroinactive competitor (codeine) is added in excess, hence some of the bound morphine is released. The released morphine is detected by an amperometric method in the range of 0.1-10 mg/L.

Later the same group developed a conductometric chemical sensor based on a molecularly imprinted polymer with benzyltriphenylphosphonium ions chosen as a template. This MIP based sensor shows higher conductivity response when exposed to the analyte.[132] Thus conductometric sensing was perhaps the first electrochemical sensor format used with integrated MIP technology, permitting direct analysis of rebinding events without the requirement for a secondary competing species.

Direct electrochemical detection of an inert template was reported by Piletsky and co-workers. They explored the MIP´s ability to change the conformation or surface potential upon binding with the template. The "gate effect", had been used for quantifying the analyte concentration. The authors achieved levels of analyte detection in the micromolar range. [103, 160, 161]

A glucose sensor based on capacitive detection has been developed by Cheng and co-workers.[162] The sensitive layer was prepared by electropolymerisation of o-phenylenediamine on a gold electrode in the presence of the template (glucose). When glucose binds to the imprint sites, there will be an additional layer decreasing the capacitance and the sensor shows a linear response between 0.1 - 20 mM with the detection limit of 0.05 mM.

A sensor system for the herbicide 2,4-D has been developed based on specific recognition of the analyte by a MIP and electrochemical detection using disposable screen-printed electrodes. An integrated sensor was developed by coating the imprinted polymer particles directly onto the working electrode. Following incubation of the modified electrode in a solution containing the analyte and the probe, the bound fraction of the probe is quantified.[121]

A voltammetric sensor for the determination of diclofenac/ vanillylmandelic acid was developed based on MIP-modified electrodes. Thin layers of MIPs for template have been prepared by spin coating the surface of a glassy carbon electrode with the monomer mixture (template, methacrylic acid, a cross-linking agent and solvent), followed by in situ photopolymerisation. After extraction of the template molecule the rebinding is monitored by differential pulse voltammetry.[163, 164]

Sode and co-workers had mixed the imprinted particles with carbon paste to generate fructosyl valine specific electrodes which offers another relatively simple route towards electrochemical sensors based on amperometry.[165, 166]

Field effect transistors exploit a change in gate potential as a consequence of analyte binding to a selective matrix on the gate (MIPs, in this case), to produce a signal from the resulting change in output current of the device. Mosbach´s group had combined a field-effect device with a MIP. Thin polymer membranes containing MIP against L-phenylalanine anilide were prepared and

applied as sensing layer in field-effect transistors. The sensor could distinguish between the template (L-phenylalanine anilide) and related compounds (tyrosinanilide, phenylalaninol).[105]

Molecular recognition sites for the nucleotides adenosine 5′-monophosphate, guanosine 5′-monophosphate, cytosine 5′-monophosphate and uridine 5′-monophosphate was imprinted in an acrylamide-phenylboronic acid copolymer membrane. MIP membranes are assembled on the gate surface of an ISFET device by radical polymerisation. The ISFET response is due to the charging of the polymer membrane as a result of the formation of the nucleotide-boronate complex.[106]

Recently Willner et al described an imprinting technique for methyl viologen (MV^{2+}). Polyphenol is electropolymerised on a Au electrode to yield an imprinted film for Donor-acceptor interactions provide the driving force for the formation of the imprinted sites. The imprinted polymer reveals selectivity toward the association of MV^{2+}, and the polymer-bound MV^{2+} enables vectorial electron transfer between the electrode and redox label dissolved in the bulk electrolyte solution.[167]

1.4.4.4 Calorimetric sensing

Use of microcalorimeters to study MIP/analyte interactions started in 2001. Lin and co-workers made a thermodynamic investigations of MIP/2,4-D interactions using isothermal titration calorimetry. They postulated a binding mechanism from a thermodynamic point of view and explained the role of electrostatic, π-stacking and steric complementarity interactions between MIP and template.[168]

Wulff used isothermal titration calorimetry to study MIP/template interaction. The overall heats of rebinding of phenyl-β-D-mannopyranoside to a phenyl boronic acid containing MIP was endothermic.[169]

Microgels were imprinted using L-Boc-phenylalanine anilide (L-BFA) and studies of ITC revealed an exothermic enthalphy of rebinding. Significant differences were observed between the binding enthalpy of the original template L-BFA and those of D-BFA, L- Boc -phenylalanine, L- Boc-tryptophan, and L- Boc-tyrosine. [170]

Chou and co-workers prepared MIP films using lysozyme and cytochrome c as template. Microcalorimeter studies indicated that the MIPs were able to selectively recognise their natural template species.[171]

Apart from microcalorimeters, an enzyme thermistor can been used to study the MIP/analyte interaction. The first report on the combination of MIP with enzyme thermistor to follow a catalytic reaction was described by Lettau et al in 2006.[172] The authors claimed that the enzyme-like catalysis and antibody-like binding can be seen in a bifunctional MIP using a thermistor for the first time.

This thesis describes the integration of covalent MIPs with a thermistor for the first time which are detailed in the Results and Discussion section. The principle of measurement with an enzyme thermistor is described in the following section

1.5 Enzyme Thermistor

The technique of microcalorimetry was described to measure the heat accompanying a biochemical reaction which could be endothermic or exothermic. Most enzymatic reactions are usually associated with high enthalpy changes in the range of 20-100 KJ/mol (Table 4). The thermistor based calorimeters are popularly known as enzyme thermistors and were designed in the early 1970´s by Mosbach and Danielsson.[173, 174] Thermometric measurement is based on the sum of all enthalpy changes in a reaction mixture. The experimental set up is illustrated in Figure 7.

Table 4. Molar enthalpy changes of enzyme-catalysed reactions

Enzyme	Substrate	-ΔH (KJ/mol)
Catalase	Hydrogen peroxidase	100
Cholesterol oxidase	Cholesterol	53
Glucose oxidase	Glucose	80
Hexokinase	Glucose	28 (75)*
Lactate dehydrogenase	Sodium pyruvate	62
NADH dehydrogenase	NADH	225
β-Lactamase	Penicillin G	67 (115)*
Trypsin	Benzoyl-L-argininamide	29
Urease	Urea	61
Uricase	Urate	49

*The ΔH values were obtained in Tris buffer (protonation enthalpy -47.5 kJ/mol)

The total heat evolved in a reaction is proportional to its molar enthalpy

$Q = -n_p \Delta H$

Where Q = total heat, n_p = moles product and ΔH = molar enthalpy change.

It is also dependent on the heat capacity C_s of the system including the solvent

$Q = Cs \Delta T$

The temperature change ΔT recorded by the enzyme thermistor is thus dependent on the molar enthalpy change and on the heat capacity

$\Delta T = - n_p \Delta H / Cs$

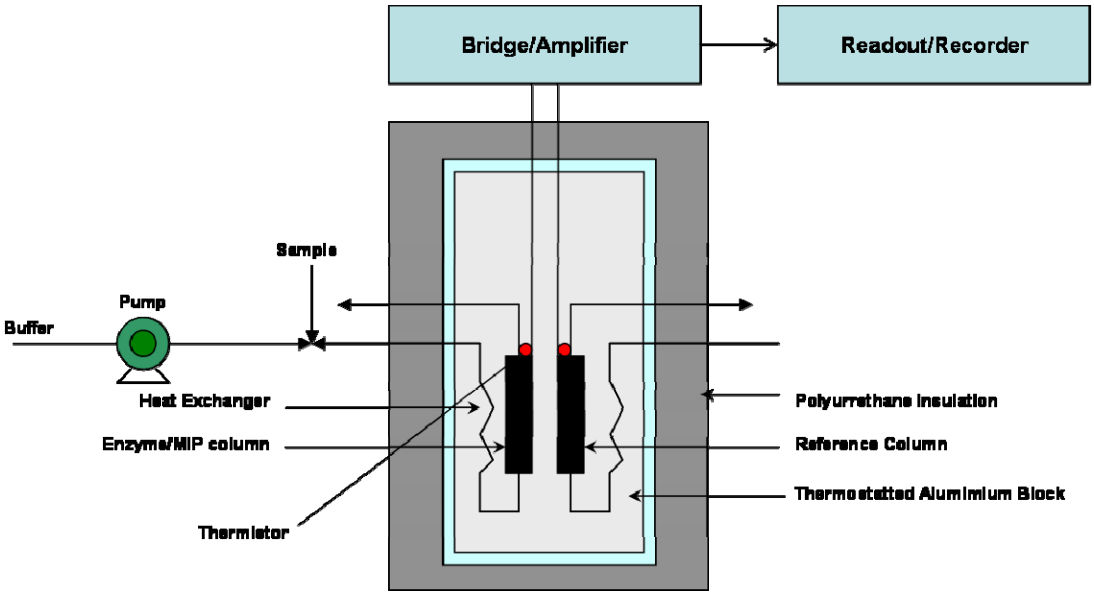

Figure 8. Experimental arrangement of an enzyme thermistor system

1.6 Boronic Acid for Saccharide Recognition

The molecular imprints described in this doctoral thesis employ boronic acid as a functional monomer, hence this section primarily describes the interaction of a boronic acid with saccharides in general. The primary interaction between boronic acids and a diol is covalent and involves the rapid and reversible formation of a cyclic boronic acid ester (Figure 8). The array of hydroxyl groups present on saccharides provides an ideal scaffold for these interactions and has led to the

development of boronic acid based MIPs for saccharides. Molecular imprinting of saccharides using boronic acid was pioneered by Wulff and his co-workers.

Figure 9. Boronate ester formation [175]

The association constant K_{eq} between various diols and phenyl boronic acid was quantified first by Lorand and Edwards and quite recently reevaluated by Springsteen and Wang at pH 7.4 and is denoted in Table 5. The association constant for the boronic acid–diol complex (K_{eq}) is found by titrating a boronic acid-ARS (Alizarin Red) solution with the target diol compound. This titration perturbs the equilibrium and therefore results in a change of the fluorescence intensity of the solution. The extent to which the diol moiety changes the fluorescence intensity depends on the binding affinity between boronic acid and diol. 1,2-dihydroxyphenyl containing compounds such as ARS and catechol, have very high affinities for PBA with K_{eq} values of 1300 and 830 M^{-1},

respectively. This is followed by sorbitol, fructose, tagatose, mannitol, sorbose, and 1,4-anhydroerythritol with K_{eq} values in the range of 110–370 M^{-1}. Compounds such as arabinose,

ribose, sialic acid, *cis*-1,2-cyclopentanediol, glucoronic acid, galactose, xylose, and mannose have moderate affinities for PBA with K_{eq} values in the range of 13–30 M^{-1}. D-glucose, diethyl tartrate, maltose, lactose, and sucrose only have weak affinities for PBA with K_{eq} values in the range of 0.67– 4.6 M^{-1}.

Table 5. Association constants (K_{eq}) calculated by Springsteen and Wang [175] with phenylboronic acid at pH 7.4, 100 mM phosphate buffer

Diol	K_{eq} (M^{-1})	Diol	K_{eq} (M^{-1})
Alizarin Red	1300	Sialic acid	21
Catechol	830	cis-1,2-Cyclopentane diol	20
D-sorbitol	370	Glucuronic acid	16
D-fructose	160	D-galactose	15
D-tagatose	130	D-xylose	14
D-mannitol	120	D-mannose	13
L-sorbose	120	D-glucose	4.6
1,4-Anhydroerythritol	110	Diethyl tartarate	3.7
D-erythronic-g-lactone	30	Maltose	3.5
L-arabinose	25	Lactose	1.6
D-ribose	24	Sucrose	0.67

1.7 Biological Significance of the Template used - Fructosyl Valine (Fru-Val)

This section describes the biological importance of the template used in this thesis for the synthsesis of molecular imprints. Quantification of glycated proteins is imperative owing to its vital role as a marker in clinical diagnosis.[176] The elevated blood sugar reacts non-enzymatically with either an N-terminal amino group or a lysyl ε-amino group of serum proteins and forms an unstable Schiff's base which rearranges to form a stable ketoamine termed as Amadori product. This is schematically represented in Figure 10. Glucose in the blood glycates the hemoglobin in red blood cells to glycated hemoglobin (HbA1c). As the lifespan of the red blood cell is approximately 120 days, the quantification of this Amadori product serves as an

important index in the diabetes control. Clinically desirable measurement ranges from 100–500 μM.

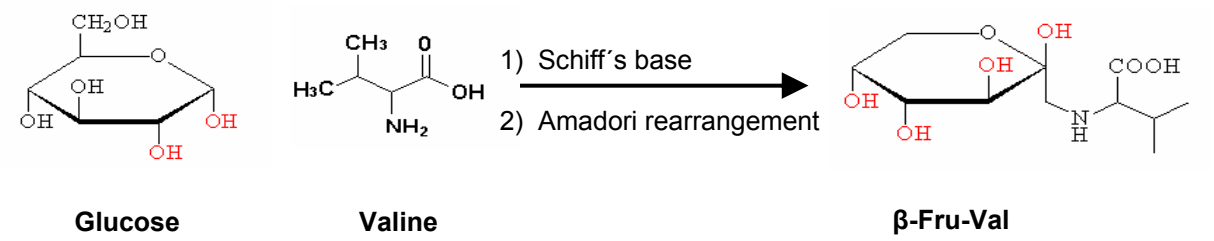

Figure 10. Reaction between glucose and valine to form fructosyl valine

Figure 11 represents the correlation between the mean blood glucose level and HbA1c. HbA1c is measured by ion-exchange chromatography, electrophoresis, immunochemical methods or by HPLC. Other long-lived proteins have been found to undergo glycation *in vivo*, such as lens crystallins, collagen, low-density lipoprotein, albumin and fibronectin. [177] An amperometric immunosensor based on antibodies as recognition element was reported.[178] In this work, membrane immobilised haptoglobin was used as an affinity matrix to bind hemoglobin and later enzyme labelled anti-HbA1c antibodies were then bound to HbA1c. In spite of the sensor's ability to measure in a clinically relevant range, the longer measurement times seem to be a disadvantage. Recently, there arose an increasing interest in developing sensors based on natural and artificial recognition elements for fructosyl-valine, the N-terminal Amadori product of HbA1c.

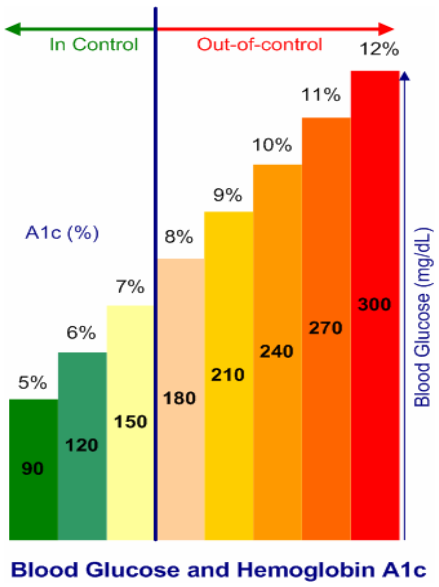

Figure 11. Correlation between HbA1c and mean blood glucose levels
(adapted from www.embeediagnostics.com)

2. OBJECTIVES

2 OBJECTIVES

In recent years, molecular imprinting has emerged as an attractive alternative to substitute natural biomolecules in sensors. Molecularly imprinted polymers (MIPs) are traditionally prepared using organic solvents during their synthesis. MIPs are generally hydrophobic and when required to operate in highly aqueous media give rise to non-specific binding. One approach to improve this situation is a systematic study of the influence of cross-linker as 75-80% of the MIP matrix is made up of cross-linkers. The approach aims at the reduction in the degree of non-specific binding in the obtained imprinted polymer.

One of the serious problems associated with the development of MIP sensors lies in the absence of a generic procedure for the transduction of the polymer-template binding event into an online detectable signal. To address this problem we aim to develop a new thermometric method for studying MIP/analyte interactions.

The aim of the thesis was to

1. develop covalently imprinted polymers based on phenylboronic acid diester for the detection of fructosyl valine and fructose and to compare them with pinacol imprinted polymers,

2. study the influence of cross-linking agent on MIP selectivity and to minimise the unspecific binding in batch binding studies,

3. develop a label-free thermometric method for studying MIP/analyte interactions,

4. investigate the cross-reactivity of MIP with glucose and disaccharides using a thermometric MIP sensor.

The approaches taken towards the selective recognition of the aforementioned targets, as well as the achievements of this doctoral research will be detailed in the Results and Discussion section.

3. MATERIALS AND METHODS

3 MATERIALS AND METHODS

3.1 Materials

3.1.1 Chemicals and biochemicals

Acetic acid	Roth, Germany
Acetone	Roth, Germany
Acetonitrile	Roth, Germany
2-Aminoethanesulfonic acid	Sigma, Germany
Anthrone	Fluka, Germany
2,2`-azobis(2-methylbutyronitile)	Fluka, Germany
Cellobiose	Sigma, Germany
Dioxane	Fluka, Germany
Ethanol	Fluka, Germany
Ethyleneglycol dimethacrylate	Fluka, Germany
D(-)-Fructose	Merck, Germany
D(+)-Glucose	Merck, Germany
Glucose oxidase	Sigma, Germany
Magnesium chloride hexahydrate	Fluka, Germany
D-Maltose	Serva Feinbiochemica, Germany
Methanol	Sigma-Aldrich, Germany
Nitrobenzene	Aldrich, Germany
Nitrotetrazolium blue chloride	Sigma, Germany
Peroxidase	Sigma, Germany
Pinacol	Aldrich, Germany
Pyridine	Roth, Germany
Sodium carbonate decahydrate	Merck, Germany
D-Sucrose	Serva Feinbiochemica, Germany
Sulfuric acid	Fluka, Germany
Tetramethylbenzidine dihydrochloride hydrate	Sigma, Germany
Trimethylolpropane trimethacrylate	Aldrich, Germany
2,4,6-Trinitrobenzenesulfonic acid	John Matthey GmbH,Germany
L (-)-Valine	Merck, Germany
4-Vinylphenyl boronic acid	Aldrich, Germany

3.1.2 Instruments

Ballmill S100	Retsch, Germany
Differential Scanning Calorimetry DSC 200	Netzsch, Germany
Enzyme Thermistor Model 9000	Lund University, Sweden
HPLC	Rainin, USA
FT-IR 6000	BioRad, Germany
Microtiter plate	Nunc, Denmark
Nitrogen sorption MT 3000	Micromeritics Tristar, Germany
Persistaltic pump Minipuls 3	Gilson, France
pH-Meter Calimatic F61	Knick, Germany
Scanning electron microscope Gemini LEO 1550	Carl Zeiss, Germany
Tabletop centrifuge 5415 D	Eppendorf, Germany
Thermogravimetry TG 209	Netzsch, Germany
UV spectrophotometer 160A	Shimadzu, Japan
YMC ODS-AM C18 column	YMC Inc., USA

3.1.3 Buffers and reagents

Buffers :

Carbonate buffer: Dissolve 28.6 g of $Na_2CO_3.10H_2O$ (MW = 286.14) in 1000 ml of water. Buffer will of course be of pH 11.4 at 28°C. The final concentration was 100 mmol/L. Add 100 ml of HPLC grade methanol and mix well.

Taurine buffer: Dissolve 6.2 g of taurine (2-Aminoethanesulfonic acid, Mr = 125.15) in 1000 ml of pure water. Adjust the pH to 8.8 using 10% NaOH. The final concentration was 50 mmol/L. Add 100 ml of HPLC grade MeOH and mix well.

Taurine buffer with $MgCl_2$: Dissolve 6.2 g of taurine and $MgCl_2.6H_2O$ (Mr = 203.31) in 1000 ml of pure water. Adjust the pH to 8.8 using NaOH using 10% NaOH. The final concentration was 50 mmol/L containing 20 mmol/L of magnesium chloride. Add 100 ml of HPLC grade MeOH and mix well.

Reagents :

Anthrone -Sulphuric acid reagent:

10 mg of anthrone, 10 mg of L-tryptophan were dissolved in 100 ml of 75% conc.H_2SO_4. The reagent is stable for 7 days when stored at 4 ^oC in an amber coloured bottle.

TNBS reagent:

10 mM TNBS was dissolved in water and used.

NBT reagent:

10 mM NBT was dissolved in 100 mM carbonate buffer, pH 11.4

3.2 Methods

3.2.1 Synthesis of template, functional monomer and template-functional monomer complex

3.2.1.1 Synthesis of fructosyl valine (template)

Fructosyl valine (Fru-Val) (Figure 11) was synthesised as previously reported [179]. A mixture of 18.8 g L-valine (0.16 mol) in 400 ml pyridine and 400 ml acetic acid was stirred for 30 min at room temperature. To this suspension 40 g (0.22 mol) of glucose were added, purged with nitrogen for 5 min and stirred for four days at room temperature.

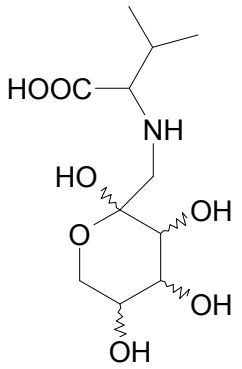

Figure 12. Structure of fructosyl valine

After four days the dark brown mixture was filtered and the solvent was evaporated. Recrystallisation from methanol resulted in a slightly yellowish amorphous product with a yield of 10 g (16 %). Purification was done using a preparative HPLC with YMC ODS-AM C18 column

with a Refractive index detector. A flow rate of 7 ml/min was used. The eluent used was water and it was efficient to separate glucose and valine from fructosyl valine. HPLC profiles were shown in Figure 12. Glucose was eluted first followed by valine and fructosyl valine. The collected Fru-Val fractions were combined and lyophilised to a colourless powder. The purity was checked by ^{1}H and ^{13}C NMR spectroscopy; all analytical data including the mass were in agreement with an earlier report.[179]

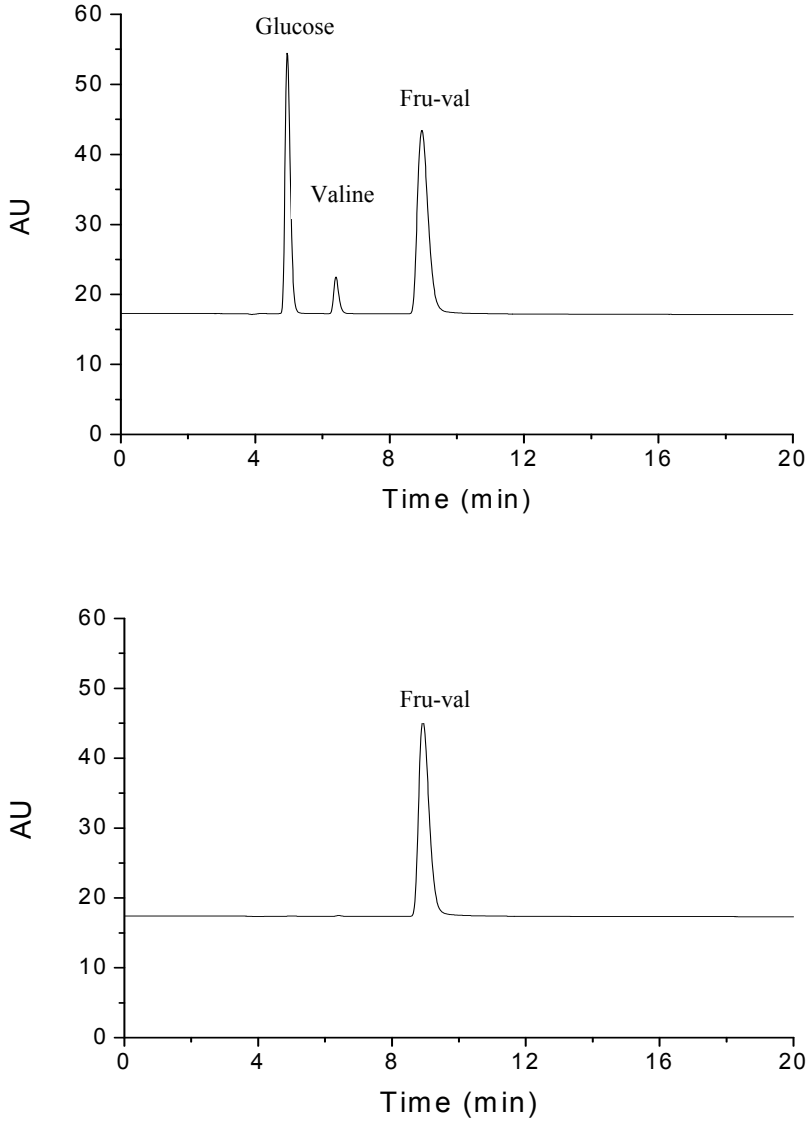

Figure 13. Analytical HPLC chromatograms of unpurified and purified fructosyl valine. Column used: YMC-AM, 4,6x250 mm, Mobile phase: Water, Flow rate: 1 ml/min, Detection: UV 200 nm

3.2.1.2 Synthesis of functional monomer (Vinyl Phenyl Boroxine)

Boroxine was synthesised according to an earlier report.[180] 5 g (0.033 mol) of 4-vinylphenyl boronic acid was dissolved in 300 ml of absolute toluene, and 100 µl of nitrobenzene was added. The mixture was heated to 137° C for 2 h by using a Dean-Strak trap. After the removal of water the reaction was stopped and cooled to room temperature and the remaining toluene was removed under reduced pressure. The product obtained was analysed by MS, NMR and IR.

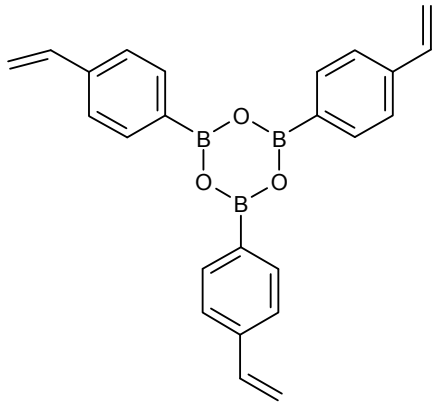

Figure 14. Structure of 4-vinyl phenyl boroxine

3.2.1.3 Synthesis of template-functional monomer complexes

Synthesis of *N*-[*β* -D-fructopyranosyl-(1)]-L-valine2,3; 4,5-bis-O- ((4-vinylphenyl)boronate)

The procedure reported for the synthesis of vinylphenyl boronic acid esters of sugars was applied to synthesise fructosyl valine–vinylphenyl boronic acid ester.[180] 1.53 g (5.5 mmol) of fructosyl valine was esterified with 1.45 g (3.7 mmol) of tris(4-vinylphenyl) boroxine in 300 ml dry dioxane containing 20 µl of nitrobenzene by azeotropic distillation. After complete reaction the remaining dioxane was removed under reduced pressure. In analogy the same procedure was applied for the synthesis of fructose and pinacol vinylphenyl boronic acid esters.

Synthesis of *β* -D-fructopyranose 2,3;4,5-bis-O- ((4-vinylphenyl)boronate)

In analogy the procedure was applied for the synthesis of *β* -D-fructopyranose 2,3;4,5-bis-O- (4-vinylphenyl)boronate); all analytical data were in agreement with the earlier work of Wulff.[180]

Synthesis of 4-vinylphenyl boronic acid pinacol esters

0.5 g (4 mmol) of pinacol was esterified with 2.9 g (3.7 mmol) of tris(4-vinylphenyl) boroxine in the same manner as described for fructose. After recrystallisation from hexane, 0.9 g (95%) of the desired boronate ester was obtained.

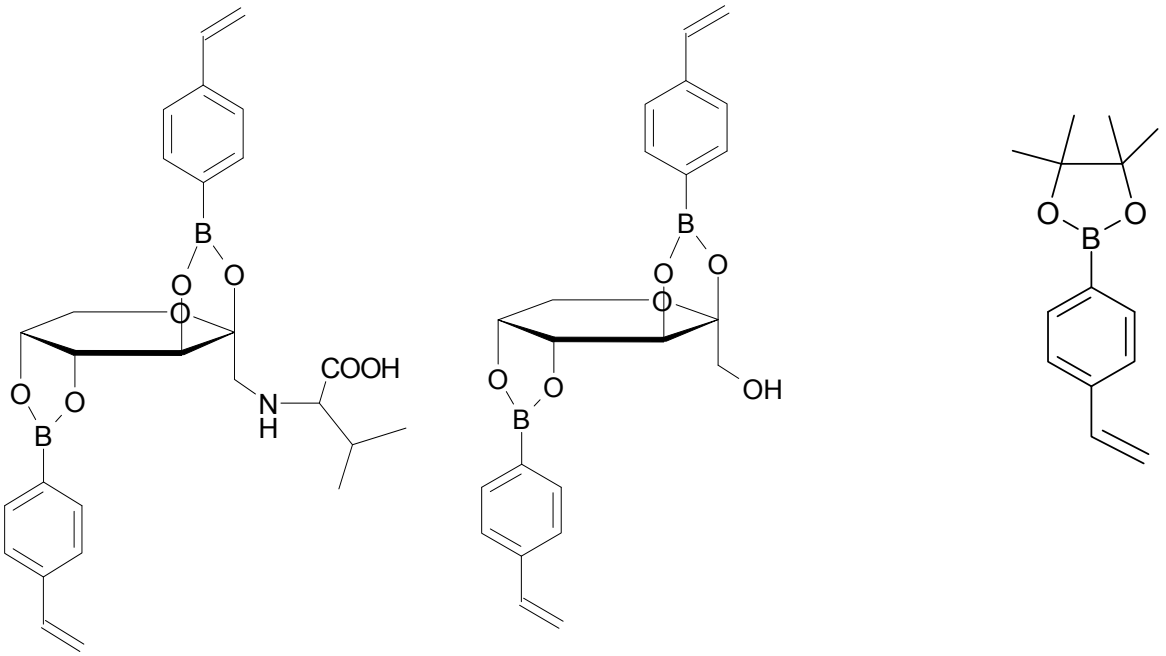

Figure 15. Structures of i) Fru-Val boronate ii) Fructose-boronate and iii) Pinacol-boronate esters

3.2.2 Preparation of molecularly imprinted polymers

1g (1.5 mmol) of Fru-Val vinylphenyl boronate ester was dissolved in 1 ml of toluene:acetonitrile (1:1). 8.54 ml (45.3 mmol) of ethylene glycol dimethacrylate (EDMA) and 0.65 g (3.98 mmol) of AIBN were added, mixed well and purged with nitrogen for 10 min. The polymerisation was initiated and carried out at 65ºC for 48 h. For the final curing of polymer the temperature was increased to 95ºC and kept constant for the next 24 h. The same procedure was applied for the synthesis of TRIM cross-linked polymers where 8.49 ml (26.5 mmol) of TRIM was used instead of EDMA. The bulk polymer monoliths were crushed in a mortar and ground in a ball mill (Retsch type S 100, Germany) for 10 min at 400 rpm and wet sieved (mesh 25 µm) using acetone to remove the fines. To remove the template, polymer particles were washed with 500 ml of water/methanol (1:1, v/v). Final washing was done with 100 ml methanol. The polymer particles were dried overnight at 50°C and then stored at room temperature. The preparation is schematically represented in Figure 15.

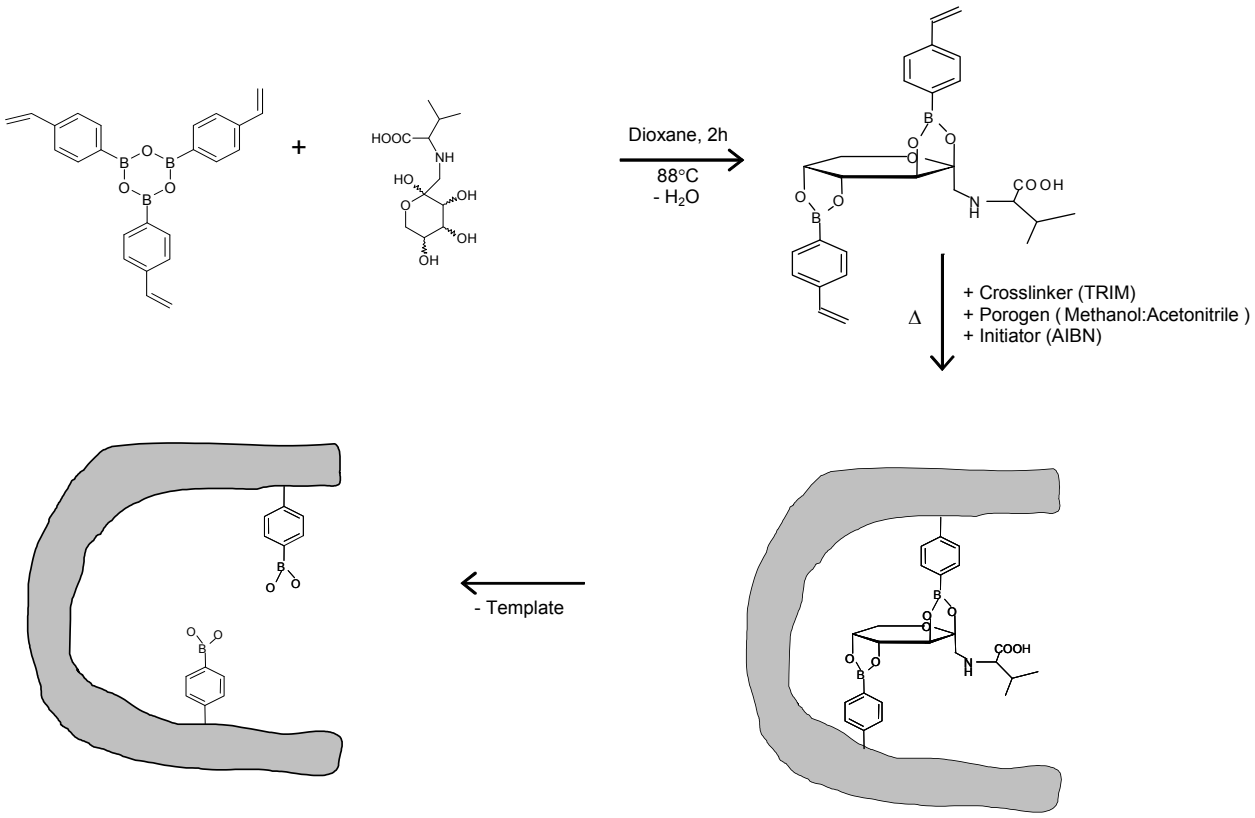

Figure 16. Molecular imprinting of fructosyl valine

3.2.3 Batch binding studies with fructosyl valine, fructose and valine

To 10 mg of polymer 1 ml of Fru-Val in 100 mM sodium carbonate buffer (pH 11.4) containing 10% methanol was added and incubated for 12h at 26ºC. After 12h the mixtures were centrifuged at 13000 rpm for 10 min and the supernatants were used to determine the unbound fructosyl valine. Therefore 500 µl of supernatant and 100 µl of 10 mM NBT in 100 mM sodium carbonate buffer (pH 11.4) were added, mixed well and incubated at 37ºC for 1h. The absorbance of the blue reaction product was measured at 530 nm with a Shimadzu 160-A UV-Vis spectrophotometer. The Fru-Val concentrations in the supernatants were calculated using a Fru-Val calibration curve as illustrated in Figure 16.

The binding of fructose and valine to the polymer was investigated in the same way. However, the unbound fructose and valine within the supernatants were quantified using the anthrone method[181] and TNBS method[182], respectively.

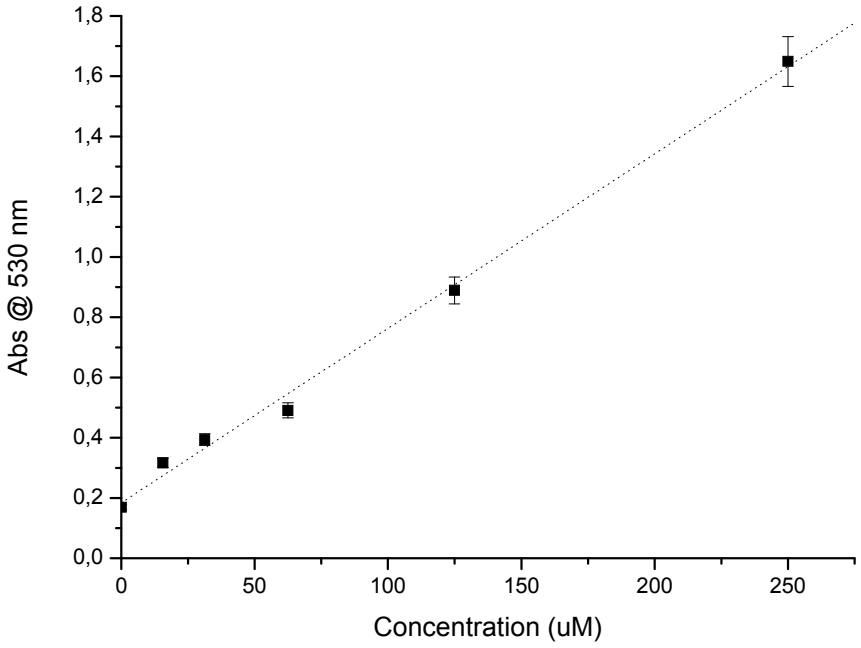

Figure 17. Calibration curve for fructosyl valine

3.2.4 Temperature stability experiments

MIP and control polymer of approximately 50 mg in 100 mM sodium carbonate buffer pH 11.4 containing 10% methanol were incubated separately at 50° and 80°C for 36 h. The batch rebinding study with Fru-Val was performed with the heat treated polymers. In another set MIP and control polymer were autoclaved at 121° C for 20 minutes. The binding studies were carried out with Fru-Val as described in section 2.4

3.2.5 Thermogravimetric analysis

Thermogravimetric analysis was carried out using a Netzsch TG 209 at the MPI of Colloids and Interfaces, Golm. The samples (~ 3 mg) were placed on a heating block, which was heated with a heating rate of 20 K min^{-1} under N_2 atmosphere.

3.2.6 Scanning electron microscopy

Scanning electron microscopy (SEM) images were recorded with a Gemini Leo 1550 instrument (Carl Zeiss, Oberkochen, Germany) at an operating voltage of 3 keV at the MPI of Colloids and Interfaces, Golm.

3.2.7 Nitrogen sorption measurements - BET analysis

Nitrogen adsorption and desorption measurements of MIPs were performed on a Micrometrics Tristar 3000 automatic adsorption instrument at the MPI of Colloids and Interfaces, Golm. Before measurements, 100-150 mg of the samples were heated at 60ºC under vacuum (10^{-5} Pa) for at least 12 h. The analysis was carried out at liquid nitrogen temperature (-196 ºC). The specific surface area was calculated by applying the BET method.

3.2.8 MIP-Thermistor set-up and measurements

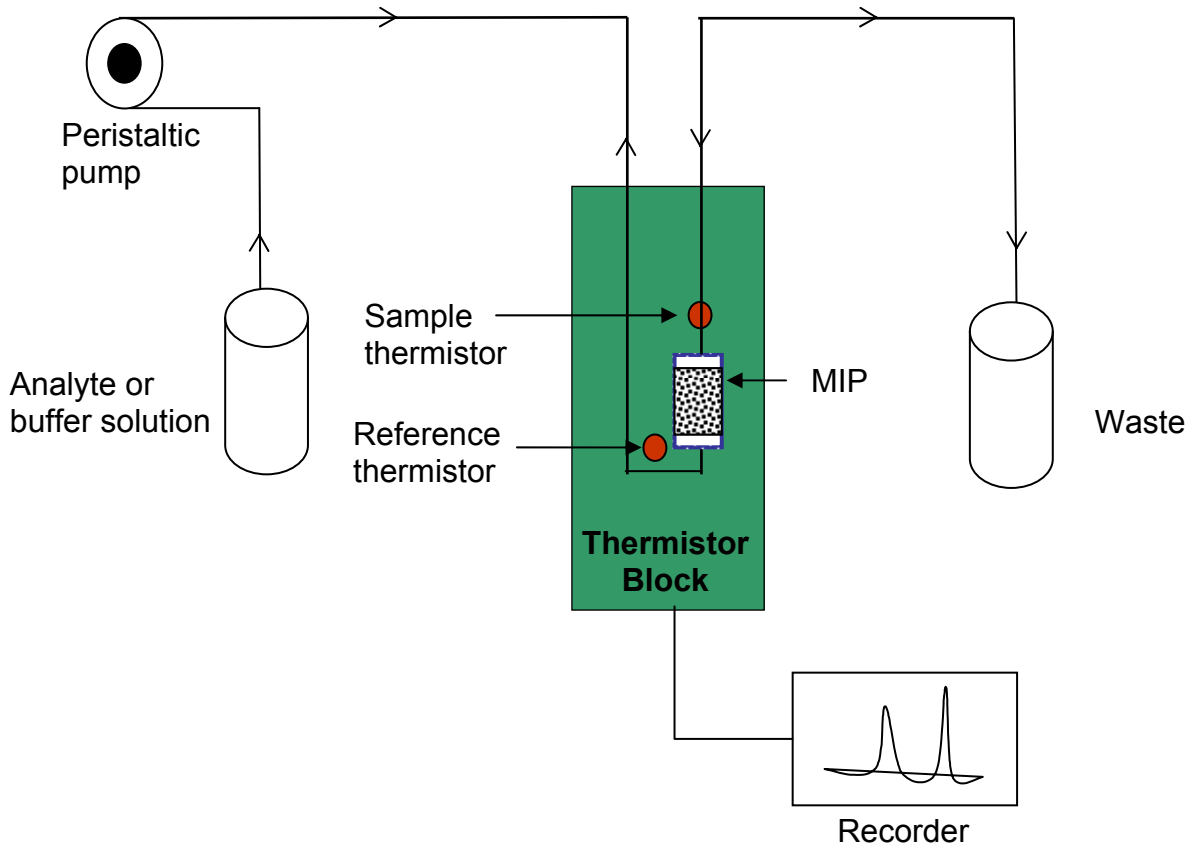

Figure 18. MIP-Thermistor setup

The set-up for the MIP-thermistor is shown in Figure 17. It consists of a peristaltic pump (Minipuls 3, Gilson, France), an injection valve (Type Eva-selector from Eppendorf, Germany), a sensor device, a Wheatstone bridge equipped with a chopper-stabilised amplifier and a recorder.

During the operation, the sensor was kept in an aluminium calorimeter block insulated with polyurethane foam to minimise interferences from changes in the environmental temperature. The signal generated due to the binding of analyte to the MIP column was registered with the Wheatstone bridge. At maximum sensitivity this bridge produces a 100 mV change in the recorder signal for a temperature change of 0.001 °C. For the test of polymers a 500µl reactor containing 100 mg of MIP or control polymer was used. A constant flow rate of 1 ml/min was used in all experiments. The analytes were pumped first for 10 minutes followed by buffer for the next 10 minutes. [183]

3.2.9 Polarimeter measurements

Polarimeter experiments were carried out in a JASCO P-1020 polarimeter. The analyte was dissolved either in water or in 100 mM carbonate buffer, pH 11.4 containing 10% methanol and filled in polarimeter cell and measured at 589 nm.

3.2.10 NMR measurements

NMR experiments were recorded at 300 MHz on a Bruker Avance 300 spectrometer. Uniformly labelled ^{13}C fructose and glucose were dissolved in deuterated water or in in 85% D_2O/10% MeOD/5% ND_3, pH 11 and stored at room temperature for 10 days to attain equilibrium before measuremenets. The NMR spectra of fructose and glucose is shown in Appendix (Chapter 7).

4 RESULTS & DISCUSSION

4.1 Batch Binding Studies with Molecularly Imprinted Polymers against Fructosyl Valine

4.1.1 Introduction

In this work, fructosyl valine – vinyl phenyl boronate diester was synthesised and subsequently polymerised with an excess of di- and tri-functional cross-linkers namely ethyleneglycol dimethacrylate (EDMA) and trimethylolpropane trimethacrylate (TRIM), respectively. This study is the first example illustrating the influence of cross-linking agents on molecular recognition of a glycated amino acid. Fructosyl-valine (Fru-Val) binding polymers were generated by covalent imprinting (Figure 15). Control polymers were generated by using the fructose and pinacol (2, 3-dimethyl-2,3-butanediol) as templates.

4.1.2 Batch binding studies - media optimisation

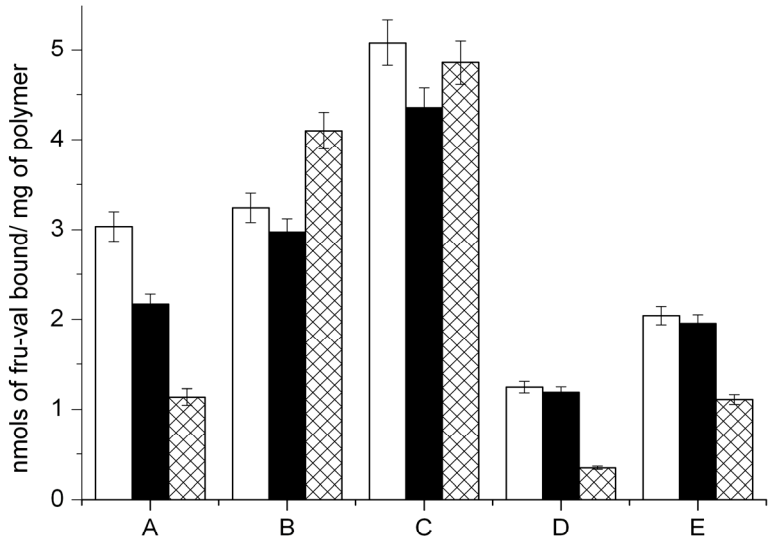

Figure 19. Fru-Val bound per polymer weight for different buffer composition on TRIM cross-linked polymers. Fru-Val imprinted polymer (white); Fructose imprinted polymer (black); Pinacol imprinted polymer (cross-bars). 10 mg of TRIM cross-linked polymer + 0.1 ml of methanol + 1 ml of 0.1 mM Fru-Val in buffer A to E; 12 h; 26ºC

A 10% methanol + 90% 100 mM sodium carbonate, pH 11.4;
B 25% methanol + 75% 100 mM sodium carbonate, pH 11.4;
C 50% methanol + 50% 100 mM sodium carbonate, pH 11.4;
D 10% methanol + 90% 50 mM taurine/ NaOH, 20 mM $MgCl_2$ pH 8.8;
E 10% methanol + 90% 50 mM taurine/ NaOH, pH 8.8

To find out the conditions under which the binding of Fru-Val to the MIP(Fru-Val) is much higher than the binding to the MIP(Frc) and control polymer the pH and the methanol concentration of the binding buffer were varied. Since most of the phenyl boronic acids have pK_a values in the range of 4.5-8.8,[184] buffers with pH values of 8.8 and 11.4 were chosen. Figure 19 shows, as expected, a higher Fru-Val binding at pH 11.4. With 10% methanol + 90% 100 mM sodium carbonate buffer, pH 11.4, the highest difference in binding between imprinted and control polymer was obtained. Under this condition, the binding of Fru-Val to the MIP(Fru-Val) was 1.4 fold higher than to the MIP(Frc) and 2.7 fold higher than to the control polymer.

By increasing the methanol content up to 50% in the media this difference is diminished. Methanol mediates the interaction between the hydrophilic template and the hydrophobic backbone of the polymer. Even though an increase in the methanol content enhances the binding a striking decrease in the specificity was observed. Hence 10% methanol in the buffer is optimal for selective binding of the template.

4.1.3 Influence of cross-linking agent on binding

Since the nature of the cross-linking agent has a great influence on the specificity of a MIP[185], molecularly imprinted polymers were prepared in parallel with two different cross-linkers. Therefore, both EDMA and TRIM were chosen as cross-linkers in the current study which compares for the first time the influence of two cross-linking agents on the specificity of MIPs for a glycated amino acid. The structure of cross-linkers is shown in Figure 20.

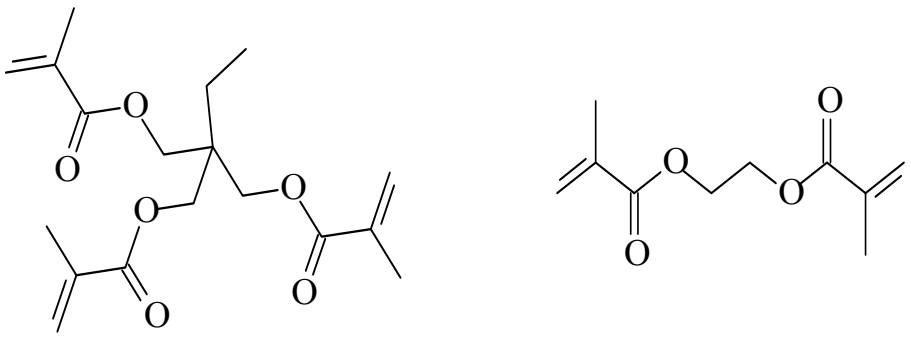

Figure 20. Structure of cross-linkers used. TRIM (left) and EDMA (right)

The pore size distribution and pore volume of the polymer particles was measured by nitrogen adsorption and desorption. The average pore diameter and pore volume for TRIM cross-linked polymers were 149 Å and 0.040 ml/g respectively, in comparison to EDMA cross-linked polymers with 33 Å and 0.007 ml/g, respectively. Thus, polymers prepared with TRIM have a macroporous structure which would enhance the mass transport as compared with the counterpart [186]. The polymer morphology of TRIM and EDMA cross-linked polymers analysed by SEM shows that the particles are highly granular in nature with irregular particle size ranging from 25-50 μm (Figure 21).

MIP(Fru-Val)-EDMA MIP(Fru-Val)-TRIM

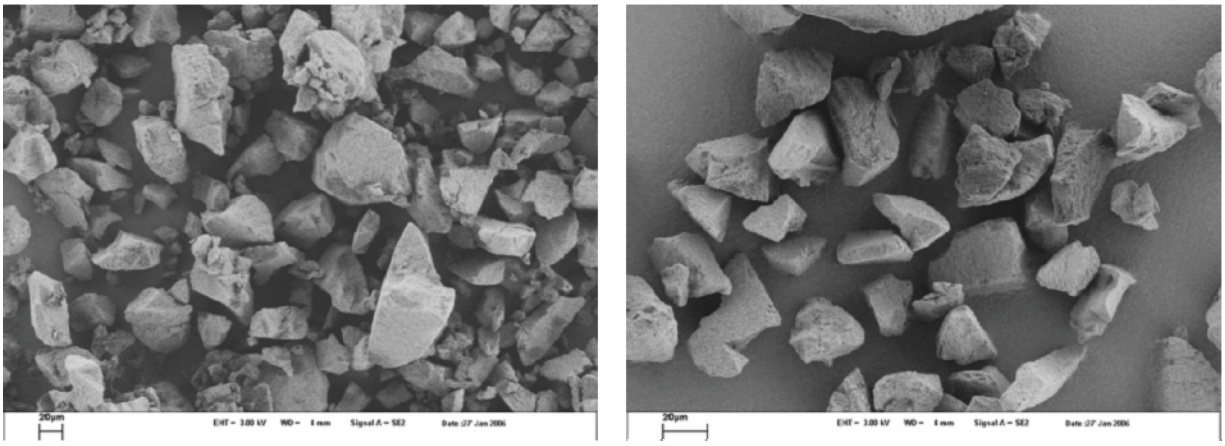

Control-EDMA Control-TRIM

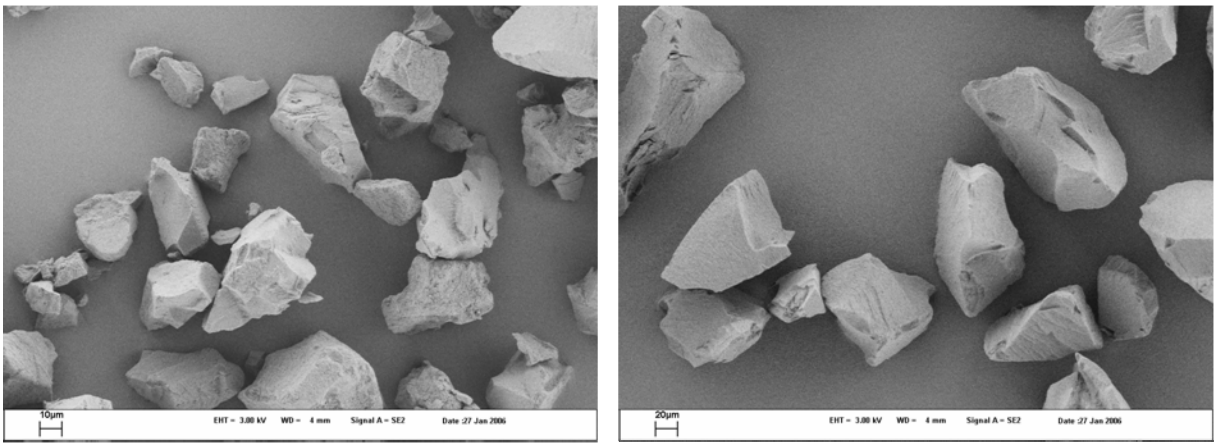

Figure 21. Scanning electron microscopy (SEM) images of MIP(Fru-Val) and control polymer cross-linked with EDMA (left) and TRIM (right)

Earlier studies reported that for sugar templates EDMA - a cross-linker with two vinyl groups- is superior to divinylbenzene (DVB).[185] This is attributed to the fact that the EDMA which is

non-aromatic and more polar than the aromatic DVB results in a more flexible network which eases the template removal. In contrast, for selective recognition of theophylline, DVB was more suitable than EDMA, due to the fact that the hydrophobic nature of DVB shows lower unspecific binding[187]. TRIM contains three vinyl groups and has been shown to be an ideal cross-linker in comparison with DVB and EDMA for imprinting penicillin[188] , R-phenylbutyric acid[189] and protected dipeptides[186].

To evaluate whether EDMA or TRIM cross-linked MIPs show better selectivities for Fru-Val, the binding of Fru-Val to the polymers synthesised with both cross-linkers was investigated. In general the EDMA cross-linked polymers showed higher Fru-Val binding but less selectivities. Both pinacol imprinted polymers bound Fru-Val unspecifically but, as expected, to a less extent than the other MIPs. The fructose imprinted and Fru-Val imprinted polymers showed a different binding behavior to Fru-Val depending on the cross-linker used. Whereas the binding of Fru-Val to the EDMA cross-linked polymers is similar, the binding to the TRIM cross-linked polymer differs.

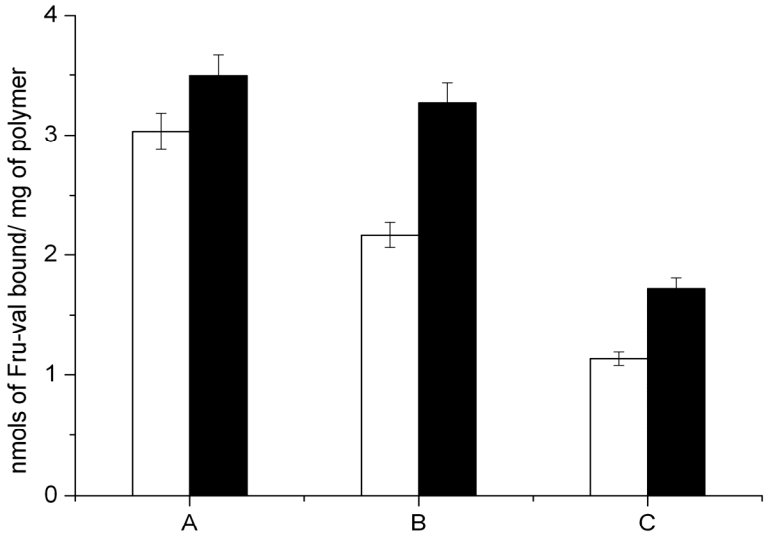

Figure 22. Fru-Val bound per polymer weight for TRIM and EDMA cross-linked MIPs A, Fru-Val imprinted polymer; B, Fructose imprinted polymer; C, Pinacol imprinted polymer; TRIM cross-linked (white); EDMA cross-linked (black); 10 mg polymer + 0.1 ml of methanol + 1 ml of 0.1 mM Fru-Val in 10% methanol+ 90% 100 mM sodium carbonate, pH 11.4; 12 h; 26ºC

When 100 µM Fru-Val was applied the TRIM cross-linked MIP(Fru-Val) binds 1.4 and 2.7 fold more Fru-Val than the MIP(Frc) and control polymer, respectively, whereas the EDMA cross-

linked MIP(Fru-Val) binds only 1.1 and 2 fold more Fru-Val than the MIP(Frc) and control polymer, respectively (Figure 22). Obviously with TRIM as cross-linker a better complementarity to the template is obtained than with EDMA making TRIM a better cross-linker for fructosyl valine imprinting.

That TRIM cross-linked MIPs can exhibit better selectivities than EDMA cross-linked polymers is in accordance to the work of Kempe[20]. She compared both cross-linking agents for the generation of non-covalently imprinted polymers for protected amino acids and dipeptides and found better separation and resolution factors for the TRIM cross-linked polymers. Unless otherwise stated further studies were carried out with the polymers prepared with TRIM.

4.1.4 Equilibration time

The equilibrium experiment was performed for 12 h. In this way the kinetic effects can be avoided and equilibrium conditions can be expected. Binding studies carried out at different time intervals showed that after 3 h equilibrium was reached (Figure 23).

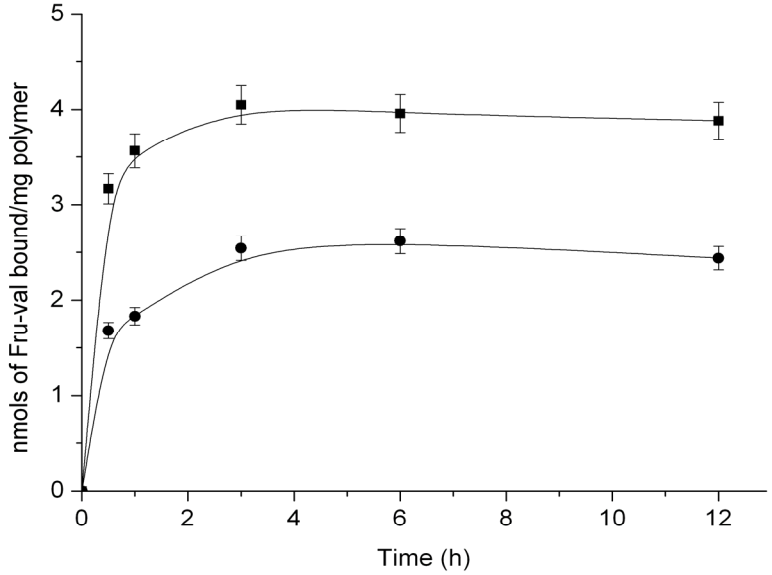

Figure 23. Time dependence for Fru-Val binding to Fru-Val imprinted (squares) and pinacol imprinted (circles) polymers. 10 mg TRIM cross-linked polymer + 0.1 ml of methanol + 1 ml of 0.1 mM Fru-Val in 10% methanol+ 90% 100 mM sodium carbonate, pH 11.4; 0- 12 h; 26ºC.

4.1.5 Concentration dependence

Figure 24 shows the concentration dependence of Fru-Val binding for MIP(Fru-Val) and control polymer, respectively. For both polymers a similar Fru-Val binding was observed at saturating Fru-Val concentrations (> 5mM) with a binding capacity of about 40 nmol Fru-Val/ mg MIP. The theoretical capacity of the polymer would be 300 nmol/ mg by taking into consideration that all template molecules during the polymerisation process resulted in binding pockets. The difference in the experimental and theoretical capacities is attributed to the fact that not all template molecules used resulted in the formation of accessible binding pockets. At 0.2 mM the "imprinting factor", i.e. the ratio of binding to the MIP(Fru-Val) and the control polymer, was ~4.5, whereas this ratio was reduced to ~1.2 at saturation concentrations. It can be concluded that the number of binding sites is similar but the affinity of the MIP(Fru-Val) is higher. Evaluation of batch binding studies reveals the half saturation values of 0.4 mM for MIP(Frc) and 1 mM for control polymer.

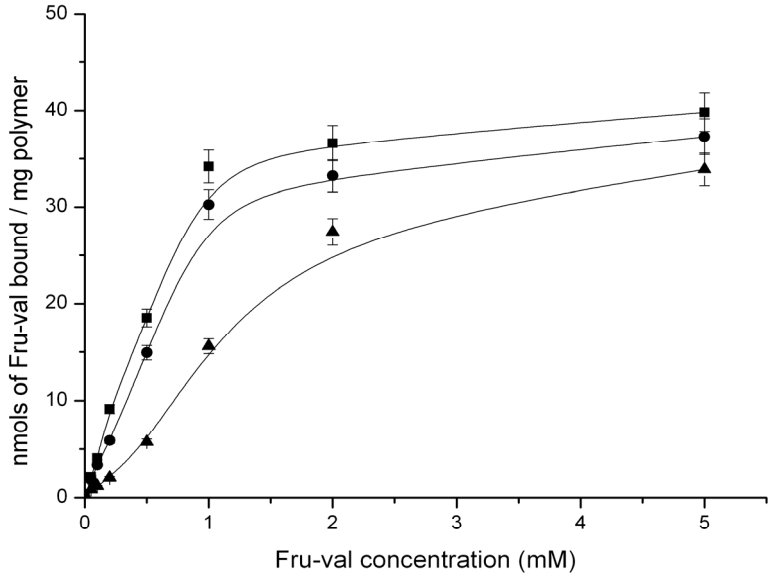

Figure 24. Concentration dependency for Fru-Val binding to Fru-Val imprinted (squares), fructose imprinted (circles) and pinacol imprinted (triangles) polymers. 10 mg TRIM cross-linked polymer + 0.1 ml of methanol + 1 ml of 0-5 mM Fru-Val in 10% methanol+ 90% 100 mM sodium carbonate, pH 11.4; 12 h; 26ºC

4.1.6 Cross-reactivity

In order to characterise the specificity of the imprinted polymers, the binding of Fru-Val, fructose and valine was compared (Figure 25). As expected, the MIP(Fru-Val) has a higher affinity for Fru-Val (1.8 fold) than for fructose, and the MIP(Frc) has a slightly higher affinity for fructose (1.2 fold) than for Fru-Val. These results confirm the imprinting effect. Valine shows only a very low binding to the polymers, which is important for future applications to distinguish between glycated and non-glycated hemoglobin.

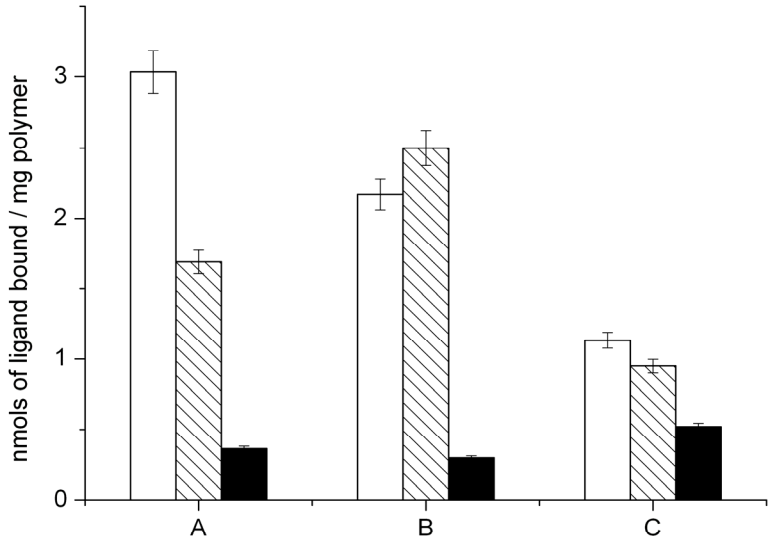

Figure 25. Binding capacities (nmoles / mg) for Fru-Val imprinted (A), fructose imprinted (B) and pinacol imprinted (C) polymers. Ligands: 0.1 mM Fru-Val (white), 0.1 mM fructose (slant lines), 1 mM valine (black). 10 mg TRIM cross-linked polymer + 0.1 ml of methanol + 1 ml ligand in 10% methanol+ 90% 100 mM sodium carbonate, pH 11.4; 12 h; 26ºC

4.1.7 MIP stability

The imprinted and control polymer were tested for their binding ability after heating the polymers for 36 h in buffer to 50°, 80 °C and for 20 min to 121°C. There was no loss in binding activity until 80°C. However at 121°C a decrease was observed (Table 6). The loss of recognition might be due to the deboronation reaction taking place at higher temperatures. It was shown in an earlier report that the incubation of phenyl boronic acid at 100°C in 0.1 N NaOH for 8 h leads to deboronation.[190] This effect will not influence the application of MIP in binding assays where the binding is carried out at RT.

Table 6. Binding activity of imprinted polymers for 0.1 mM Fru-Val after heating in buffer

Temperature	Fru-Val imprinted polymer (nmol Fru-Val/ mg)	Pinacol imprinted polymer (nmol Fru-Val/ mg)
26°C (36 h)	3.07	1.27
50°C (36 h)	2.99	1.30
80°C (36 h)	3.21	1.25
121°C (20 min)	1.41	1.11

Thermogravimetric analysis indicates that TRIM cross-linked MIPs were stable up to 250°C. No polymer glass transition was observed in the DSC analysis of MIPs in the temperature range of –20°C to 200°C which indicates a high stability of the polymer matrices.

4.1.8 Conclusions

Covalent imprinting is suitable for the generation of fructosyl valine binding polymers. The application of a covalent Fru-Val-boronic acid ester as template resulted in polymers which can distinguish between fructosyl valine, and the control substances fructose and pinacol. With respect to specificity the advantage of the cross-linker TRIM over EDMA was demonstrated. The optimal binding for fructosyl valine was found to occur at pH 11.4. The Fru-Val imprinted polymer has a higher affinity for Fru-Val than for fructose and valine. The MIP matrices are stable at higher temperatures and the recognition is unaltered until 80°C. Since the functional group of the polymers targets the sugar part of Fru-Val the developed imprinting technique used should also be applicable for the development of MIPs against other glycated amino acids and peptides.

4.2 Thermometric MIP Sensor for Fructosyl Valine

4.2.1 Introduction

Although the imprinting procedure appears to be attractive, simple and straight-forward bioanalytical applications of MIPs are still limited because they have low yields of high affinity binding sites. MIP/analyte interaction has originally been evaluated by batch binding procedures measuring the uptake of the analyte and by HPLC analysis. Label-free measurements are based on QCM, field effect transistors, surface plasmon resonance, and, quite recently, on calorimetry. [31, 106, 108, 123, 130, 151, 155, 156, 160, 165, 168-170, 172, 191-198]. The aim of the present study was the label-free interaction analysis of phenylboronic acid-containing MIPs with their respective diols – fructosyl valine, fructose and pinacol - by using a thermistor. Furthermore thermometric analysis was used to investigate the cross-reactivity and shape selectivity.

4.2.2 Short term interaction of Fru-Val with MIP and control polymer

To investigate whether the MIP/analyte interactions can directly be followed MIP(Fru-Val) or control polymer was filled in the reactor and thermometric measurements were performed in a thermistor.

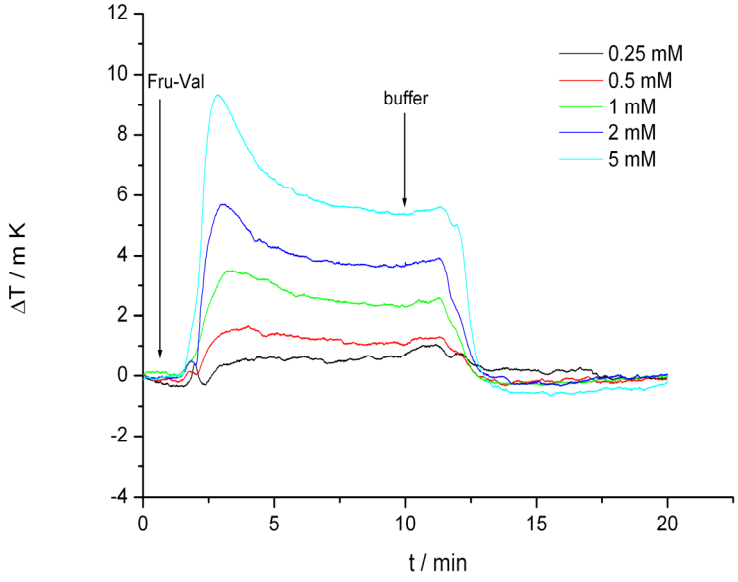

Figure 26. Time dependent thermogram for the interaction of Fru-Val with the MIP (Fru-Val) in a thermistor. Fru-Val flow at 0 min and start of washing at 10 min with 100 mM sodium carbonate (pH 11.4)/10% methanol

The specific interaction of Fru-Val is due to the formation of reversible covalent bonds of boronic acid entities with the diols within the micro cavities of MIP(Fru-Val). This binding event generates an exothermic peak signal followed by an almost steady state signal (Figure 26). Bulgrin et al have reported for the binding of boronic acid to other diols/carbohydrates an enthalphy of -11 to -21 kJ/mol.[199] Moreover our observation is in agreement with batch calorimetric measurements of esterfication of phenylboronic acid and propandiol in acetonitrile solution which gave an exothermic value of -17.5 kJ/mol.[200] However, the measured enthalpy for the binding of phenyl-β-D-mannopyranoside to a phenyl boronic acid containing MIP is endothermic.[169]

When the flow is changed from the analyte (Fru-Val) to the neat buffer (after 10 min) the signal decreases down to the baseline. However, no endogenous peak is visible, which would reflect the desorption process of bound Fru-Val from the binding sites. In contrast to the MIP(Fru-Val) the non-specific interaction with the control polymer generates negligible temperature changes (Figure 27).

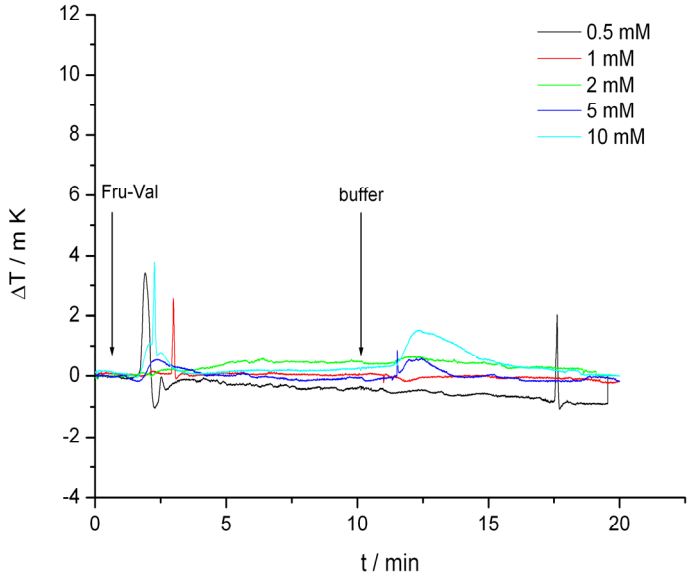

Figure 27. Time dependent thermogram for the interaction of Fru-Val with the control (pinacol imprinted) in a thermistor. Fru-Val flow at 0 min and start of washing at 10 min with 100 mM sodium carbonate (pH 11.4)/10% methanol

4.2.3 Concentration dependence of Fru-Val binding

The adsorption peak signals (at 2.5 min) plotted against the concentration of Fru-Val generates binding curves for the interaction of Fru-Val to the MIP(Fru-Val) and the control polymer (Figure 28). It can be seen that even at 5mM Fru-Val the maximal heat change is not yet reached.

Unfortunately, data for higher concentrations could not be obtained, since a great fluctuation in the temperature changes took place, obviously due to the higher viscosity of the media.

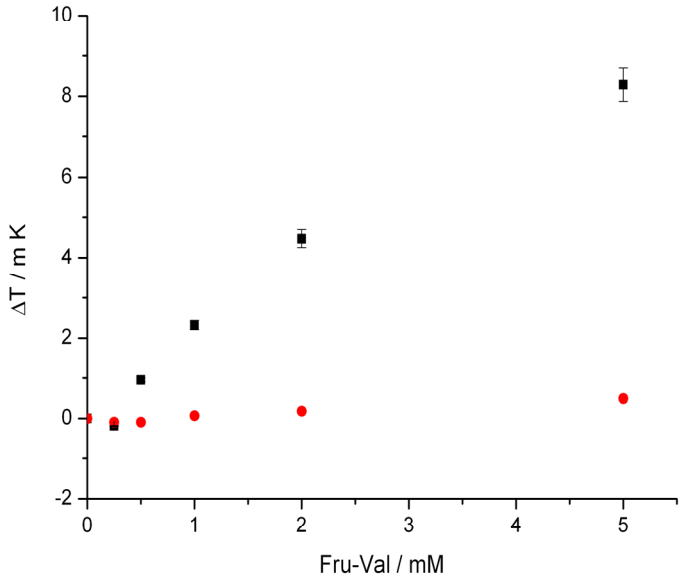

Figure 28. Concentration dependency for Fru-Val binding. Temperature changes at peak position (2.5 min) for different Fru-Val concentration for MIP (squares) and control polymer (circles)

Binding to the control polymer results in considerably smaller temperature changes. Thus a very clear difference in binding behavior between the polymers is seen. Earlier batch binding studies have given an "imprinting factor" (IF) of 1.4 - i.e. the ratio of binding at equilibrium to the MIP(Fru-Val) and to the control polymer, whereas a ratio of the respective signals of 41 was obtained in the flow-through mode. The big difference between the enthalpies for specific covalent binding of the carbohydrate to the boronic acids and non-specific adsorption to the polymer matrix may explain the higher "apparent imprinting factor". On the other hand binding studies in the batch do not discriminate the non-specific adsorption because the concentration change is the sum of both specific and non-specific interactions. Table 7 lists the binding characteristics of MIP(Fru-Val)

Table 7. Binding characteristics of fructosyl valine imprinted polymer

MIP	Fru-Val binding capacity (nmol / mg)	Half saturation value (mM)	IF* Batch	IF ** Thermometric
MIP (Fru-Val)	40	0.4 mM	1.4	41
Control	30	1 mM		

IF* is the ratio of Fru-Val binding to MIP(Fru-Val) to control polymer at 5 mM
IF** is the ratio of heat generation due to Fru-Val binding to MIP(Fru-Val) to control polymer at 5 mM

Batch binding procedures based on the incubation of the MIP(Fru-Val) with the analyte revealed that the equilibrium is reached within almost 2 h whereas the binding in the present flow-through set-up, with an average residence time of 0.1 min, does not at all approach equilibrium. From the short term interaction of Fru-Val to MIP(Fru-val) it can be concluded that after 10 min almost 20% of the equilibrium value is attained and only a very small fraction of the binding cavities are occupied.

As illustrated in Figure 26 the steady state signal for the MIP(Fru-val) depends on the Fru-Val concentrations. In our earlier investigations such a steady state heat signal has been typical for catalytic reactions. [172] In the case of the control polymer this effect has not been detected, so it can be concluded that it arises only from the imprinting.

MIPs possess a certain ratio of perfect and less perfect binding sites, which leads to different binding kinetics. To figure out whether the observed steady state temperature signal is attributed to a slow Fru-Val binding the temperature changes at steady state were monitored for several hours. We observed a stable signal over a period of 4 h. Colorimetric measurements of Fru-Val concentrations indicate that the concentration of Fru-Val was lowered by 10% in the effluent. The amount of Fru-Val which is consumed within 4 h exceeds the theoretical binding capacity of the reactor by a factor of almost 4. Therefore the slow binding will not explain the long term steady state heat signal.

4.2.4 Interaction of Fru-Val with MIP in a loop

In order to characterise the heat generation up to the establishment of equilibrium we constructed an experimental setup comparable with the batch binding studies. For this reason 10 ml of the Fru-Val solution were pumped in a closed loop through the MIP reactor containing 100 mg of the polymer. In this way in both configurations the same volume ratio of the MIP to the substrate was used.

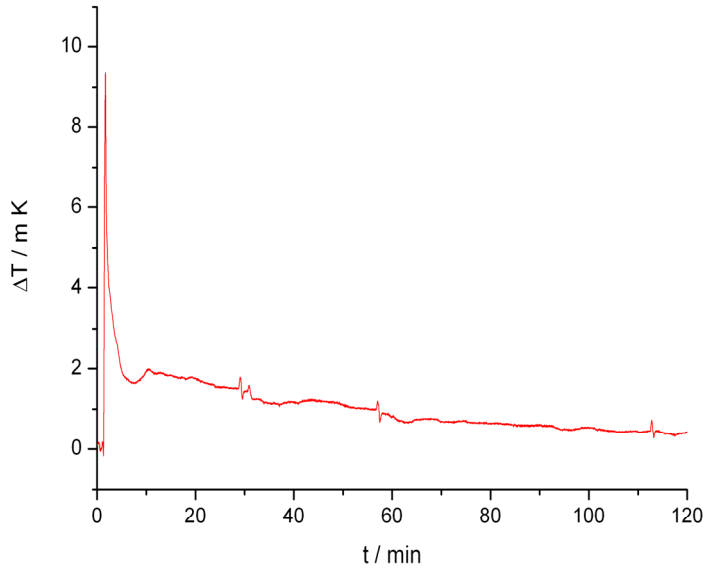

Figure 29. Time dependent thermogram for 5 mM Fru-Val pumped continuously in a loop through the MIP thermistor

The flow of a 5 mM Fru-Val solution through the MIP reactor generated an initial peak signal which was followed by a slowly decaying signal (Figure 29). Two hours after the start the measuring curve reached the base line, indicating the establishment of equilibrium. Switching the stream to the neat buffer resulted in an endothermic signal which reflects the desorption of the Fru-Val from the polymer.

Measurement of the Fru-Val concentrations during the loop experiment revealed that almost 5 µmol have been consumed within the first 60 min. The concentration of the analyte remains almost unchanged at the value of 4.5 mM over the next 180 min. The amount of Fru-Val which is consumed reflects almost 15% of the content of boronic acid moieties. These results, i.e., the time to reach the equilibrium and the binding capacity of the MIP(Fru-Val), are in agreement with the batch binding studies. The thermistor signal parallels the progress of adsorption, consumption and subsequent desorption.

It is very interesting to note that long term MIP/analyte interactions yield a stable heat signal, whereas the interactions in the loop mode the signal decrease down to the baseline. The reason might be that in long term the fresh analyte is continuously delivered which causes stable heat signals whereas in loop mode the conversion of the analyte reaches equilibrium. [201]

4.2.5 Short term interaction of pinacol with MIP and control polymer

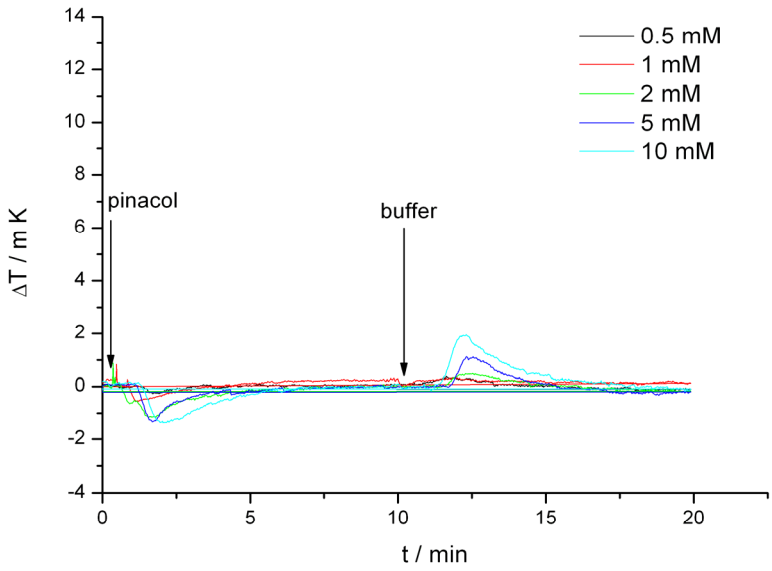

Figure 30. Time dependent thermogram for the interaction of pinacol with the control polymer (pinacol imprinted) in a thermistor. Pinacol flow at 0 min and start of washing at 10 min with 100 mM sodium carbonate (pH 11.4)/10% methanol

Pinacol was used as a template to generate the control polymer and is expected to bind to the functional group (boronic acid) of the polymers. However, the interaction of pinacol with the MIP(Fru-Val) generates very small heat changes (Figure 30).

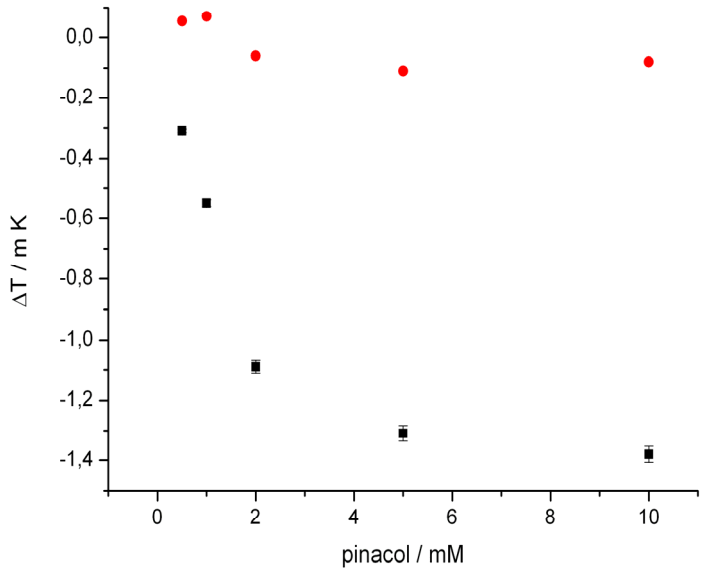

Figure 31. Concentration dependency for pinacol binding. Temperature changes at peak position (2.5 min) for different pinacol concentrations for control polymer (squares) and MIP (circles)

The binding of pinacol to the control polymer leads to an endothermic peak which might be associated with the adsorption of pinacol. When the flow is changed from the pinacol containing buffer to the neat buffer desorption of pinacol is clearly seen as a heat signal in an opposite direction. It should be considered that apart from enthalpy contributions due to the selective esterfication there are also enthalpy changes originating from solvation/desolvation of the analytes or local movements of polymer chains close to the binding sites.[169] The small endothermic signals of pinacol binding to the control polymer reflect a negligible contribution of the esterification to the overall process. Earlier, Shinkai and co-workers have reported a low binding of pinacol to the boronic acid receptor in acetonitrile.[202] The adsorption peaks (at 2.5 min) plotted against the concentration of pinacol generates a binding curve for the interaction of pinacol to the MIP and control polymer (Figure 31).

4.2.6 MIP cross-reactivity and shape selectivity

One of our goals is to develop a MIP sensor which can differentiate between Fru-Val - the N-terminal glycated amino acid present in hemoglobin A1c (HbA1c) - and Val - the N-terminal amino acid in the pristine hemoglobin (HbA0). Hence, the specificity of the MIP sensor was investigated by applying valine and fructose.

Table 8. Temperature changes at peak due to the interaction of Fru-Val, Valine and Fructose to MIP and control polymer

Analyte	**MIP(Fru-Val) ΔT (m K)**	**Control polymer ΔT (m K)**
5 mM Fru-Val	8.2	0.2
5 mM Valine	0.03	0.15
5 mM Fructose	3.47	0.13

Table 8 compares the temperature changes at peak position for the interaction of Fru-Val, fructose and valine with the MIP(Fru-Val) and control polymer. Interaction of valine with the MIP(Fru-Val) or control polymer generates a temperature change below 0.1 mK. Hence valine is neither recognised by imprinted nor by control polymer. Interaction of Fru-Val to MIP(Fru-Val) gives an up to 270 fold higher temperature change compared to valine. This clearly shows that the MIP sensor is selective to Fru- Val in comparison to valine.

Binding of 0.1 mM Fru-Val to MIP(Fru-Val) generates 2.4 fold higher temperatures than fructose binding. Hence the polymer imprinted with Fru-Val shows higher affinity towards Fru-Val than valine and fructose. These results are very important for the further application to distinguish glycated haemoglobin (HbA1c) from non-glycated one (HbA0).

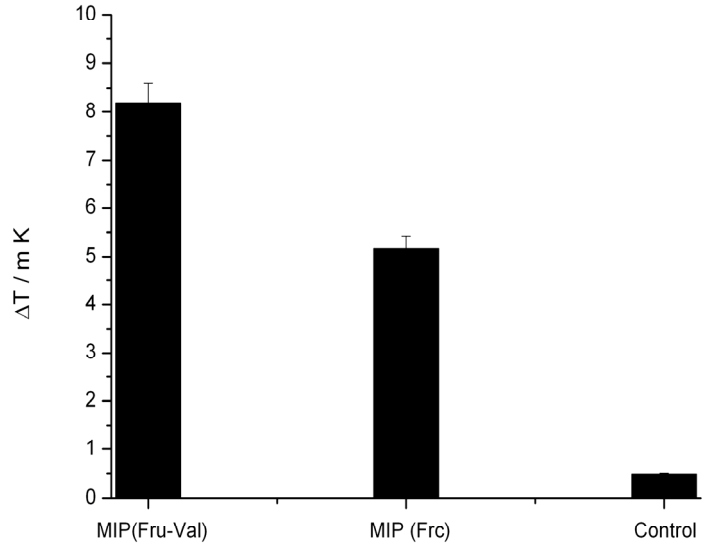

Figure 32. Binding of Fru-Val to Fru-Val imprinted, fructose imprinted and control polymer

Earlier reports have demonstrated the importance of spatial requirements (shape selectivity) on molecular recognition.[180, 203-205] In our experiments we wanted to evaluate the role of shape selectivity by the calorimetric method. Hence we compared the binding of Fru-Val to MIP(Fru-Val) and MIP(Frc). The comparison is summarised in Figure 32 which reveals that the MIP(Fru-Val) gives 1.6 fold higher heat signal and therewith an uptake compared to the MIP(Frc). This clearly shows that apart from interaction with boronic acid the shape of the cavity plays a vital role in molecular recognition.

4.2.7 Conclusions

For the first time a fructosyl valine imprinted polymer obtained *via* a covalent approach has been integrated in a thermistor for the label-free online detection of Fru-Val concentrations in a range of 0.25 - 5 mM. The big difference between the enthalpy for the specific covalent binding of the diol functionalities of the desired carbohydrates by two aromatic boronic acid moieties and for the non-specific adsorption to the polymer matrix leads to a higher "apparent imprinting factor" as compared with the batch procedure. Our results demonstrate a label-free non-optical method of detecting binding events with MIPs.

4.3 Studies with Molecularly Imprinted Polymers against Fructose

4.3.1 Introduction

In this work, fructose-vinyl phenyl boronate ester was synthesised and then polymerised with an excess of the di- and tri-functional cross-linkers ethylenglycol dimethacrylate (EDMA) and trimethylolpropane trimethacrylate (TRIM), respectively. The influence of cross-linking agents on binding of fructose is compared. Further fructose imprinted TRIM cross-linked polymers were used as a recognition element to construct a thermometric MIP sensor. The results obtained from the batch binding studies were compared with the thermometric detection method. A detailed investigation on the interaction of fresh and equilibrated fructose with MIP(Frc) was described.

4.3.2 Batch binding studies - Comparison between EDMA and TRIM cross-linked polymers

The polymer morphology and texture of the dry cross-linked polymer particles analysed by SEM shows that particles are highly granular in nature with irregular particle size between 25-50 μm which is typical for bulk polymers (Figure 33).

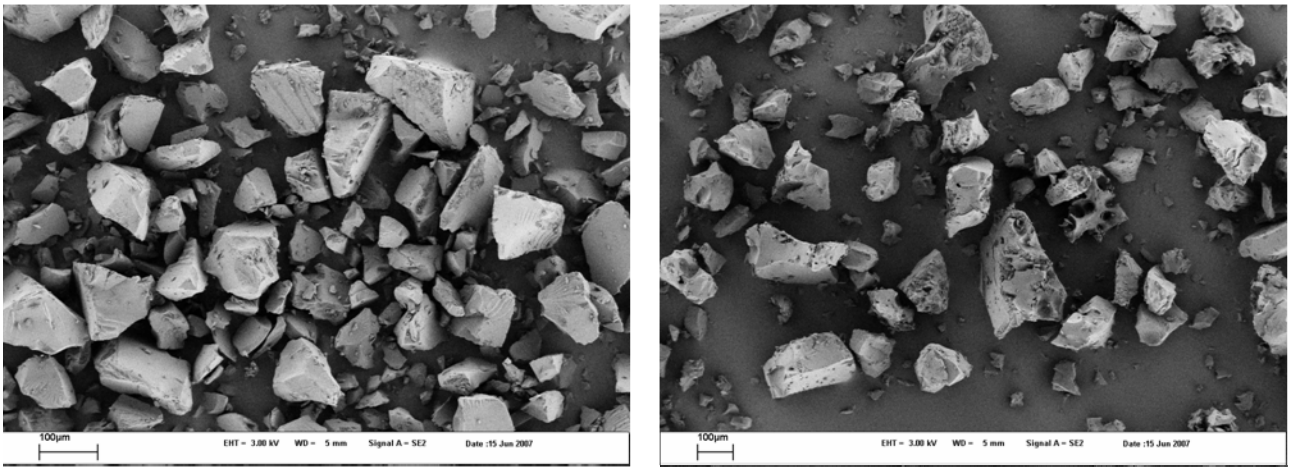

Figure 33. Scanning electron microscopy (SEM) images of MIP(Frc) particles cross-linked with EDMA (left) and TRIM (right)

Batch binding of fructose was investigated with fructose imprinted polymer, fructosyl valine imprinted polymer and control polymer (Figure 34). In batch studies 1M fructose stock solution in water is diluted with 100 mM sodium carbonate buffer, pH 11.4 containing 10% methanol to the desired concentration and incubated with MIP or control polymer for 12 h at room temperature. The unbound fructose was quantified using Anthrone method.[181]

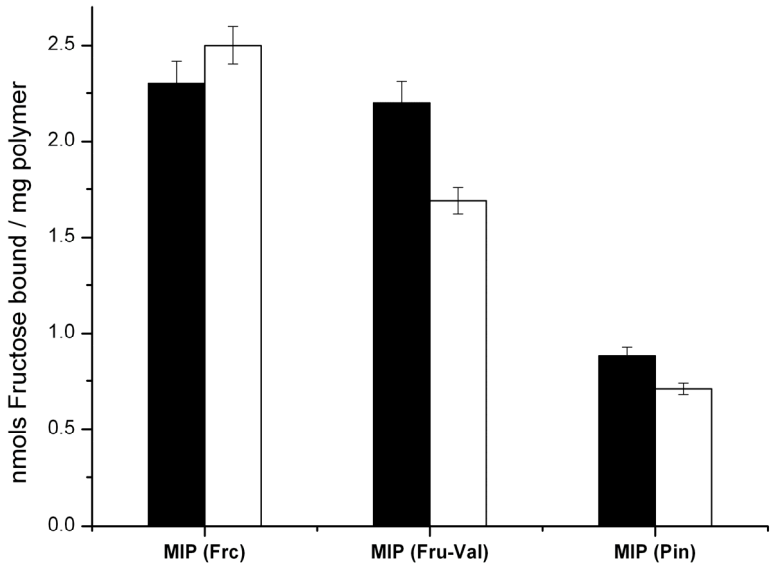

Figure 34. Comparison of fructose binding to TRIM and EDMA cross-linked MIP(Frc), MIP(FV) and control polymers. TRIM cross-linked (white); EDMA cross-linked (black); 10 mg polymer + 1 ml of 0.1 mM fructose in 10% methanol+ 90% 100 mM sodium carbonate, pH 11.4; 12 h; 26ºC.

The fructose imprinted and Fru-Val imprinted polymers showed a different binding behavior to fructose depending on the cross-linker used. EDMA cross-linked polymers showed higher unspecific binding compared with TRIM cross-linked polymers. When 0.1 mM fructose is applied the TRIM cross-linked fructose imprinted polymer binds 3.5 fold more fructose than control polymer and 1.4 fold more fructose than Fru-Val imprinted polymer. The EDMA cross-linked fructose imprinted polymer binds only 2.6 fold more fructose than the control polymer and almost the same amount is bound to the Fru-Val imprinted polymer. Hence with TRIM as cross-linker a better complementarity to the template is obtained than with EDMA making TRIM a better cross-linker for fructose imprinting. The finding that the TRIM cross-linked MIPs exhibit better selectivities than EDMA cross-linked polymers is in accordance with our earlier report on fructosyl valine MIPs.[206] These results show that the cross-linking agent is not merely an inert compound but plays a decisive role in promoting positive interactions with the template to afford molecular recognition.

4.3.3 Batch binding studies to determine the equilibrium time

Batch binding studies were carried out for different time intervals by incubating the MIP suspension with 0.1 mM fructose in 100 mM carbonate buffer /pH 11.4 containing 10 %

methanol to determine the time taken to reach equilibrium. Figure 35 shows that equilibrium was reached after 2 h. For further binding studies an incubation period of 2 h was therefore considered as sufficient.

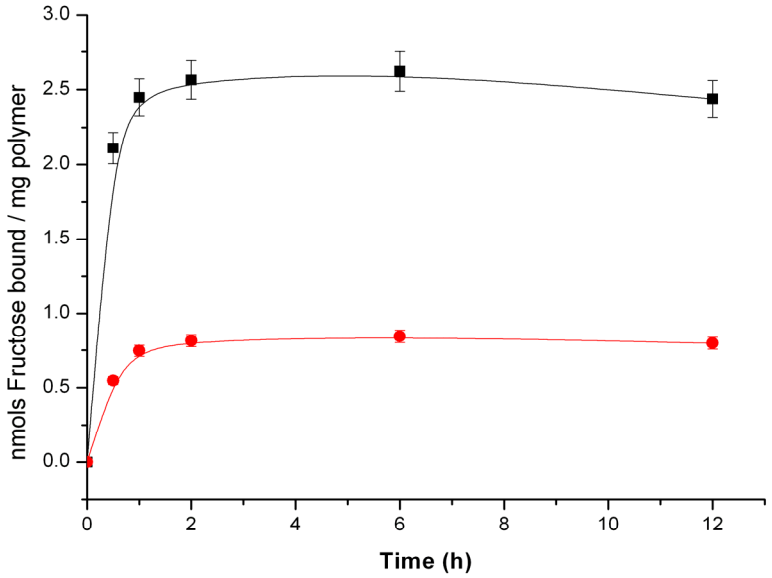

Figure 35. Time dependence for fructose binding to MIP(Frc) (squares) and control (circles) polymers.10 mg TRIM cross-linked polymer + 1 ml of 0.1 mM fructose in 10% methanol + 90% 100 mM sodium carbonate, pH 11.4; 0- 12 h; 26ºC

4.3.4 Concentration dependence of fructose binding in batch

Figure 36 shows the concentration dependence of fructose binding to the MIP(Frc) and the control polymer. Eventhough the theoretical capacity of the polymer would be 300 nmol/ mg we found that at saturating fructose concentrations the binding capacity of MIP(Frc) was about 40 nmol/mg MIP. The difference may be attributed to the fact that not all template used in imprinting resulted in accessible binding sites. At 0.2 mM fructose the ratio of binding to the MIP(Frc) and to the control polymer , i.e "imprinting factor" (IF) was ~ 3.8, whereas this ratio was reduced to ~ 1.5 at saturation concentrations. Evaluation of batch binding studies reveals the half saturation values of 0.5 mM for MIP(Frc) and1 mM control polymer.

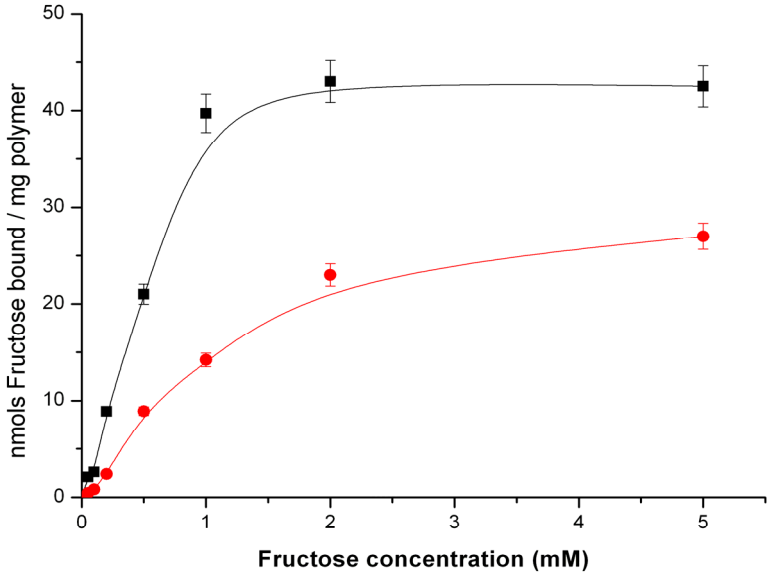

Figure 36. Concentration dependency for fructose binding to fructose imprinted (black squares) and pinacol imprinted (red circles) polymers. 10 mg TRIM cross-linked polymer + 1 ml of 0-5 mM fructose in 10% methanol+ 90% 100 mM sodium carbonate, pH 11.4; 12 h; 26ºC

4.3.5 Thermometric study - Interaction of freshly dissolved fructose with MIP and control polymer

For thermometric studies, MIP(Frc) was packed in a column and placed in a thermistor. The MIP is used as recognition element and the thermistor serves as a transducer. The binding of

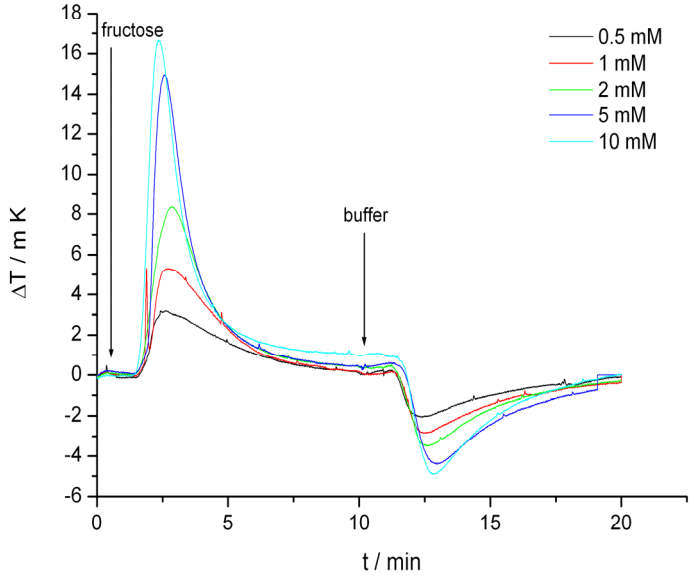

Figure 37. Time dependent thermogram for the interaction of freshly dissolved fructose with the MIP(Frc) in a thermistor. Fructose flow at 0 min and start of washing at 10 min with 100 mM sodium carbonate (pH 11.4)/10% methanol

freshly dissolved fructose to MIP(Frc) is due to the formation of reversible covalent linkage with the boronic acid within the micro cavities of MIP and generates an exothermic adsorption peak signal then decreasing down to the baseline (Figure 37). When the flow is changed from the analyte containing buffer to the neat buffer (after 10 min of analyte flow) an endothermic peak is observed reflecting the desorption of bound fructose from the cavities. On the other hand the non-specific interaction with the control polymer generates negligible endothermic adsorption and desorption heat signals (Figure 38).

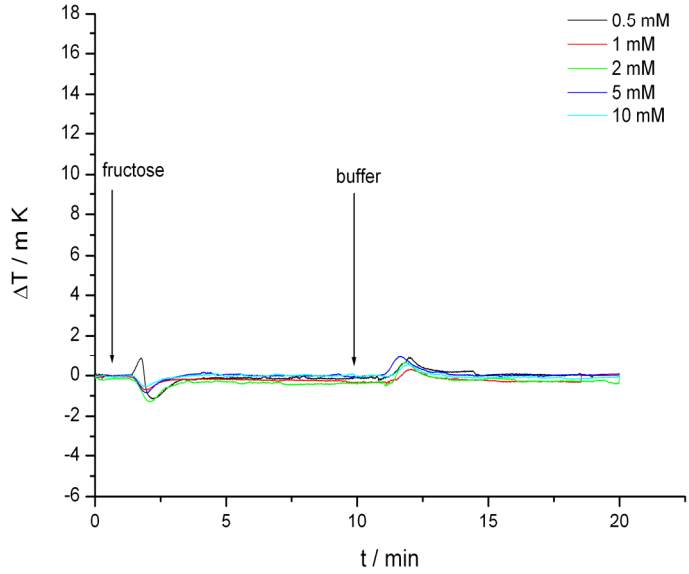

Figure 38. Time dependent thermogram for the interaction of freshly dissolved fructose with the control polymer (pinacol imprinted) in a thermistor. Fructose flow at 0 min and start of washing at 10 min with 100 mM sodium carbonate (pH 11.4)/10% methanol

The adsorption peaks (at 2.5 min) plotted against the concentration of fructose generate a binding curve for the interaction of fructose to the MIP(Frc) and the control polymer (Figure. 39). For the MIP the signal rises linearly up to 5 mM fructose and saturates at higher concentrations. Binding to the control polymer results in a considerably smaller temperature increase in the order of 0.2 m K. Thus a very clear difference in the binding behavior between the polymers is seen. The experiments were performed in triplicates and the MIP-sensor shows very good reproducibility.

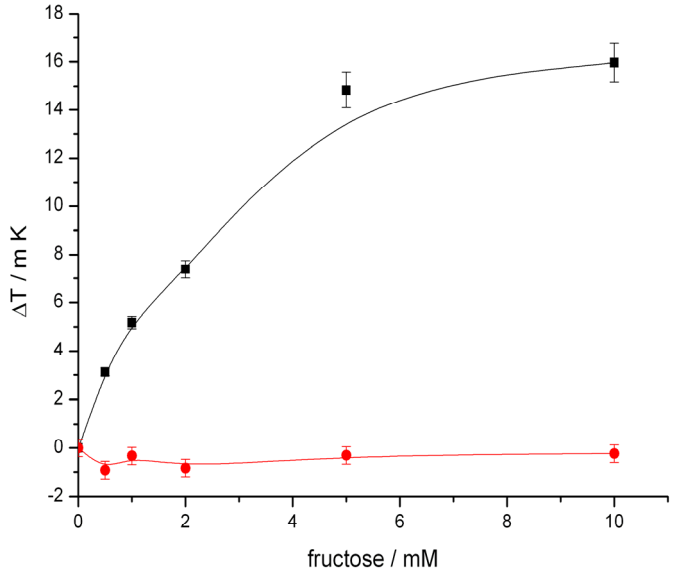

Figure 39. Temperature changes at the peak position (2.5 min) for different concentrations of fresh fructose with MIP(Frc) (black squares) and control polymer (red circles)

The much higher imprinting factor obtained in the flow technique compared to the batch measurement may be due to the fact that the former, measure events that are sensitive to the high affinity binding sites, and the unspecific adsorption of fructose to control polymer is associated with smaller enthalpy changes whereas the latter covers all cavities. By combining the shape effect and the predominance of heat generation by esterification an "apparent imprinting factor" of 28 is found which exceeds the respective value of batch binding studies by a factor of 18. When we compare thermistor results with batch binding studies the binding of fructose to MIP(Frc) is concentration dependant and saturates at 2 mM. The reason is that in batch the incubation time is around 2 h where the equilibrium is attained, whereas in thermometric study the equilibrium is not reached within 10 minutes of interaction. Table 9 lists the binding characteristics of MIP(Frc)

Table 9. Binding characteristics of fructose imprinted polymer

MIP	Fructose binding capacity (nmol / mg)	Half saturation value (mM)	IF* Batch	IF ** Thermometric
MIP (Frc)	40	0.5 mM	1.5	28
Control	25	1 mM		

IF* is the ratio of fructose binding to MIP(Frc) to control polymer at 5 mM
IF** is the ratio of heat generation due to fructose binding to MIP(Frc) to control polymer at 5 mM

4.3.6 Thermometric study - Interaction of equilibrated fructose with MIP and control polymer

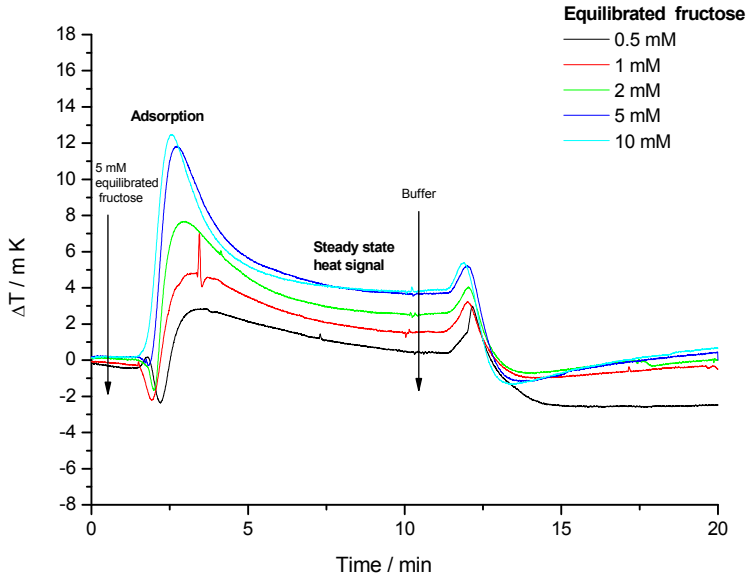

Figure 40. Time dependent thermogram for the interaction of equilibrated fructose with the MIP(Frc) in a thermistor. Fructose flow at 0 min and start of washing at 10 min with 100 mM sodium carbonate (pH 11.4)/10% methanol

Figure 40 illustrates the interaction of fructose equilibrated for two weeks in 100 mM sodium carbonate buffer/10% methanol, pH 11.4 to the MIP(Frc). Interaction of equilibrated fructose to the MIP(Frc) generates a small endothermic peak followed by an exothermic peak, smaller than that for freshly dissolved fructose, which is associated with the adsorption process followed by an exothermic steady state signal. When the flow is changed from the analyte to the neat buffer (at the 10 th minute) after a small exothermic peak the signal decreases down to the baseline, which would indicate the desorption process of bound fructose from the binding sites. This is in contrast to the interaction of MIP(Frc) with the freshly dissolved fructose as shown in Figure 36.

The interaction of equilibrated fructose with the control polymer shows an endothermic adsorption and exothermic desorption signal (Figure 41). Fructose (fresh and equilibrated) interactions with the control polymer does not show any concentration dependency in the investigated concentration range. The interaction of fresh fructose with the control polymer causes a much lower thermometric signal compared with the equilibrated fructose. It is interesting to compare these results with an earlier experiment where interaction of pinacol with control polymer shows a concentration

dependent endothermic binding and exothermic desorption signal (as shown in Figure 30). MIP/Fru-Val interactions studied in the thermistor also exert an exothermic heat change.

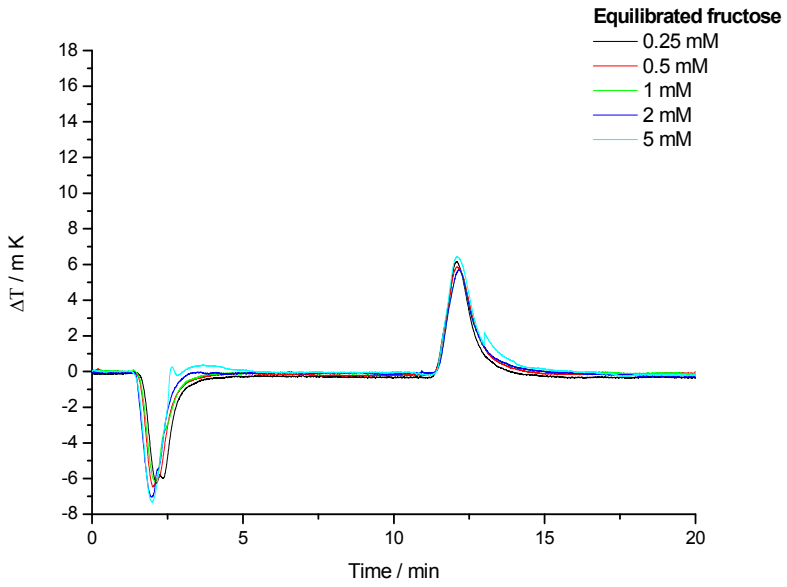

Figure 41. Time dependent thermogram for the interaction of equilibrated fructose with the control polymer in a thermistor. Fructose flow at 0 min and start of washing at 10 min with 100 mM sodium carbonate (pH 11.4)/10% methanol

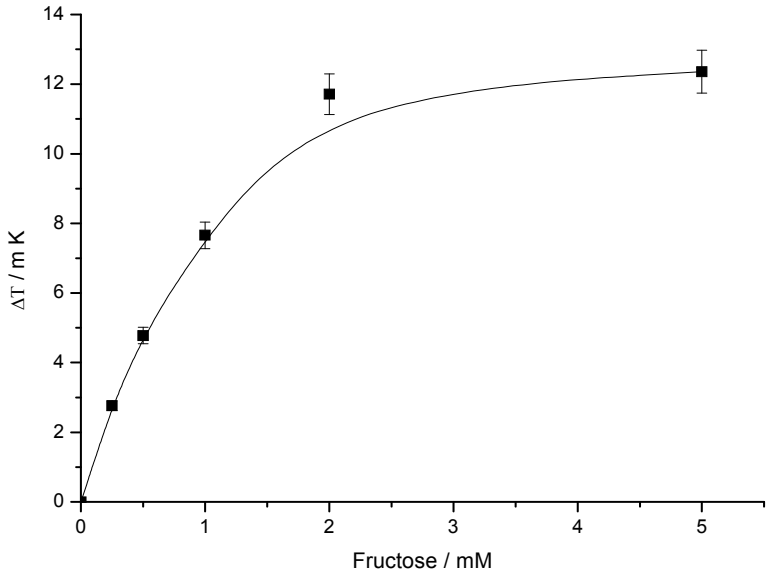

Figure 42. Concentration dependent heat changes for equilibrated fructose binding to MIP(Frc). Temperature changes at peak position (2.5 min) for different fructose concentrations

The adsorption peak signals (at 2.5 min) plotted against the concentration of fructose generates a binding curve for the interaction of equilibrated fructose to the MIP (Figure 42). It can be seen that at 5mM fructose the maximal heat change is reached.

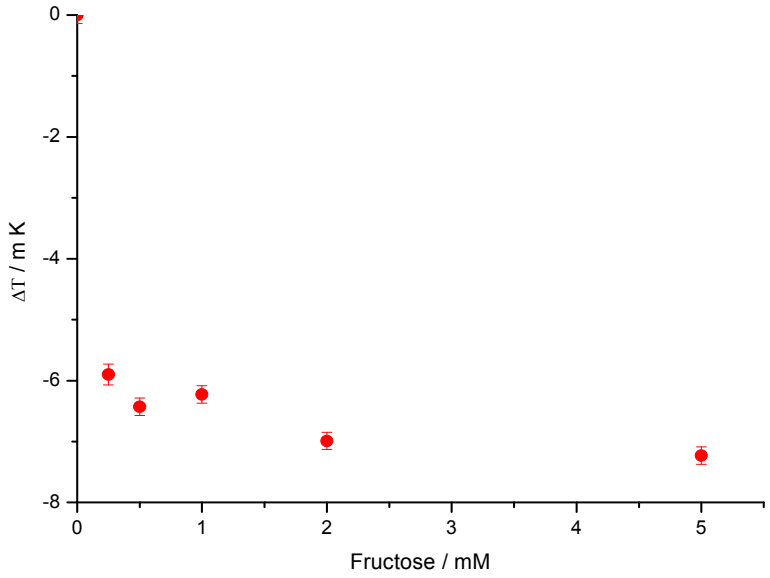

Figure 43. Concentration dependent heat changes for the interaction of equilibrated fructose to control polymer. Temperature changes at peak position (2.5 min) for different fructose concentrations

Figure 43 illustrates the concentration dependence of the interaction of equilibrated fructose with the control polymer. Since the equilibrium is not reached, only apparent half saturation values can be given as 0.6 mM for MIP(Frc). In case of fresh fructose the apparent half saturation value would be ~ 2 mM.

Table 10 indicates the effect of different media on MIP/equilibrated fructose interactions at the peak as well as at the steady state. We found that higher heat changes are observed under alkaline conditions. For instance at pH 11.4, a 30 fold higher signal at the peak and a 13 fold higher signal at steady state was observed in comparison to pH 7.1. The reason for such a higher thermometric signal at alkaline conditions is the fact that the boronic acid is present in its tetrahedral anionic form rather than the triagonal form at neutral conditions. Springsteen reported that the nature of the buffer and its composition affect the binding of boronic acid with diols, and the K_{eq} value of D-fructose at pH 8.5 was found to be 560 M^{-1} which was 120 fold higher than the K_{eq} value observed at pH 5.8.[175] It is clear that the pH and the buffer play an influential role on the complexation of fructose with boronic acid containing MIP. Batch binding studies carried out at different media also mirror this result.

Table 10. Comparison of the effect of different media on the interaction of equilibrated fructose at the peak and steady state heat signal

5 mM equilibrated fructose in the media	ΔT Peak (m K)	ΔT Steady state (m K)
100 mM carbonate buffer, pH 11.4 + 10 % MeOH	12.3	3.9
1 mM carbonate buffer, pH 10.7 + 10 % MeOH	4.8	1.6
1.2 mM NaOH pH 11.4 + 10 % MeOH	2.8	1.2
85% water + 5% NH_3 in water + 10% ACN, pH 11.4	2.6	1.1
100 mM phosphate buffer, pH 7.1 + 10 % MeOH	0.3	0.3
100 mM acetate buffer, pH 5.5 + 10 % MeOH	-0.3	-0.2

4.3.7 Long term interaction of equilibrated fructose with MIP

To assess whether the observed steady state temperature signal in Figure 40 is attributed to a slow binding the the steady state was monitored for several hours. From Figure 44 we can see that the heat signal was stable over a period of 2 h. Therefore slow binding will not explain the long term steady state heat signal.

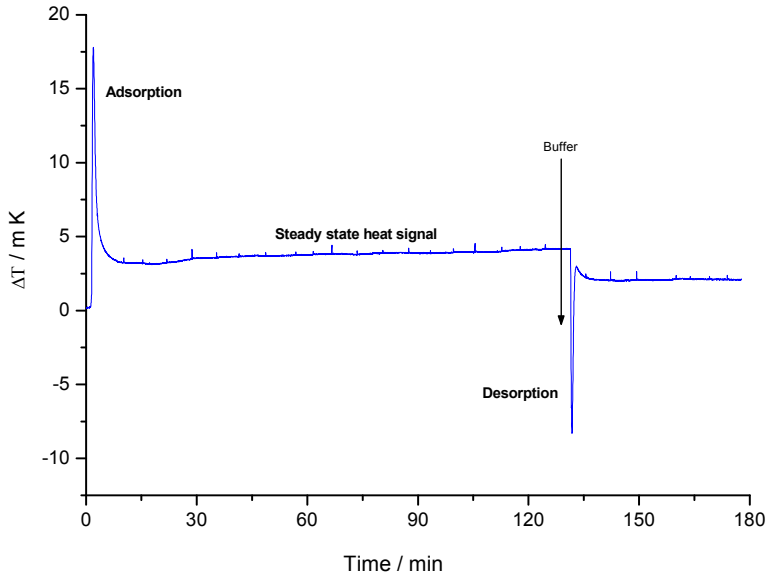

Figure 44. Time dependent thermogram representing long term interaction of equilibrated fructose with MIP(Frc)

It is very interesting to note that the interaction of a fresh fructose solution with MIP(Frc) does not yield a steady state signal whereas the interactions with equilibrated fructose give a stable steady state heat signal. The reason might be that only an equilibrated fructose contains a substance which causes a steady state heat change. Equilibrated fructose exists in deuterated water at pH 7.0 in a complex equilibrium between the five isomeric forms namely β-D-fructopyranose (68%), β-D-fructofuranose (23%), α-D-fructopyranose (2%), α-D-fructofuranose (6%) and open chain from (0.7%).[207]

4.3.8 Polarimetry and NMR studies with fresh and equilibrated fructose

Figure 45 shows the specific rotation of fructose in carbonate buffer, pH 11.4. The aim of this experiment was to determine the time taken by fructose in different media to reach equilibration. In water the equilibrium is attained within hours whereas under alkaline conditions it takes almost 10 days to reach equilibrium. The first phase of conversion after dissolving the fructose is predominantly β-D-fructopyranose to β-D-fructofuranose in water and subsequent conversion involves mainly α to β interconversions for the two ring forms.

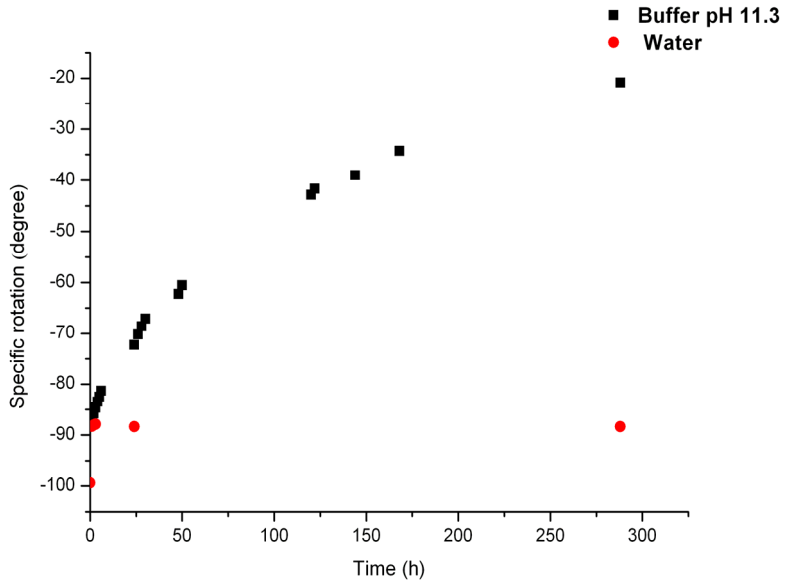

Figure 45. Equilibration of fructose followed in a polarimeter. Fructose was dissolved in water (red circles) and in 100 mM carbonate buffer pH 11.4 containing 10% methanol (black squares)

Recently investigators reported that in aqueous alkaline media the saccharide must possess synperiplanar diol functionality to complex with the boronic acid. As the boron- oxygen bond lengths are known to be relatively short and the formation of thermodynamically stable boronate

ester complexes will require the interacting diol to be synperiplanar which is possible for furanoses. Hence the boronic acid in cavities should complex with the β-D-fructofuranose.[207] Figure 46 represents the different isomeric forms of fructose present in water after equilibration.

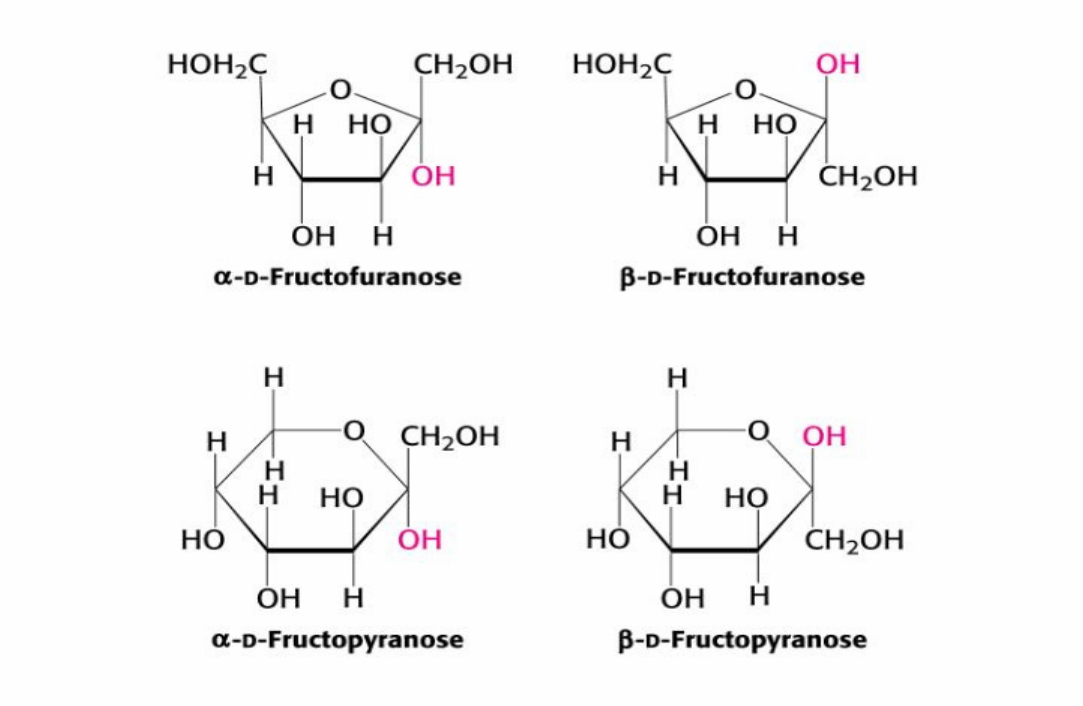

Figure 46. Different forms of fructose present in water

Uniformly ^{13}C labelled fructose and glucose were dissolved in deuterated water, and the NMR spectrum was recorded after one day. Fructose and glucose were also dissolved in 85% D_2O/10% MeOD/5% ND_3, pH 11 and stored at room temperature for 10 days to attain equilibrium. Parts of the ^{13}C NMR spectrum shown in Figure 47, represents the signals of C2 obtained between 90 and 110 ppm. Chemical shifts (relative to MeOD) corresponding to all carbons can be assigned for fructose at neutral conditions and are in agreement with an earlier report.[208] On comparing the spectra of fructose allowed to equilibrate under alkaline conditions (b) with neutral conditions (a) we found that the peaks corresponding to the C2 of furanoses between 102 -106 ppm cannot be seen. But we observed a broad peak in this region probably due to the deprotanation. There were two new peaks P1 and P2 around 97 and 92 ppm, respectively. They are doublets indicating that the carbon atom has only one carbon in its neighbourhood which indicates the formation of glucose.

When we compare the glucose spectrum c & d, C1 of pyranoses can be seen both at neutral and at alkaline conditions. In alkaline conditions there is a new set of peaks P3 appearing around 98 ppm. On comparing a,b,c and d it can be clearly seen that peaks p1 and p2 of fructose corresponds to C1 of α and β pyranoses of glucose. This indicates that probably at alkaline conditions fructose is

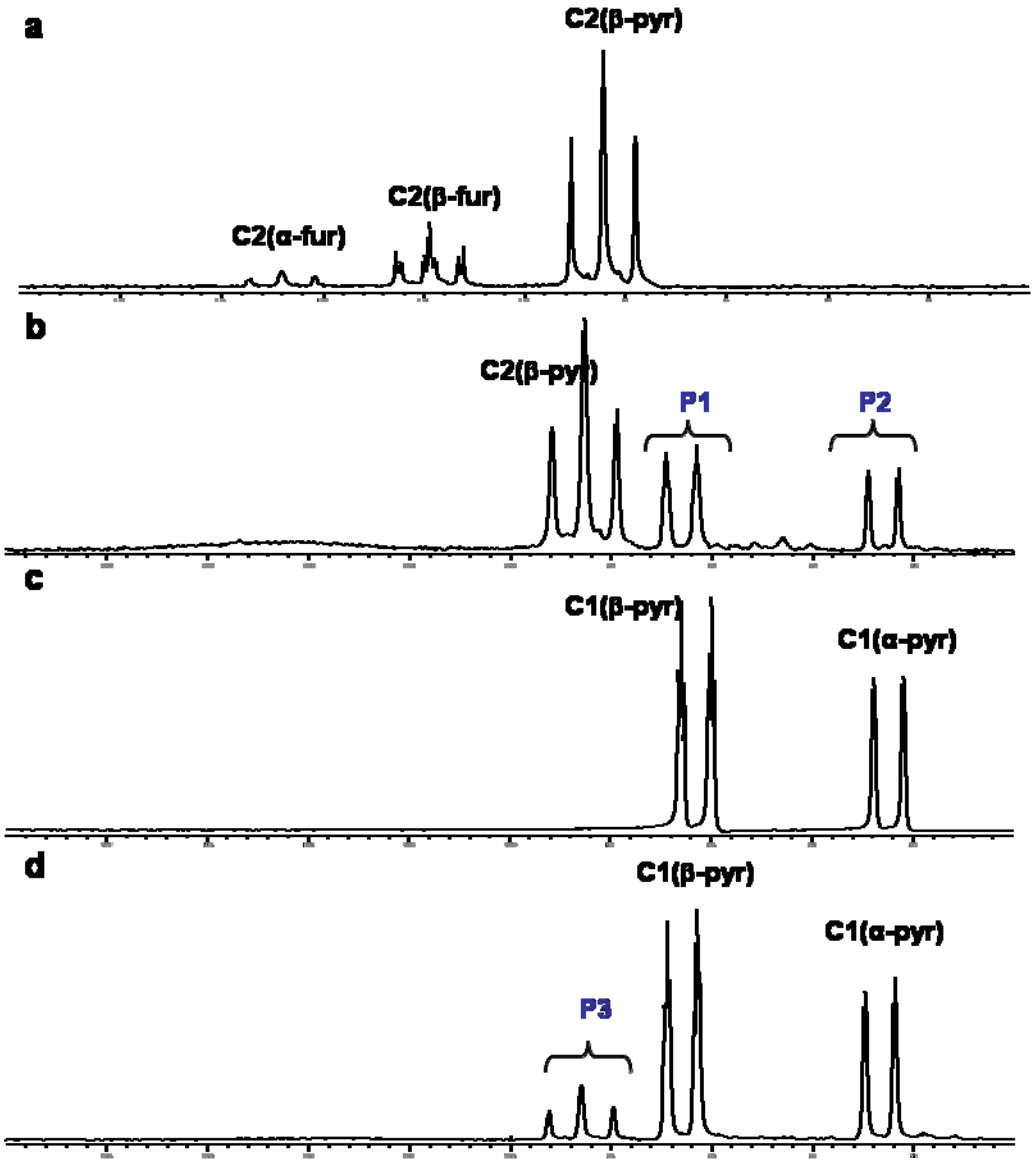

Figure 47. NMR spectrum representing anomeric carbon at position 2 of uniformly labelled fructose and glucose. a) fructose in D_2O b) fructose in 85% D_2O/10% MeOD/5% ND_3, pH 11 c) glucose in D_2O d) glucose in 85% D_2O/10% MeOD/5% ND_3, pH 11

partly converted to glucose via keto-enol tautomerisation. Signal P3 of glucose might be representing the C2 of β-fructopyranose. It is known from Lobry de Bruyn Alberda Van Ekenstein rearrangement that the conversion of aldoses and ketoses may occur under alkaline conditions. Treatment of D-glucose with 0.035% aqueous sodium hydroxide solution for 100 h results in a mixture containing D-fructose (28%), D-mannose (3%) and unchanged D-glucose (57%).

When fructose at alkaline conditions was tested for glucose using an amperometric glucose sensor for quantification, we found no detectable amount of glucose. Probably this conversion is too low to be quantified. Further to determine whether MIP is catalysing the transformation of one form of fructose to the other we had used uniformly labelled fructose in our experiments to record the NMR spectrum. The NMR spectra of fructose solution from the thermistor inlet and outlet are quite similar, since the conversion is almost 10% which means that product yield is too low to be quantified. (Figure 48)

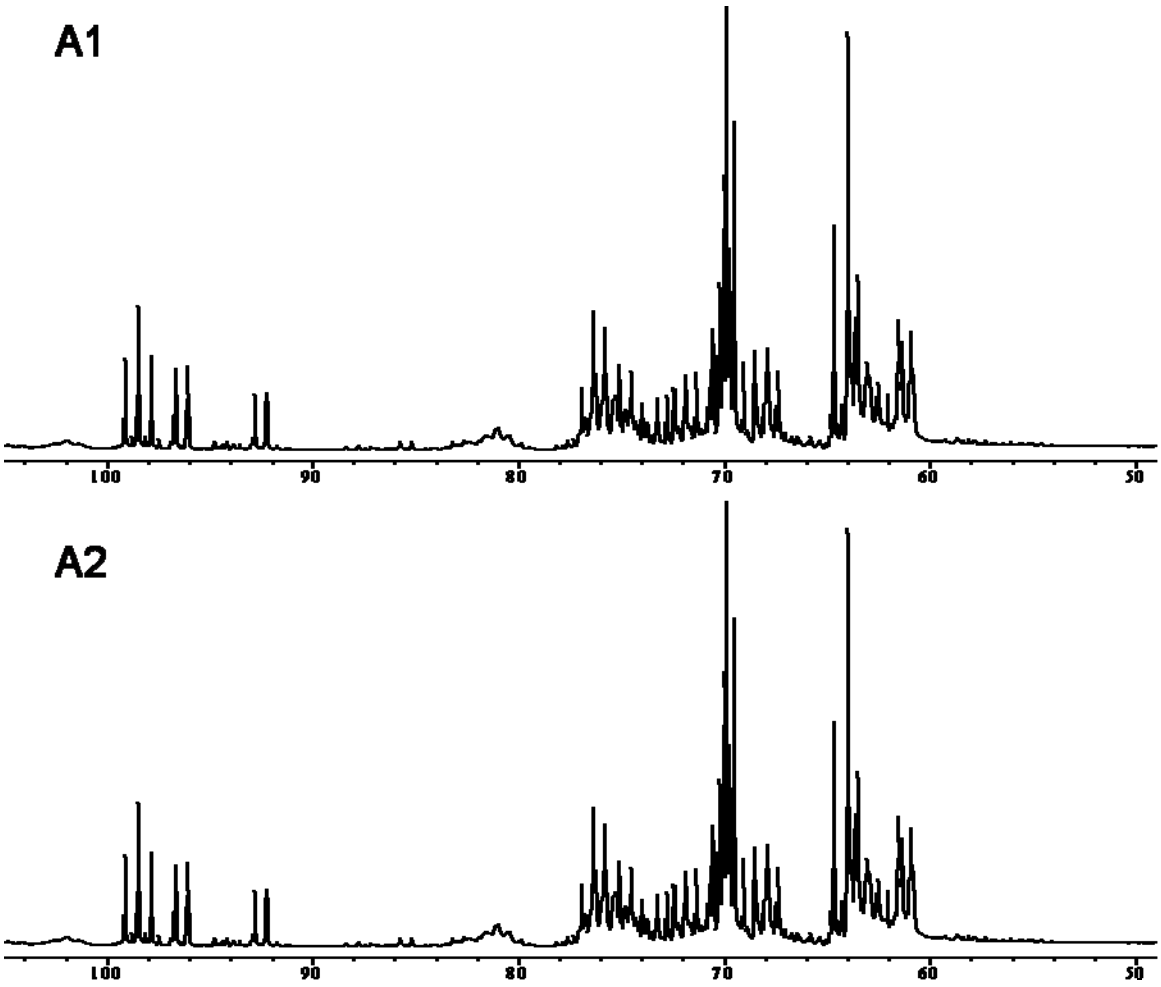

Figure 48. NMR spectrum representing uniformly labelled fructose in 85% D_2O/10% MeOD/5% ND_3, pH 11 at A1) thermistor intlet A2) thermistor outlet

The synthesis of MIPs was carried out in organic solvents and the resultant MIP should be specific for β-D-fructopyranose. But the binding studies were carried out under aqueous alkaline conditions where the β-D-fructofuranose is the dominant form. Our results clearly indicate that the interaction of MIP between different forms of fructose leads to different thermogram patterns. But with our present data the reasons for the observed difference in thermogram patterns therefore remain unclear.

4.3.9 Interaction of a model compound with MIP

Tetrahydroxy cyclohexane (THC) (Figure 49) was synthesised as a model compound to study whether the esterification of the boronic acid would have an endothermic or exothermic thermogram pattern. Unlike fructose this molecule does not allow ring opening and from this experiment the reason for the steady state signal described in the chapter before can further be resolved.

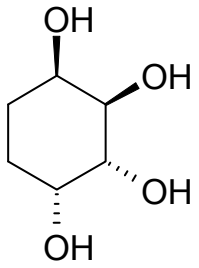

Figure 49. Structure of the model compound tetrahydroxy cyclohexane

Figure 50 shows the thermogram pattern obtained for the interaction of THC (Red) and equilibrated fructose (Black) with MIP. Interaction of THC with MIP gives rise to an endothermic heat signal and when switched to the neat buffer the desorption of THC from MIP cavities is seen as a peak in the exothermic direction. No steady state heat generation was observed. Interaction of equilibrated fructose to control polymer also exhibits a similar endothermic adsorption and exothermic desorption.

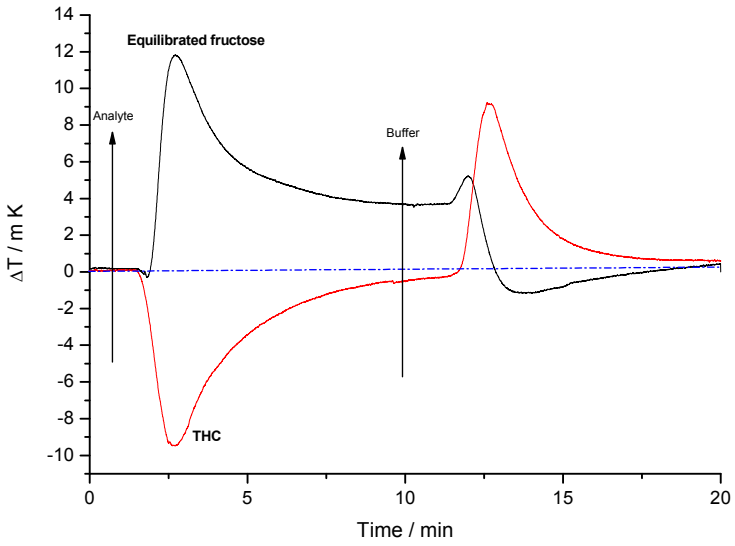

Figure 50. Time dependent thermogram for the interaction of 5 mM equilibrated fructose and 5 mM tetrahydroxy cyclohexane with MIP(Frc) in a thermistor. Fructose or THC flow at 0 min and start of washing at 10 min with 100 mM sodium carbonate (pH 11.4)/10% methanol

Thermogram pattern of MIP/THC interaction is in direct contrast with the thermogram pattern obtained with equilibrated fructose. This result further confirms that the steady state signal is due to some kind of species present in fructose after equilibration at pH 11.4. The MIP/THC interaction gave an endothermic heat signal which might be associated with the change in the solvation profile in comparison with fructose. It should be considered that sugars might deprotonate at alkaline conditions whereas the model compound is neutral. Probably in case of fructose deprotonation at pH 11.4 might be the reason for an exothermic signal and in case of THC deprotonation does not occur at this pH which might also be a reason for the opposite signal.

4.3.10 Conclusions

The influence of cross-linking agent on binding of fructose shows the advantage of TRIM over EDMA. For the first time fructose imprinted polymer has been integrated in a thermistor for the label-free online detection of fructose in a range of 0.5-5 mM. The concentration dependence exhibited by fructose with MIP(Frc) and by pinacol with control polymer shows that apart from functional monomer the shape complementarities of the imprinted cavity to the corresponding template plays a significant role in molecular recognition. Interaction of fresh and equilibrated fructose with the MIP and the control polymer leads to different thermograms. Probably the reason for steady state heat generation is the different form of fructose present after equilibration. The effect of media/pH was investigated and a higher thermometric signal is obtained under alkaline conditions.

4.4 Studies on Evaluation of MIP Cross-reactivity

4.4.1 Introduction

MIPs were found to show a remrakable cross-reactivity with the molecules analogous to the imprinted template. In this study MIP cross-reactivity was evaluated for the monosaccharide glucose. Further, detailed investigations on interaction of fresh and equilibrated glucose with MIP are discussed. Later the interaction of disachharides with MIP(Frc) is studied to characterise the cross-reactivity.

4.4.2 Cross-reactivity with glucose

4.4.2.1 Interaction of freshly dissolved glucose with MIP and control

Thermograms obtained due to the interaction of fresh glucose with MIP and control polymer are represented in Figures 51 and 52. The interaction of glucose to MIP(Frc) which is due to the formation of reversible covalent linkage with the boronic acid within the micro cavities of MIP generates an exothermic peak signal which decreases down to the baseline within 5 minutes. When the flow is changed from the analyte (glucose) containing buffer to the neat buffer (after 10 min of analyte flow) a small endothermic peak is seen which indicates the desorption of bound glucose from the cavities. This behaviour is coincident with that of freshly dissolved fructose. However, for fructosyl valine a long lasting steady state has been found after an initial adsorption peak (Figure 26). The mechanism behind this effect which is also found with fructose or glucose equilibrated at pH 11.4 for two weeks is probably a catalytic conversion. At 5 mM the interaction of fresh fructose with MIP(Frc) gave a thermometric peak value of 14.8 mK whereas fresh glucose yielded only 3.2 mK. The 4 fold higher heat value indicates that the MIP(Frc) preferentially binds fructose.

On contrary to the MIP, the interaction of fresh glucose with control polymer yields an endothermic adsorption and exothermic desorption signal. This is in accordance with the interaction of fresh fructose with control polymer. There is no concentration dependent interaction of fresh glucose with control polymer which is similar to the interaction of fresh fructose with control polymer.

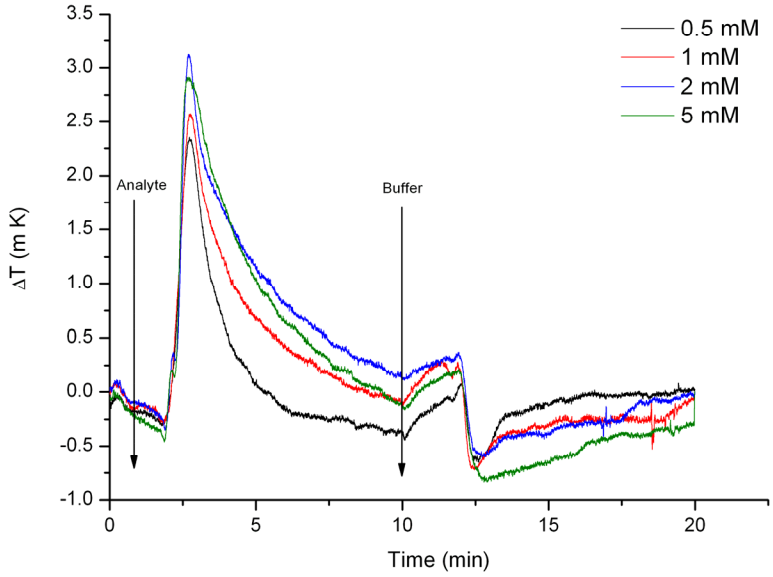

Figure 51. Time dependent thermogram for the interaction of fresh glucose with the MIP (Frc) in a thermistor. Glucose flow at 0 min and start of washing at 10 min with 100 mM sodium carbonate (pH 11.4) containing 10% methanol

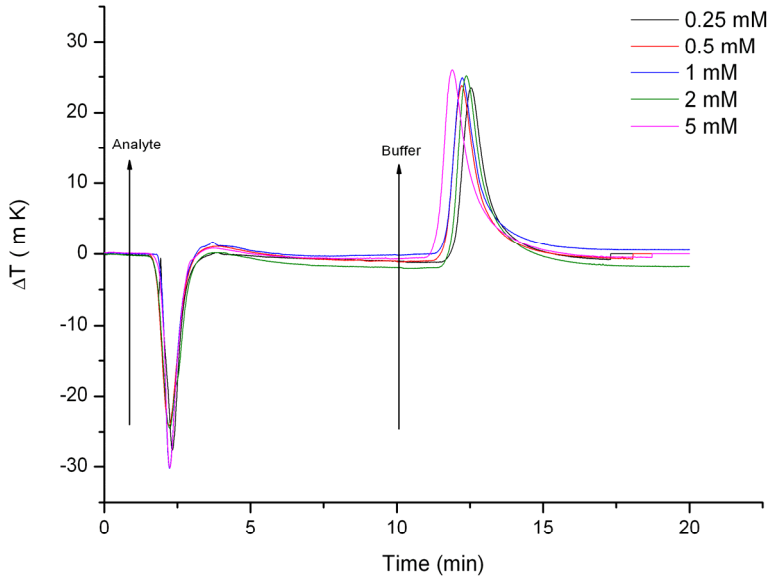

Figure 52. Time dependent thermogram for the interaction of fresh glucose with the control polymer in a thermistor. Glucose flow at 0 min and start of washing at 10 min with 100 mM sodium carbonate (pH 11.4) containing 10% methanol

The fresh glucose from the thermistor was collected at the adsorption peak and at the desorption peak and was quantified using an amperometric glucose sensor. From the glucose concentration profile of fresh glucose (Figure 53), it is evident that during the initial adsorption the content of

glucose is lowered by 29% in the effluent. 15 μmoles of glucose are bound by MIP in the first 10 minutes. At the desorption peak there is some glucose liberation.

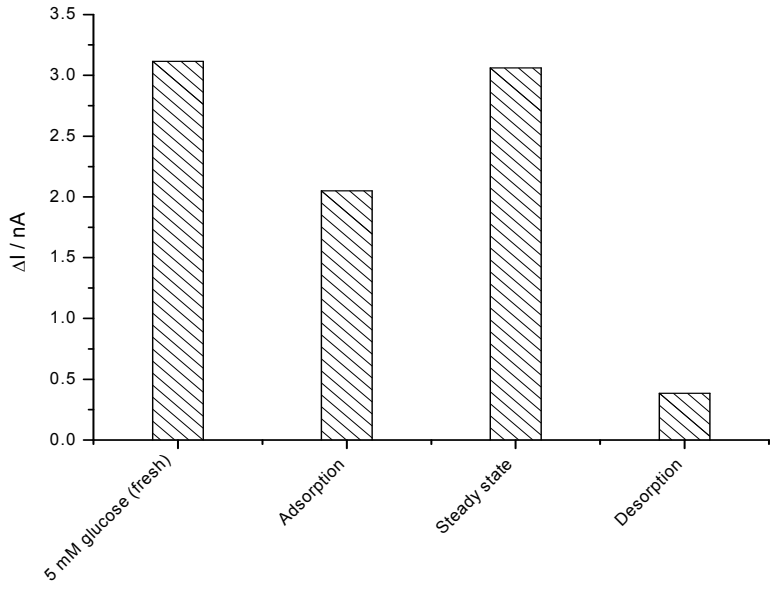

Figure 53. Concentration profile of fresh glucose as analysed using an amperometric glucose sensor

4.4.2.2 Short term interaction of equilibrated glucose with MIP and control polymer

Interaction of equilibrated glucose with the MIP(Frc) generates an exothermic peak signal followed by an exothermic steady state signal. (Figure 54) When the flow is changed from the analyte to the neat buffer (after 10 min) the signal decreases down to the baseline after a small endothermic peak. At 5 mM the interaction of equilibrated glucose with MIP(Frc) yields a roughly 25% lower adsorption peak in comparison with the interaction of equilibrated fructose. The interaction of 5 mM equilibrated glucose with MIP(Frc) yields a 3-fold higher adsorption signal than the fresh glucose.

In contrary to MIP(Frc), the interaction of equilibrated glucose with the control polymer generates endothermic adsorption and exothermic desorption signals (Figure 55). These interactions do not show any concentration dependency which was also not observed in the case of equilibrated fructose as described earlier.

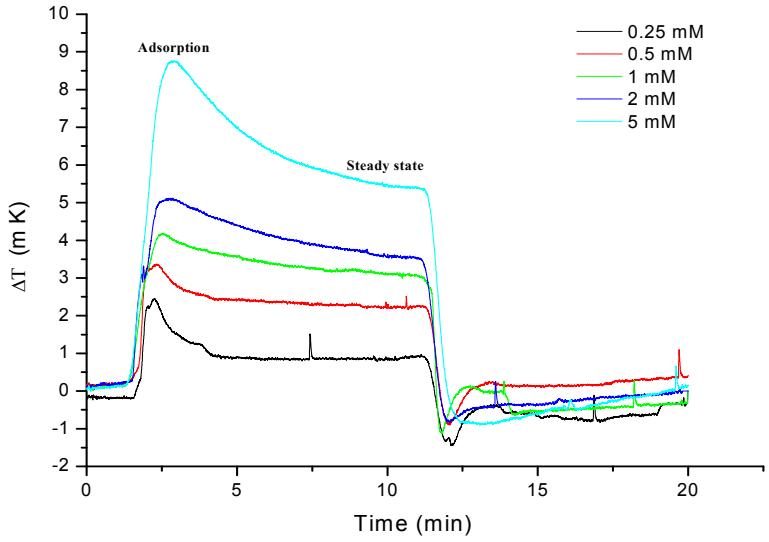

Figure 54. Time dependent thermogram for the interaction of equilibrated glucose with the MIP (Fructose imprinted) in a thermistor. Glucose flow at 0 min and start of washing at 10 min with 100 mM sodium carbonate (pH 11.4)/10% methanol

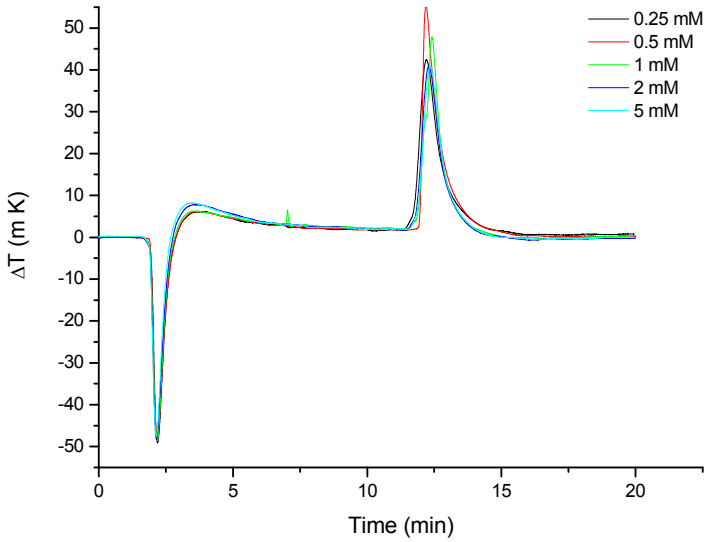

Figure 55. Time dependent thermogram for the interaction of equilibrated glucose with the control polymer in a thermistor. Glucose flow at 0 min and start of washing at 10 min with 100 mM sodium carbonate (pH 11.4) with 10% methanol

To elucidate the reasons for such a steady state heat signal the equilibrated glucose from the thermistor was collected at the adsorption peak, the steady state and at the desorption peak and was quantified using an amperometric glucose sensor. The results are represented in Figure 56.

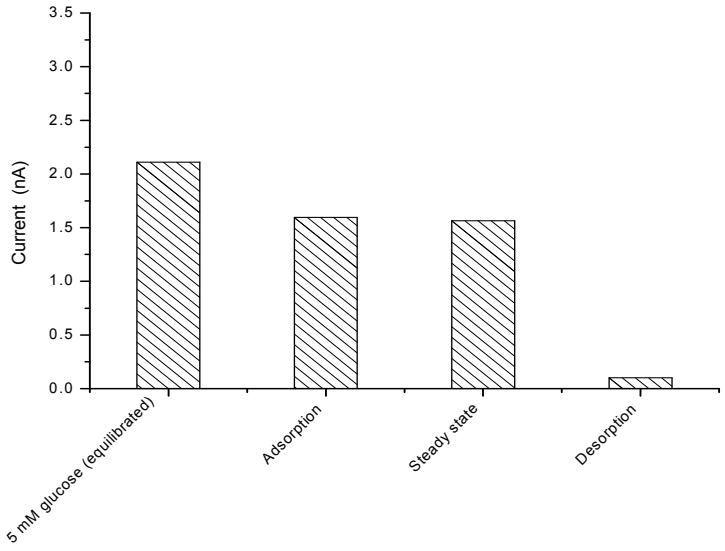

Figure 56. Concentration of the effluent for equilibrated glucose as analysed using an amperometric glucose sensor

From the glucose concentration profile, it is evident that during the adsorption as well as at steady state there is consumption of glucose and at the desorption peak there is some liberation of glucose Concentration of glucose in effluent at the adsorption peak as well as at the steady state was lowered by 23%. 10 μmoles of glucose would be bound in 10 min of flow which reflects roughly 30% of the boronic acid present in the MIP.

4.4.2.3 Long-term interaction of equilibrated glucose with MIP and control polymer

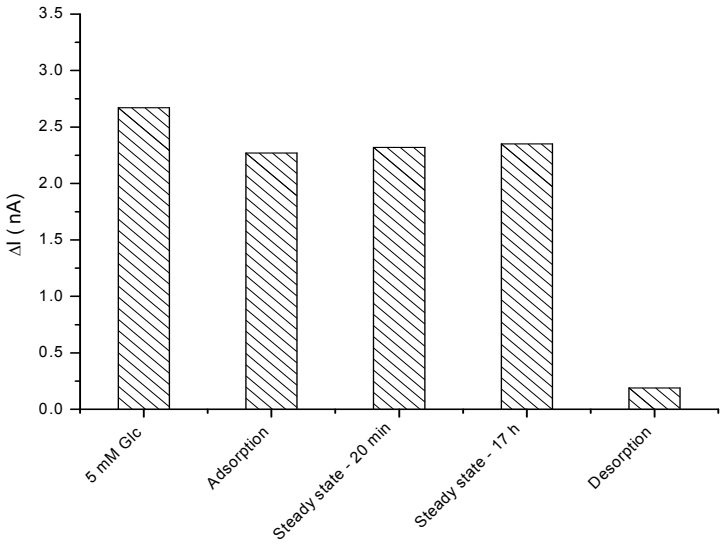

Figure 57. Concentration of the effluent long term interaction as analysed using an amperometric glucose sensor

To assess whether the observed steady state temperature signal is attributed to a slow binding kinetics the temperature changes were monitored for several hours. We observed a stable signal over a period of 17 h. Amperometric measurements of glucose indicate that the concentration of glucose was lowered by 10 % at the adsorption peak. At steady state, glucose is lowered by 10% (Figure 57). This consumption of glucose at steady state exceeds the binding capacity of MIP by more than 2 fold. Hence the steady state heat signal cannot be explained in terms of the slow binding. Continuous glucose consumption by MIP indicates that there is a reaction associated with this heat generation.

4.4.2.4 Interaction of glucose with MIP in a Loop

In order to characterise the heat generation up to the establishment of equilibrium we realised an experimental setup comparable with the batch binding studies. For this reason 10 ml of the equilibrated glucose solution were pumped in a closed loop through the MIP reactor containing 100 mg of the polymer. In this way in both configurations the same volume ratio of MIP to substrate was used.

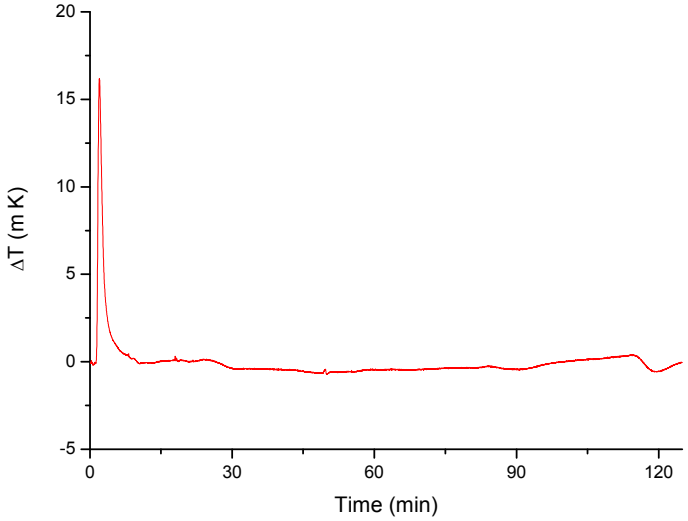

Figure 58. Time dependent thermogram for 5 mM equilibrated glucose pumped continuously in a loop through the MIP thermistor

The flow of a 5 mM equilibrated glucose solution through the MIP reactor generated an initial peak signal which was followed by a slowly decaying signal. (Figure 58) 15 minutes after the start the measuring curve reached the base line, indicating the establishment of equilibrium. Switching the stream to the neat buffer resulted in an endothermic signal which reflects the splitting of the bound fructose from the polymer (not shown).

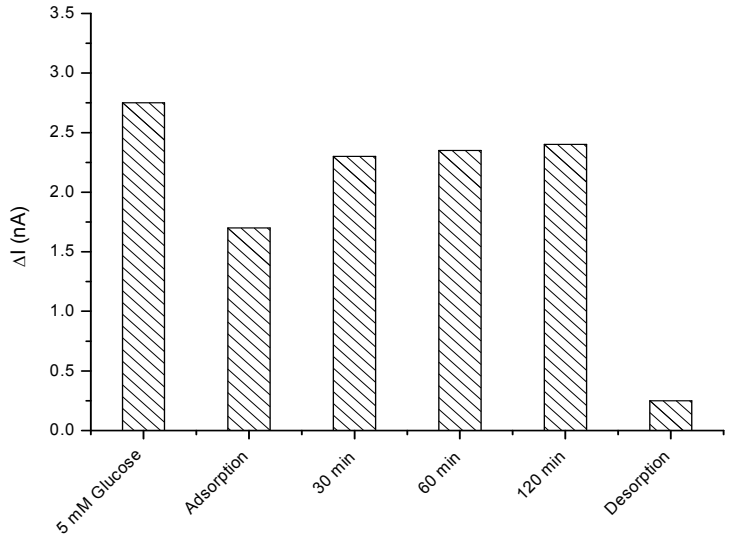

Figure 59. Glucose concentration profile in a loop experiment analysed using an amperometric glucose sensor

Measurement of the glucose concentrations during the loop experiment revealed that almost 10 µmol have been bound within the first 60 min (Figure 59). The concentration of the analyte remains almost unchanged at the value of 4.5 mM over the next 120 min. The amount of glucose which is bound to the MIP reflects almost 30% of the content of the boronic acid moieties.

It is important to note that long term MIP(Frc)/equilibrated glucose interactions give a stable heat signal whereas for interactions in the loop mode the signal decreases down to the baseline. The reason might be that in long term the fresh analyte is continuously delivered which causes stable heat signals whereas in loop mode the conversion of the analyte reaches equilibrium.

Equilibrated glucose exists in deuterated water in a complex equilibrium between the five isomeric forms namely β-D-glucopyranose (60.9%), β-D-glucofuranose (0.15 %), α-D-glucopyranose (38.8 %), α-D-glucofuranose (0.14 %) and open chain from (0.0024 %). However, glucose equilibrated at pH 11.4 should contain a species which is not present at pH 7 because the steady state is found only with the long term equilibrated glucose. The measurements in the effluent of the MIP reactor indicate that almost 10% of the total β-D-glucose are consumed at the steady state. This amount exceeds the theoretical binding capacity of the reactor, therefore a catalytic reaction would explain the results presented.

4.4.3 Cross-reactivity with disaccharides

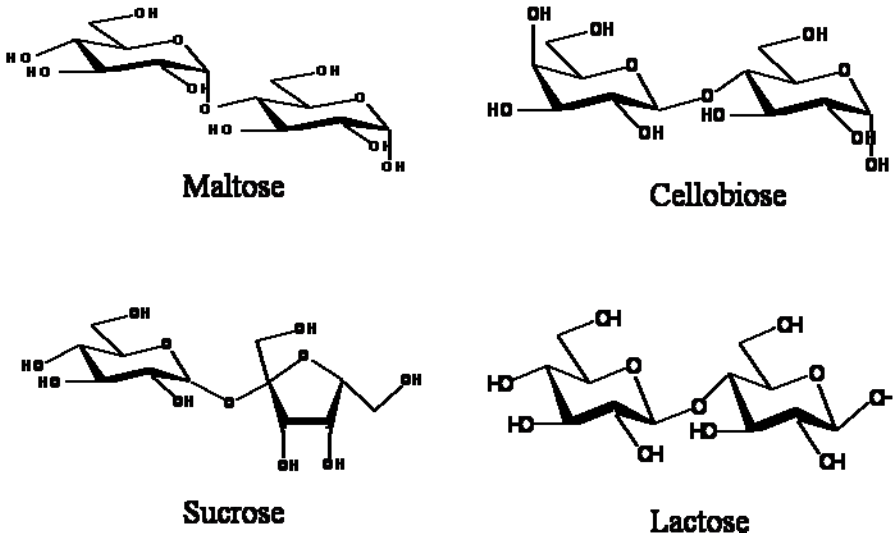

Figure 60. Structure of disaccharides used to evaluate MIP cross-reactivity

The structure of different compounds used to evaluate the cross-reactivity is illustrated in Figure 60. Interaction of fructose to MIP generates at least a 4 fold higher heat signal in comparison with maltose and cellobiose. Interaction of sucrose which contains fructose generates a negligible heat signal (Figure 61). The reason for the lower signal is due to the ´shape selectivity´ of the MIP(Frc) and the decreased affinity to the boronic acid residues. At pH 7.4 phenyl boronic acid in solution was found to have lower association constants for disaccharides (maltose 2.5 M^{-1}; lactose 1.6 M^{-1}; sucrose 0.67 M^{-1}) as compared with monosaccharides (fructose 160 M^{-1}) ; glucose 4.6 M^{-1}).[175]

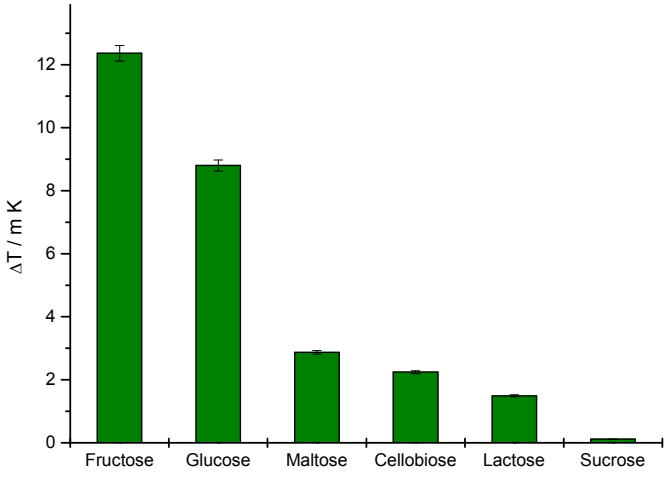

Figure 61. Cross-reactivity of MIP with disaccharides

In the present study the MIP(Frc) shows almost the same binding for maltose and cellobiose and the selectivity towards fructose is approximately 4 fold higher than towards the disaccharides. Striegler had synthesised disaccharide imprinted polymers based on metal coordination interactions and found that the cellobiose imprinted polymer binds 1.7 fold more cellobiose than maltose. On the other hand maltose imprinted polymer shows much lower selectivity and binds only 1.2 fold more maltose than cellobiose. Further maltose imprinted polymer binds less maltose (5 μmol of maltose/ g MIP) compared with glucose (100 μmol of glucose/ g MIP).[209, 210] The difference in the imprinting, binding conditions is attributed to the observed differences in the selectivity.

Earlier Mattiasson et al. reported a calorimetric assay procedure for the determination of cellobiose in the range of 0.05-5 mM. Cellobiose is hydrolysed by β-glucosidase and the glucose formed is calorimetrically measured by an enzyme thermistor containing co-immobilised glucose oxidase and catalase. [211] It is interesting that the MIP against fructose allows direct measurement of cellobiose.

4.4.4 Conclusions

A MIP-thermistor sensor was successfully used to evaluate the cross-reactivity. The cross-reactivity experiment indicates that MIP(Frc) shows higher heat signal to fructose in comparison with the glucose and other disaccharides used in the study. Sucrose is not recognised by MIP. Steady state heat generation should be due to a not yet identified form of sugar present after equilibration at alkaline conditions. Continuous heat generation for 17 h reflects the consumption of β-D-glucose. Amperometric quantification of glucose in the effluent indicates that the consumption of glucose exceeds the theoretical binding capacity of the MIP. Therefore a catalytic reaction would explain the results described in this study.

5.0 SUMMARY

5 SUMMARY

This thesis describes the design, synthesis and evaluation of molecularly imprinted polymers (MIPs) targeting fructosyl valine (Fru-Val), the N-terminal constituent of hemoglobin A1c ß-chains. The main effort was focused towards the development of an imprinted material that would be able to selectively bind Fru-Val.

The covalent approach was used for the first time for the synthesis of molecularly imprinted polymers for a glycated amino acid. It is well known that aryl boronic acid derivatives can react with 1,2 or 1,3-cis-diols in organic or aqueous solvents and offer the possibility to synthesise defined template-monomer constructs. Such controlled stoichiometry leads to the formation of sugar-boronate adducts in a defined geometry and thereby should result in homogeneous binding sites for the sugar.

MIPs were synthesised using the most common cross-linker in molecular imprinting, ethyleneglycol dimethacrylate (EDMA), a cross-linking monomer that comprises both rigidity and moderate hydrophilic/hydrophobic character. However, the aim was to synthesise materials capable of operating in highly aqueous environments, with a minimal non-specific binding. Trifunctional trimethylolpropane trimethacrylate (TRIM) was also used as a cross-linker. The non-specific binding, as estimated by the binding of Fru-Val on the control polymers, was drastically reduced when TRIM was used as a cross-linker for imprinting Fru-Val.

Batch experiments had shown that the MIP(Fru-Val) has a higher affinity for Fru-Val than for fructose and valine. From the batch binding experiments with MIP(Fru-Val) it can be concluded that by optimising the polymer matrix and by tailoring the binding conditions it is possible to minimise the unspecific binding. Taking into account the known advantages of imprinted polymers, e.g. robustness, thermal and chemical stability, imprinted materials were successfully used as a recognition element in the sensor.

It has always been very difficult to transform the binding event into a measurable signal. This is one of the major problems that hinder the development of MIP sensors. Here we demonstrated the possibility to use a "thermometric" approach for the detection of binding events between the MIP and analyte. The big difference between enthalpy for the specific covalent binding of the *vicinal* diol functionalities of the desired carbohydrates by two aromatic boronic acid moieties and non-

specific adsorption to the polymer matrix leads to a higher “apparent imprinting factor” as compared with the batch procedure. It is important to expand this method for a variety of other analytes.

In our thermometric studies with MIP(Frc) we found that the interaction of fresh and equilibrated fructose with MIP(Frc) shows the different thermogram patterns. A similar trend was also observed in the case of glucose. Apart from an exothermic binding process a stable steady state exothermic signal was observed for 17 h with equilibrated glucose. Further measurement of glucose in the effluent of the MIP reactor using an amperometric glucose sensor indicates that almost 10-20 % of the total β-D-glucose is consumed at the steady state. As the glucose consumption exceeds the theoretical binding capacity of the reactor, a catalytic reaction would explain the results presented. Investigations based on NMR have failed to identify the reaction product as the yield is too low to be quantified.

In conclusion I showed that the thermometric approach provides new insight on studying MIP/analyte interactions. One of the serious problems associated with the development of MIP sensors which lies in the absence of a generic procedure for the transduction of the polymer-template binding event into a detectable signal has been addressed by developing the "thermometric" approach. I hope that this thesis, and the studies it is based upon, will facilitate these developments and help to promote the use of MIP sensors for practical use.

6. REFERENCES

6 REFERENCES

1. F. Scheller, F. Schubert, D. Pfeiffer, R. Hintsche, I. Dransfeld, R. Renneberg, U. Wollenberger, K. Riedel, M. Pavlova, M. Kuhn, H.-G. Muller, P.M. Tan, W. Hoffmann, and W. Moritz, *Research and development of biosensors. A review.* Analyst, 1989. **114**:653-662.
2. D.R. Thevenot, K. Toth, R.A. Durst, and G.S. Wilson, *Electrochemical biosensors: Recommended definitions and classification.* Biosensors and Bioelectronics, 2001. **16**:121-131.
3. F.W. Scheller, F. Schubert, and J. Fedrowitz, *Frontiers in Biosensorics.* 1997.Birkäuser Verlag , Switzerland
4. F.W. Scheller, U. Wollenberger, A. Warsinke, and F. Lisdat, *Research and development in biosensors.* Current Opinion in Biotechnology, 2001. **12**:35-40.
5. R. Wilson and A.P.F. Turner, *Glucose oxidase: An ideal enzyme.* Biosensors and Bioelectronics, 1992. **7**:165-185.
6. B.R. Eggins, *Biosensors: An Introduction.* 1996. Wiley-Teubner, Stuttgart, Germany
7. S.F. D'Souza, *Microbial biosensors.* Biosensors and Bioelectronics, 2001. **16**:337-353.
8. I. Karube, T. Matsunaga, S. Mitsuda, and S. Suzuki, *Microbial electrode BOD sensors.* Biotechnology and Bioengineering, 1977. **19**:1535-1547.
9. J. Wannlund and M. DeLuca, *A sensitive bioluminescent immunoassay for dinitrophenol and trinitrotoluene.* Analytical Biochemistry, 1982. **122**:385-393.
10. K.R. Rogers, J.J. Valdes, and M.E. Eldefrawi, *Acetylcholine receptor fiber-optic evanescent fluorosensor.* Analytical Biochemistry, 1989. **182**:353-359.
11. J.C. Fernando, K.R. Rogers, N.A. Anis, J.J. Valdes, R.G. Thompson, A.T. Eldefrawi, and M.E. Eldefrawi, *Rapid detection of anticholinesterase insecticides by a reusable light addressable potentiometric biosensor.* Journal of Agricultural and Food Chemistry, 1993. **41**:511-516.
12. M. Eray, N.S. Dogan, S.R. Reiken, H. Sutisna, B.J. Van Wie, A.R. Koch, D.F. Moffett, M. Silber, and W.C. Davis, *A highly stable and selective biosensor using modified nicotinic acetylcholine receptor (nAChR).* BioSystems, 1995. **35**:183-188.
13. D. Leech, *Affinity biosensors.* Chemical Society Reviews, 1994. **23**:205-213.
14. J. Wang and M.S. Lin, *Mixed plant tissue-carbon paste bioelectrode.* Analytical Chemistry, 1988. **60**:1545-1548.
15. F. Schubert and F.W. Scheller, *Organelle electrodes.* Methods in Enzymology, 1988. **137**:152-160.
16. J. Wang, *From DNA biosensors to gene chips.* Nucleic Acids Research, 2000. **28**:3011-3016.
17. M. Polyakov, *Adsorption properties and structure of silica gel.* Zhurnal Fizicheskoi Khimii, 1931:799.
18. L. Pauling, *A Theory of the Formation of Antibodies.* Journal of the American Chemical Society, 1940. **62**:2643-2657.
19. S. Mudd, *A Hypothetical Mechanism of Antibody Formation.* Journal of Immunology, 1932. **23**:423-427.
20. F. Breinl, Haurowitz, F., *Chemical examinations on the precipitate from haemoglobin and anti-haemoglobin serum and comments on the nature of antibodies.* Z. Physiol. Chem., 1930. **192**:45-57.
21. S.C. Zimmerman and N.G. Lemcoff, *Synthetic hosts via molecular imprinting - are universal synthetic antibodies realistically possible?* Chemical Communications, 2004:5-14.

22. F.H. Dickey, *The Preparation of Specific Adsorbents.* Proceedings of the National Academy of Sciences of the United States of America, 1949. **35**:227-229.
23. T. Takagishi and I.M. Klotz, *Macromolecule-Small Molecule Interactions; Introduction of Additional Binding Sites in Polyethyleneimine by Disulfide Cross-linkages.* Biopolymers, 1972. **11**:483-491.
24. G. Wulff and A. Sarhan, *Use of Polymers with Enzyme-Analogous Structures for Resolution of Racemates.* Angewandte Chemie. International Ed. In English, 1972. **11**:341.
25. R. Arshady and K. Mosbach, *Synthesis of Substrate-Selective Polymers by Host-Guest Polymerization.* Macromolecular Chemistry and Physics, 1981. **182**:687-692.
26. G.A. Theodoridis and I.N. Papadoyannis, *Novel advanced approaches in sample preparation and analyte detection for bioanalysis.* Current Pharmaceutical Analysis, 2006. **2**:385-404.
27. S. Wei and B. Mizaikoff, *Recent advances on noncovalent molecular imprints for affinity separations.* Journal of Separation Science, 2007. **30**:1794-1805.
28. B. Sellergren, *Noncovalent molecular imprinting: Antibody-like molecular recognition in polymeric network materials.* TrAC - Trends in Analytical Chemistry, 1997. **16**:310-320.
29. B. Sellergren, *Imprinted chiral stationary phases in high-performance liquid chromatography.* Journal of Chromatography A, 2001. **906**:227-252.
30. P.A.G. Cormack and A.Z. Elorza, *Molecularly imprinted polymers: synthesis and characterisation.* Journal of Chromatography B-Analytical Technologies in the Biomedical and Life Sciences, 2004. **804**:173-182.
31. R.J. Ansell, D. Kriz, and K. Mosbach, *Molecularly imprinted polymers for bioanalysis: Chromatography, binding assays and biomimetic sensors.* Current Opinion in Biotechnology, 1996. **7**:89-94.
32. A. Merkocj and S. Alegret, *New materials for electrochemical sensing IV. Molecular imprinted polymers.* TrAC - Trends in Analytical Chemistry, 2002. **21**:717-725.
33. L.M. Kindschy and E.C. Alocilja, *A review of molecularly imprinted polymers for biosensor development for food and agricultural applications.* Transactions of the American Society of Agricultural Engineers, 2004. **47**:1375-1382.
34. A. Bossi, F. Bonini, A.P.F. Turner, and S.A. Piletsky, *Molecularly imprinted polymers for the recognition of proteins: The state of the art.* Biosensors and Bioelectronics, 2007. **22**:1131-1137.
35. E.L. Holthoff and F.V. Bright, *Molecularly templated materials in chemical sensing.* Analytica Chimica Acta, 2007. **594**:147-161.
36. M.C. Blanco-Lopez, M.J. Lobo-Castanon, A.J. Miranda-Ordieres, and P. Tunon-Blanco, *Electrochemical sensors based on molecularly imprinted polymers.* Trac-Trends in Analytical Chemistry, 2004. **23**:36-48.
37. J.Q. Liu and G. Wulff, *Functional mimicry of the active site of carboxypeptidase A by a molecular imprinting strategy: Cooperativity of an amidinium and a copper ion in a transition-state imprinted cavity giving rise to high catalytic activity.* Journal of the American Chemical Society, 2004. **126**:7452-7453.
38. J.Q. Liu and G. Wulff, *Molecularly imprinted polymers with strong carboxypeptidase A-like activity: Combination of an amidinium function with a zinc-ion binding site in transition-state imprinted cavities.* Angewandte Chemie. International Ed. In English, 2004. **43**:1287-1290.
39. A. Strikovsky, J. Hradil, and G. Wulff, *Catalytically active, molecularly imprinted polymers in bead form.* Reactive & Functional Polymers, 2003. **54**:49-61.
40. A.G. Strikovsky, D. Kasper, M. Grun, B.S. Green, J. Hradil, and G. Wulff, *Catalytic molecularly imprinted polymers using conventional bulk polymerization or suspension*

polymerization: Selective hydrolysis of diphenyl carbonate and diphenyl carbamate. Journal of the American Chemical Society, 2000. **122**:6295-6296.

41. G. Wulff, T. Gross, and R. Schönfeld, *Enzyme models based on molecularly imprinted polymers with strong esterase activity.* Angewandte Chemie. International Ed. In English, 1997. **36**:1962-1964.
42. J.M. Kim, K.D. Ahn, A.G. Strikovsky, and G. Wulff, *Polymer catalysts by molecular imprinting: A labile covalent bonding approach.* Bulletin of the Korean Chemical Society, 2001. **22**:689-692.
43. J.M. Kim, K.D. Ahn, and G. Wulff, *Cholesterol esterase activity of a molecularly imprinted polymer.* Macromolecular Chemistry and Physics, 2001. **202**:1105-1108.
44. C. Alexander, L. Davidson, and W. Hayes, *Imprinted polymers: Artificial molecular recognition materials with applications in synthesis and catalysis.* Tetrahedron, 2003. **59**:2025-2057.
45. M.A. Markowitz, P.R. Kust, G. Deng, P.E. Schoen, J.S. Dordick, D.S. Clark, and B.P. Gaber, *Catalytic silica particles via template-directed molecular imprinting.* Langmuir, 2000. **16**:1759-1765.
46. K. Polborn and K. Severin, *Molecular imprinting with an organometallic transition state analogue.* Chemical Communications, 1999:2481-2482.
47. F. Locatelli, P. Gamez, and M. Lemaire, *Molecular imprinting of polymerised catalytic complexes in asymmetric catalysis.* Journal of Molecular Catalysis A: Chemical, 1998. **135**:89-98.
48. O. Brüggemann, *Catalytically active polymers obtained by molecular imprinting and their application in chemical reaction engineering.* Biomolecular Engineering, 2001. **18**:1-7.
49. W.R. Ahmad and M.E. Davis, *Transesterification on "imprinted" silica.* Catalysis Letters, 1996. **40**:109-114.
50. A. Volkmann and O. Brüggemann, *Catalysis of an ester hydrolysis applying molecularly imprinted polymer shells based on an immobilised chiral template.* Reactive and Functional Polymers, 2006. **66**:1725-1733.
51. G. Wulff, B.-O. Chong, and U. Kolb, *Soluble single-molecule nanogels of controlled structure as a matrix for efficient artificial enzymes.* Angewandte Chemie. International Ed. In English, 2006. **45**:2955-2958.
52. J. Hedin-Dahlström, J.P. Rosengren-Holmberg, S. Legrand, S. Wikman, and I.A. Nicholls, *A class II aldolase mimic.* Journal of Organic Chemistry, 2006. **71**:4845-4853.
53. P. Pasetto, S.C. Maddock, and M. Resmini, *Synthesis and characterisation of molecularly imprinted catalytic microgels for carbonate hydrolysis.* Analytica Chimica Acta, 2005. **542**:66-75.
54. A. Visnjevski, R. Schomäcker, E. Yilmaz, and O. Brüggemann, *Catalysis of a Diels-Alder cycloaddition with differently fabricated molecularly imprinted polymers.* Catalysis Communications, 2005. **6**:601-606.
55. M. Tada and Y. Iwasawa, *Advanced chemical design with supported metal complexes for selective catalysis.* Chemical Communications, 2006:2833-2844.
56. A. Visnjevski, E. Yilmaz, and O. Bruggemann, *Catalyzing a cycloaddition with molecularly imprinted polymers obtained via immobilized templates.* Applied Catalysis A - General, 2004. **260**:169-174.
57. F. Lanza and B. Sellergren, *Molecularly imprinted extraction materials for highly selective sample cleanup and analyte enrichment.* Advances in Chromatography, 2001. **41**:137-173.
58. C.F. Poole, *New trends in solid-phase extraction.* TrAC - Trends in Analytical Chemistry, 2003. **22**:362-373.

59. F. Lanza and B. Sellergren, *Molecularly Imprinted Polymers via High-Throughput and Combinatorial Techniques.* Macromolecular Rapid Communications, 2004. **25**:59-68.
60. E. Caro, R.M. Marcea, F. Borrull, P.A.G. Cormack, and D.C. Sherrington, *Application of molecularly imprinted polymers to solid-phase extraction of compounds from environmental and biological samples.* TrAC - Trends in Analytical Chemistry, 2006. **25**:143-154.
61. C. Baggiani, L. Anfossi, and C. Giovannoli, *Molecular imprinted polymers: Useful tools for pharmaceutical analysis.* Current Pharmaceutical Analysis, 2006. **2**:219-247.
62. L. Ye and K. Haupt, *Molecularly imprinted polymers as antibody and receptor mimics for assays, sensors and drug discovery.* Analytical and Bioanalytical Chemistry, 2004. **378**:1887-1897.
63. R.J. Ansell, *Molecularly imprinted polymers in pseudoimmunoassay.* Journal of Chromatography B: Analytical Technologies in the Biomedical and Life Sciences, 2004. **804**:151-165.
64. E. Turiel and A. Martin-Esteban, *Molecular imprinting technology in capillary electrochromatography.* Journal of Separation Science, 2005. **28**:719-728.
65. J. Haginaka, *Selectivity of affinity media in solid-phase extraction of analytes.* TrAC - Trends in Analytical Chemistry, 2005. **24**:407-415.
66. A.L. Hillberg, K.R. Brain, and C.J. Allender, *Molecular imprinted polymer sensors: Implications for therapeutics.* Advanced Drug Delivery Reviews, 2005. **57**:1875-1889.
67. R.J. Ansell, *Molecularly imprinted polymers for the enantioseparation of chiral drugs.* Advanced Drug Delivery Reviews, 2005. **57**:1809-1835.
68. D.A. Spivak, *Optimization, evaluation, and characterization of molecularly imprinted polymers.* Advanced Drug Delivery Reviews, 2005. **57**:1779-1794.
69. A.G. Mayes and M.J. Whitcombe, *Synthetic strategies for the generation of molecularly imprinted organic polymers.* Advanced Drug Delivery Reviews, 2005. **57**:1742-1778.
70. B. Sellergren and C.J. Allender, *Molecularly imprinted polymers: A bridge to advanced drug delivery.* Advanced Drug Delivery Reviews, 2005. **57**:1733-1741.
71. D.L. Rathbone, *Molecularly imprinted polymers in the drug discovery process.* Advanced Drug Delivery Reviews, 2005. **57**:1854-1874.
72. K. Karim, F. Breton, R. Rouillon, E.V. Piletska, A. Guerreiro, I. Chianella, and S.A. Piletsky, *How to find effective functional monomers for effective molecularly imprinted polymers?* Advanced Drug Delivery Reviews, 2005. **57**:1795-1808.
73. C. Nilsson and S. Nilsson, *Nanoparticle-based pseudostationary phases in capillary electrochromatography.* Electrophoresis, 2006. **27**:76-83.
74. V. Pichon and K. Haupt, *Affinity separations on molecularly imprinted polymers with special emphasis on solid-phase extraction.* Journal of Liquid Chromatography and Related Technologies, 2006. **29**:989-1023.
75. E. Oral and N.A. Peppas, *Hydrophilic molecularly imprinted poly(hydroxyethyl-methacrylate) polymers.* Journal of Biomedical Materials Research - Part A, 2006. **78**:205-210.
76. J.A. Garcia-Calzon and M.E. Diaz-Garcia, *Characterization of binding sites in molecularly imprinted polymers.* Sensors and Actuators, B: Chemical, 2007. **123**:1180-1194.
77. V. Pichon, *Selective sample treatment using molecularly imprinted polymers.* Journal of Chromatography A, 2007. **1152**:41-53.
78. F. BelHadj-Kaabi and V. Pichon, *Different approaches to synthesizing moleculariy imprinted polymers for solid-phase extraction.* LC-GC Europe, 2007. **20**:406-413.

79. B. Preinerstorfer and M. Lämmerhofer, *Recent accomplishments in the field of enantiomer separation by CEC.* Electrophoresis, 2007. **28**:2527-2565.
80. B. Sellergren and K.J. Shea, *Influence of Polymer Morphology on the Ability of Imprinted Network Polymers to Resolve Enantiomers.* Journal of Chromatography, 1993. **635**:31-49.
81. D. Batra and K.J. Shea, *Combinatorial methods in molecular imprinting.* Current Opinion in Chemical Biology, 2003. **7**:434-442.
82. K.J. Shea and T.K. Dougherty, *Molecular Recognition on Synthetic Amorphous Surfaces - the Influence of Functional-Group Positioning on the Effectiveness of Molecular Recognition.* Journal of the American Chemical Society, 1986. **108**:1091-1093.
83. K.J. Shea, E.A. Thompson, S.D. Pandey, and P.S. Beauchamp, *Template Synthesis of Macromolecules - Synthesis and Chemistry of Functionalized Macroporous Polydivinylbenzene.* Journal of the American Chemical Society, 1980. **102**:3149-3155.
84. C. Alexander, H.S. Andersson, L.I. Andersson, R.J. Ansell, N. Kirsch, I.A. Nicholls, J. O'Mahony, and M.J. Whitcombe, *Molecular imprinting science and technology: a survey of the literature for the years up to and including 2003.* Journal of Molecular Recognition, 2006. **19**:106-180.
85. S. Piletsky and A.P.F. Turner, *Molecular Imprinting of Polymers.* 2006. Landes Bioscience, UK
86. B. Sellergren, *Molecularly Imprinted Polymers - Man-made Mimics of Antibodies and Their Applications in Analytical Chemistry.* Elsevier Amsterdam, 2001.
87. M.J. Whitcombe, M.E. Rodriguez, P. Villar, and E.N. Vulfson, *A New Method for the Introduction of Recognition Site Functionality into Polymers Prepared by Molecular Imprinting - Synthesis and Characterization of Polymeric Receptors for Cholesterol.* Journal of the American Chemical Society, 1995. **117**:7105-7111.
88. P.K. Dhal and F.H. Arnold, *Template-Mediated Synthesis of Metal-Complexing Polymers for Molecular Recognition.* Journal of the American Chemical Society, 1991. **113**:7417-7418.
89. K. Lettau, A. Warsinke, A. Laschewsky, K. Mosbach, E. Yilmaz, and F.W. Scheller, *An esterolytic imprinted polymer prepared via a silica-supported transition state analogue.* Chemistry of Materials, 2004. **16**:2745-2749.
90. E. Yilmaz, K. Haupt, and K. Mosbach, *The use of immobilized templates - A new approach in molecular imprinting.* Angewandte Chemie. International Ed. In English, 2000. **39**:2115-2118.
91. M.M. Titirici, A.J. Hall, and B. Sellergren, *Hierarchically imprinted stationary phases: Mesoporous polymer beads containing surface-confined binding sites for adenine.* Chemistry of Materials, 2002. **14**:21-23.
92. M.M. Titirici, A.J. Hall, and B. Sellergren, *Hierarchical imprinting using crude solid phase peptide synthesis products as templates.* Chemistry of Materials, 2003. **15**:822-824.
93. C. Sulitzky, B. Ruckert, A.J. Hall, F. Lanza, K. Unger, and B. Sellergren, *Grafting of molecularly imprinted polymer films on silica supports containing surface-bound free radical initiators.* Macromolecules, 2002. **35**:79-91.
94. A.G. Mayes and K. Mosbach, *Molecularly imprinted polymer beads: Suspension fbupolymerization using a liquid perfluorocarbon as the dispersing phase.* Analytical Chemistry, 1996. **68**:3769-3774.
95. L. Ye, P.A.G. Cormack, and K. Mosbach, *Molecular imprinting on microgel spheres.* Analytica Chimica Acta, 2001. **435**:187-196.
96. L. Ye, P.A.G. Cormack, and K. Mosbach, *Molecularly imprinted monodisperse microspheres for competitive radioassay.* Analytical Communications, 1999. **36**:35-38.

97. K. Hosoya, K. Yoshizako, N. Tanaka, K. Kimata, T. Araki, and J. Haginaka, *Uniform-Size Macroporous Polymer-Based Stationary-Phase for Hplc Prepared through Molecular Imprinting Technique.* Chemistry Letters, 1994:1437-1438.
98. N. Pérez, M.J. Whitcombe, and E.N. Vulfson, *Surface imprinting of cholesterol on submicrometer core-shell emulsion particles.* Macromolecules, 2001. **34**:830-836.
99. N. Pérez, M.J. Whitcombe, and E.N. Vulfson, *Molecularly imprinted nanoparticles prepared by core-shell emulsion polymerization.* Journal of Applied Polymer Science, 2000. **77**:1851-1859.
100. M. Lehmann, H. Brunner, and G.E.M. Tovar, *Selective separations and hydrodynamic studies: A new approaoch using molecularly imprinted nanosphere composite membranes.* Desalination, 2002. **149**:315-321.
101. D. Vaihinger, K. Landfester, I. Krauter, H. Brunner, and G.E.M. Tovar, *Molecularly imprinted polymer nanospheres as synthetic affinity receptors obtained by miniemulsion polymerisation.* Macromolecular Chemistry and Physics, 2002. **203**:1965-1973.
102. S.C. Zimmerman, M.S. Wendland, N.A. Rakow, I. Zharov, and K.S. Suslick, *Synthetic hosts by monomolecular imprinting inside dendrimers.* Nature, 2002. **418**:399-403.
103. T.A. Sergeyeva, S.A. Piletsky, A.A. Brovko, E.A. Slinchenko, L.M. Sergeeva, and A.V. El'skaya, *Selective recognition of atrazine by molecularly imprinted polymer membranes. Development of conductometric sensor for herbicides detection.* Analytica Chimica Acta, 1999. **392**:105-111.
104. J. Mathew-Krotz and K.J. Shea, *Imprinted polymer membranes for the selective transport of targeted neutral molecules.* Journal of the American Chemical Society, 1996. **118**:8154-8155.
105. E. Hedborg, F. Winquist, I. Lundstrom, L.I. Andersson, and K. Mosbach, *Some Studies of Molecularly-Imprinted Polymer Membranes in Combination with Field-Effect Devices.* Sensors and Actuators a-Physical, 1993. **37-8**:796-799.
106. N. Sallacan, M. Zayats, T. Bourenko, A.B. Kharitonov, and I. Willner, *Imprinting of nucleotide and monosaccharide recognition sites in acrylamidephenylboronic acid-acrylamide copolymer membranes associated with electronic transducers.* Analytical Chemistry, 2002. **74**:702-712.
107. S.P. Pogorelova, T. Bourenko, A.B. Kharitonov, and I. Willner, *Selective sensing of triazine herbicides in imprinted membranes using ion-sensitive field-effect transistors and microgravimetric quartz crystal microbalance measurements.* Analyst, 2002. **127**:1484-1491.
108. K. Haupt and K. Mosbach, *Molecularly Imprinted Polymers and Their Use in Biomimetic Sensors.* Chemical Reviews, 2000. **100**:2495-2504.
109. L.I. Andersson, C.F. Mandenius, and K. Mosbach, *Studies on guest selective molecular recognition on an octadecyl silylated silicon surface using ellipsometry.* Tetrahedron Letters, 1988. **29**:5437-5440.
110. E.P.C. Lai, A. Fafara, V.A. VanderNoot, M. Kono, and B. Polsky, *Surface plasmon resonance sensors using molecularly imprinted polymers for sorbent assay of theophylline, caffeine, and xanthine.* Canadian Journal of Chemistry-Revue Canadienne De Chimie, 1998. **76**:265-273.
111. T.L. Panasyuk, V.M. Mirsky, S.A. Piletsky, and O.S. Wolfbeis, *Electropolymerized molecularly imprinted polymers as receptor layers in a capacitive chemical sensors.* Analytical Chemistry, 1999. **71**:4609-4613.
112. F.L. Dickert, P. Forth, P. Lieberzeit, and M. Tortschanoff, *Molecular imprinting in chemical sensing - Detection of aromatic and halogenated hydrocarbons as well as polar solvent vapors.* Fresenius' Journal of Analytical Chemistry, 1998. **360**:759-762.

113. C. Malitesta, I. Losito, and P.G. Zambonin, *Molecularly imprinted electrosynthesized polymers: New materials for biomimetic sensors.* Analytical Chemistry, 1999. **71**:1366-1370.
114. K. Haupt, K. Noworyta, and W. Kutner, *Imprinted polymer-based enantioselective acoustic sensor using a quartz crystal microbalance.* Analytical Communications, 1999. **36**:391-393.
115. B. Jakoby, G.M. Ismail, M.P. Byfield, and M.J. Vellekoop, *Novel molecularly imprinted thin film applied to a Love wave gas sensor.* Sensors and Actuators, A: Physical, 1999. **76**:93-97.
116. M. Jakusch, M. Janotta, B. Mizaikoff, K. Mosbach, and K. Haupt, *Molecularly imprinted polymers and infrared evanescent wave spectroscopy. A chemical sensors approach.* Analytical Chemistry, 1999. **71**:4786-4791.
117. D. Kriz, O. Ramström, A. Svensson, and K. Mosbach, *Introducing biomimetic sensors based on molecularly imprinted polymers as recognition elements.* Analytical Chemistry, 1995. **67**:2142-2144.
118. F.L. Dickert, M. Tortschanoff, W.E. Bulst, and G. Fischerauer, *Molecularly imprinted sensor layers for the detection of polycyclic aromatic hydrocarbons in water.* Analytical Chemistry, 1999. **71**:4559-4563.
119. D. Kriz and K. Mosbach, *Competitive amperometric morphine sensor based on an agarose immobilised molecularly imprinted polymer.* Analytica Chimica Acta, 1995. **300**:71-75.
120. R. Levi, S. McNiven, S.A. Piletsky, S.-H. Cheong, K. Yano, and I. Karube, *Optical detection of chloramphenicol using molecularly imprinted polymers.* Analytical Chemistry, 1997. **69**:2017-2021.
121. S. Kroger, A.P.F. Turner, K. Mosbach, and K. Haupt, *Imprinted polymer based sensor system for herbicides using differential-pulse voltammetry on screen printed electrodes.* Analytical Chemistry, 1999. **71**:3698-3702.
122. G.H. Chen, Z.B. Guan, C.T. Chen, L.T. Fu, V. Sundaresan, and F.H. Arnold, *A glucose-sensing polymer.* Nature Biotechnology, 1997. **15**:354-357.
123. P. Turkewitsch, B. Wandelt, G.D. Darling, and W.S. Powell, *Fluorescent Functional Recognition Sites through Molecular Imprinting. A Polymer-Based Fluorescent Chemosensor for Aqueous cAMP.* Analytical Chemistry, 1998. **70**:2025-2030.
124. F.L. Dickert and O. Hayden, *Molecular fingerprints using imprinting techniques.* Advanced Materials, 2000. **12**:311-314.
125. F.L. Dickert, O. Hayden, and K.P. Halikias, *Synthetic receptors as sensor coatings for molecules and living cells.* Analyst, 2001. **126**:766-771.
126. F.L. Dickert, O. Hayden, P. Lieberzeit, C. Haderspoeck, R. Bindeus, C. Palfinger, and B. Wirl, *Nano- and micro-structuring of sensor materials - from molecule to cell detection.* Synthetic Metals, 2003. **138**:65-69.
127. F.L. Dickert, P. Lieberzeit, and O. Hayden, *Sensor strategies for microorganism detection - from physical principles to imprinting procedures.* Analytical and Bioanalytical Chemistry, 2003. **377**:540-549.
128. P.A. Lieberzeit, A. Afzal, G. Glanzing, and F.L. Dickert, *Molecularly imprinted sol-gel nanoparticles for mass-sensitive engine oil degradation sensing.* Analytical and Bioanalytical Chemistry, 2007. **389**:441-446.
129. R. Suedee, W. Intakong, and F.L. Dickert, *The use of trichloroacetic acid imprinted polymer coated quartz crystal microbalance as a screening method for determination of haloacetic acids in drinking water.* Talanta, 2006. **70**:194-201.
130. O. Hayden and F.L. Dickert, *Selective microorganism detection with cell surface imprinted polymers.* Advanced Materials, 2001. **13**:1480-1483.

131. O. Hayden, P.A. Lieberzeit, D. Blaas, and F.L. Dickert, *Artificial antibodies for bioanalyte detection - Sensing viruses and proteins.* Advanced Functional Materials, 2006. **16**:1269-1278.
132. O. Hayden, K.-J. Mann, S. Krassnig, and F.L. Dickert, *Biomimetic ABO blood-group typing.* Angewandte Chemie. International Ed. In English, 2006. **45**:2626-2629.
133. I. Chianella, S.A. Piletsky, I.E. Tothill, B. Chen, and A.P.F. Turner, *MIP-based solid phase extraction cartridges combined with MIP- based sensors for the detection of microcystin-LR.* Biosensors and Bioelectronics, 2003. **18**:119-127.
134. C.J. Percival, S. Stanley, M. Galle, A. Braithwaite, M.I. Newton, G. McHale, and W. Hayes, *Molecular-imprinted, polymer-coated quartz crystal microbalances for the detection of terpenes.* Analytical Chemistry, 2001. **73**:4225-4228.
135. A. Kugimiya and T. Takeuchi, *Molecularly imprinted polymer-coated quartz crystal microbalance for detection of biological hormone.* Electroanalysis, 1999. **11**:1158-1160.
136. H.-S. Ji, S. McNiven, K. Ikebukuro, and I. Karube, *Selective piezoelectric odor sensors using molecularly imprinted polymers.* Analytica Chimica Acta, 1999. **390**:93-100.
137. A. Ersöz, A. Denizli, A. Özcan, and R. Say, *Molecularly imprinted ligand-exchange recognition assay of glucose by quartz crystal microbalance.* Biosensors and Bioelectronics, 2005. **20**:2197-2202.
138. D.-F. Tai, C.-Y. Lin, T.-Z. Wu, and L.-K. Chen, *Recognition of dengue virus protein using epitope-mediated molecularly imprinted film.* Analytical Chemistry, 2005. **77**:5140-5143.
139. C. Ayela, F. Vandevelde, D. Lagrange, K. Haupt, and L. Nicu, *Combining Resonant Piezoelectric Micromembranes with Molecularly Imprinted Polymers.* Angewandte Chemie. International Ed. In English, 2007 (In Press).
140. A. Graefe, K. Haupt, and G.J. Mohr, *Optical sensor materials for the detection of amines in organic solvents.* Analytica Chimica Acta, 2006. **565**:42-47.
141. S.A. Piletsky, E.V. Piletskaya, K. Yano, A. Kugimiya, A.V. Elgersma, R. Levi, U. Kahlow, T. Takeuchi, I. Karube, T.I. Panasyuk, and A.V. El'skaya, *A biomimetic receptor system for sialic acid based on molecular imprinting.* Analytical Letters, 1996. **29**:157-170.
142. S. Subrahmanyam, S.A. Piletsky, E.V. Piletska, B.N. Chen, K. Karim, and A.P.F. Turner, *'Bite-and-Switch' approach using computationally designed molecularly imprinted polymers for sensing of creatinine.* Biosensors and Bioelectronics, 2001. **16**:631-637.
143. S. Subrahmanyam, S.A. Piletsky, E.V. Piletska, B. Chen, R. Day, and A.P.F. Turner, *"Bite-and-Switch" Approach to Creatinine Recognition by Use of Molecularly Imprinted Polymers.* Advanced Materials (Weinheim, Federal Republic of Germany), 2000. **12**:722-724.
144. S.A. Piletsky, E.V. Piletskaya, A.V. El'skaya, R. Levi, K. Yano, and I. Karube, *Optical detection system for triazine based on molecularly-imprinted polymers.* Analytical Letters, 1997. **30**:445-455.
145. L. Ye and K. Mosbach, *Polymers recognizing biomolecules based on a combination of molecular imprinting and proximity scintillation: A new sensor concept.* Journal of the American Chemical Society, 2001. **123**:2901-2902.
146. D.L. Rathbone, D. Su, Y. Wang, and D.C. Billington, *Molecular recognition by fluorescent imprinted polymers.* Tetrahedron Letters, 2000. **41**:123-126.
147. N.T.K. Thanh, D.L. Rathbone, D.C. Billington, and N.A. Hartell, *Selective recognition of cyclic GMP using a fluorescence-based molecularly imprinted polymer.* Analytical Letters, 2002. **35**:2499-2509.

148. W. Wang, S. Gao, and B. Wang, *Building fluorescent sensors by template polymerization: The preparation of a fluorescent sensor for d-Fructose.* Organic Letters, 1999. **1**:1209-1212.
149. S. Gao, W. Wang, and B. Wang, *Building fluorescent sensors for carbohydrates using template-directed polymerizations.* Bioorganic Chemistry, 2001. **29**:308-320.
150. I. Surugiu, B. Danielsson, L. Ye, K. Mosbach, and K. Haupt, *Chemiluminescence Imaging ELISA Using an Imprinted Polymer as the Recognition Element Instead of an Antibody.* Analytical Chemistry, 2001. **73**:487-491.
151. I. Surugiu, J. Svitel, L. Ye, K. Haupt, and B. Danielsson, *Development of a flow injection capillary chemiluminescent ELISA using an imprinted polymer instead of the antibody.* Analytical Chemistry, 2001. **73**:4388-4392.
152. K. Haupt, *Molecularly imprinted sorbent assays and the use of non-related probes.* Reactive and Functional Polymers, 1999. **41**:125-131.
153. B.R. Arnold, A.C. Euler, A.L. Jenkins, O.M. Uy, and G.M. Murray, *Progress in the development of molecularly imprinted polymer sensors.* Johns Hopkins APL Technical Digest (Applied Physics Laboratory), 1999. **20**:190-198.
154. A.L. Jenkins, O.M. Uy, and G.M. Murray, *Polymer Based Lanthanide Luminescent Sensors for the Detection of Nerve Agents.* Analytical Communications, 1997. **34**:221-224.
155. A.L. Jenkins, O.M. Uy, and G.M. Murray, *Polymer-based lanthanide luminescent sensor for detection of the hydrolysis product of the nerve agent soman in water.* Analytical Chemistry, 1999. **71**:373-378.
156. A. Kugimiya and T. Takeuchi, *Surface plasmon resonance sensor using molecularly imprinted polymer for detection of sialic acid.* Biosensors and Bioelectronics, 2001. **16**:1059-1062.
157. T. Matsunaga, T. Hishiya, and T. Takeuchi, *Surface plasmon resonance sensor for lysozyme based on molecularly imprinted thin films.* Analytica Chimica Acta, 2007. **591**:63-67.
158. O.A. Raitman, V.I. Chegel, A.B. Kharitonov, M. Zayats, E. Katz, and I. Willner, *Analysis of NAD(P)+ and NAD(P)H cofactors by means of imprinted polymers associated with Au surfaces: A surface plasmon resonance study.* Analytica Chimica Acta, 2004. **504**:101-111.
159. D. Nopper, O. Lammershop, G. Wulff, and G. Gauglitz, *Amidine-based molecularly imprinted polymers - new sensitive elements for chiral chemosensors.* Analytical and Bioanalytical Chemistry, 2003. **377**:608-613.
160. S.A. Piletsky, E.V. Piletskaya, T.L. Panasyuk, A.V. El'skaya, R. Levi, I. Karube, and G. Wulff, *Imprinted membranes for sensor technology: Opposite behavior of covalently and noncovalently imprinted membranes.* Macromolecules, 1998. **31**:2137-2140.
161. S.A. Piletsky and A.P.F. Turner, *Electrochemical sensors based on molecularly imprinted polymers.* Electroanalysis, 2002. **14**:317-323.
162. Z. Cheng, E. Wang, and X. Yang, *Capacitive detection of glucose using molecularly imprinted polymers.* Biosensors and Bioelectronics, 2001. **16**:179-185.
163. M.C. Blanco-Lopez, M.J. Lobo-Castanon, A.J. Miranda-Ordieres, and P. Tunon-Blanco, *Voltammetric response of diclofenac-molecularly imprinted film modified carbon electrodes.* Analytical and Bioanalytical Chemistry, 2003. **377**:257-261.
164. M.C. Blanco-Lopez, M.J. Lobo-Castanon, A.J. Miranda-Ordieres, and P. Tunon-Blanco, *Voltammetric sensor for vanillylmandelic acid based on molecularly imprinted polymer-modified electrodes.* Biosensors and Bioelectronics, 2003. **18**:353-362.

165. K. Sode, S. Ohta, Y. Yanai, and T. Yamazaki, *Construction of a molecular imprinting catalyst using target analogue template and its application for an amperometric fructosylamine sensor.* Biosensors and Bioelectronics, 2003. **18**:1485-1490.
166. K. Sode, Y. Takahashi, S. Ohta, W. Tsugawa, and T. Yamazaki, *A new concept for the construction of an artificial dehydrogenase for fructosylamine compounds and its application for an amperometric fructosylamine sensor.* Analytica Chimica Acta, 2001. **435**:151-156.
167. M. Riskin, R. Tel-Vered, and I. Willner, *The Imprint of Electropolymerized Polyphenol Films on Electrodes by Donor-Acceptor Interactions: Selective Electrochemical Sensing of N,Nprime-dimethyl-4,4prime-bipyridinium (Methyl Viologen).* Advanced Functional Materials, 2007 (In Press).
168. W.-Y. Chen, C.-S. Chen, and F.-Y. Lin, *Molecular recognition in imprinted polymers: Thermodynamic investigation of analyte binding using microcalorimetry.* Journal of Chromatography A, 2001. **923**:1-6.
169. R. Kirchner, J. Seidel, G. Wolf, and G. Wulff, *Calorimetric investigation of chiral recognition processes in a molecularly imprinted polymer.* Journal of Inclusion Phenomena and Macrocyclic Chemistry, 2002. **43**:279-283.
170. A. Weber, M. Dettling, H. Brunner, and G.E.M. Tovar, *Isothermal titration calorimetry of molecularly imprinted polymer nanospheres.* Macromolecular Rapid Communications, 2002. **23**:824-828.
171. J. Rick and T.-C. Chou, *Enthalpy changes associated with protein binding to thin films.* Biosensors and Bioelectronics, 2005. **20**:1878-1883.
172. K. Lettau, A. Warsinke, M. Katterle, B. Danielsson, and F.W. Scheller, *A bifunctional Molecularly Imprinted Polymer (MIP): Analysis of binding and catalysis by a thermistor.* Angewandte Chemie. International Ed. In English, 2006. **45**:6986-6990.
173. B. Danielsson and K. Mosbach, *Enzyme thermistor devices.* Methods in Enzymology, 1976. **44**:667-676.
174. K. Mosbach and B. Danielsson, *An enzyme thermistor.* Biochimica et Biophysica Acta, 1974. **364**:140-145.
175. G. Springsteen and B.H. Wang, *A detailed examination of boronic acid-diol complexation.* Tetrahedron, 2002. **58**:5291-5300.
176. A. Lapolla, P. Traldi, and D. Fedele, *Importance of measuring products of non-enzymatic glycation of proteins.* Clin Biochem., 2005. **38**:103-115.
177. P.J. Bilan and A. Klip, *Glycation of the human erythrocyte glucose transporter in vitro and its functional consequences.* Biochem J., 1990. **268**:661-667.
178. D. Stollner, W. Stocklein, F. Scheller, and A. Warsinke, *Membrane-immobilized haptoglobin as affinity matrix for a hemoglobin-A1c immunosensor.* Analytica Chimica Acta, 2002. **470**:111-119.
179. P. Keil, H.B. Mortensen, and C. Christophersen, *Fructosylvaline. A simple model of the N-terminal residue of human haemoglobin A1c.* Acta Chem Scand B., 1985. **39**:191-193.
180. G. Wulff and S. Schauhoff, *Enzyme-Analog-Built Polymers .27. Racemic-Resolution of Free Sugars with Macroporous Polymers Prepared by Molecular Imprinting - Selectivity Dependence on the Arrangement of Functional-Groups Versus Spatial Requirements.* Journal of Organic Chemistry, 1991. **56**:395-400.
181. B.L. Somani, J. Khanade, and R. Sinha, *A modified anthrone-sulfuric acid method for the determination of fructose in the presence of certain proteins.* Anal Biochem, 1987. **167**:327-30.

182. R. Fields, *The rapid determination of amino groups with TNBS*, in *Methods in Enzymology Part B: Enzyme Structure*, C.H.W.H.a.S.N. Timasheff, Editor. 1972, Academic Press. p. 464-468.
183. R. Rajkumar, A. Warsinke, M. Katterle, H. Mohwald, and F. Scheller, *Synthesis and thermometric application of a molecularly imprinted polymer for fructosyl valine.* Tissue Engineering, 2007. **13**:889-890.
184. X.C. Liu, J.L. Hubbard, and W.H. Scouten, *Synthesis and Structural Investigation of 2 Potential Boronate Affinity-Chromatography Ligands Catechol [2-(Diisopropylamino) Carbonyl]Phenylboronate and Catechol [2-(Diethylamino)Carbonyl, 4-Methyl]Phenylboronate.* Journal of Organometallic Chemistry, 1995. **493**:91-94.
185. G. Wulff, J. Vietmeier, and H.G. Poll, *Enzyme-Analog Built Polymers .22. Influence of the Nature of the Cross-Linking Agent on the Performance of Imprinted Polymers in Racemic-Resolution.* Makromolekulare Chemie-Macromolecular Chemistry and Physics, 1987. **188**:731-740.
186. M. Kempe, *Antibody-Mimicking polymers as chiral stationary phases in HPLC.* Analytical Chemistry, 1996. **68**:1948-1953.
187. S. Striegler, *Designing selective sites in templated polymers utilizing coordinative bonds.* Journal of Chromatography B: Analytical Technologies in the Biomedical and Life Sciences, 2004. **804**:183-195.
188. J. Cederfur, Y. Pei, M. Zihui, and M. Kempe, *Synthesis and screening of a molecularly imprinted polymer library targeted for penicillin G.* J Comb Chem, 2003. **5**:67-72.
189. F.A. El-Toufaili, A. Visnjevski, and O. Bruggemann, *Screening combinatorial libraries of molecularly imprinted polymer films casted on membranes in single-use membrane modules.* J Chromatogr B Analyt Technol Biomed Life Sci, 2004. **804**:135-9.
190. S. Kaess, *Anwendung der Matrizenpolymerisation auf die Racemattrennung nicht derivatisierter Monosaccharide und Untersuchungen zur Eignung der 2-N,N-Dimethylaminophenylboronsäure als Haftgruppe.* PhD Thesis, 1988. Heinrich Heine University, Duesseldorf.
191. T. Takeuchi and J. Haginaka, *Separation and sensing based on molecular recognition using molecularly imprinted polymers.* Journal of Chromatography B, 1999. **728**:1-20.
192. D. Kriz, M. Kempe, and K. Mosbach, *Introduction of molecularly imprinted polymers as recognition elements in conductometric chemical sensors.* Sensors and Actuators, B: Chemical, 1996. **33**:178-181.
193. L.I. Andersson, *Molecular imprinting: developments and applications in the analytical chemistry field.* Journal of Chromatography B, 2000. **745**:3-13.
194. K. Yano and I. Karube, *Molecularly imprinted polymers for biosensor applications.* TrAC - Trends in Analytical Chemistry, 1999. **18**:199-204.
195. G. Vlatakis, L.I. Andersson, R. Mueller, and K. Mosbach, *Drug assay using antibody mimics made by molecular imprinting.* Nature (London, United Kingdom), 1993. **361**:645-7.
196. A.G. Mayes and K. Mosbach, *Molecularly imprinted polymers: Useful materials for analytical chemistry?* TrAC - Trends in Analytical Chemistry, 1997. **16**:321-332.
197. S. Vidyasankar and F.H. Arnold, *Molecular Imprinting: selective materials for separations, sensors and catalysis.* ,Curr. Opin. Biotechnol, 1995. **6**:218.
198. C.J. Allender, *Molecularly imprinted polymers: Technology and applications.* Advanced Drug Delivery Reviews, 2005. **57**:1731-1732.
199. J.M. Conner and B. V.C., *Equilibria between borate ion and some polyols in aqueous solution.* Journal of Inorganic and Nuclear Chemistry, 1967. **29**:1953-1961.

200. G. Wulff and H.G. Poll, *Enzyme-Analog Built Polymers .23. Influence of the Structure of the Binding-Sites on the Selectivity for Racemic-Resolution.* Makromolekulare Chemie-Macromolecular Chemistry and Physics, 1987. **188**:741-748.
201. R. Rajkumar, A. Warsinke, M. Katterle, H. Mohwald, and F. Scheller, *Thermometric MIP Sensor for Fructosyl Valine.* Biosensors and Bioelectronics, 2007.In Press
202. S. Hideyuki, M. Takeuchi, and S. Shinkai, *Spectroscopic detection of diols and sugars by a colour change in boronic acid-appended spirobenzopyrans.* J. Chem. Soc., Perkin Trans. 2, 1996:1-3.
203. D. Spivak, M.A. Gilmore, and K.J. Shea, *Evaluation of binding and origins of specificity of 9-ethyladenine imprinted polymers.* Journal of the American Chemical Society, 1997. **119**:4388-4393.
204. G. Wulff, *Selective bindingh to polymers Via covalent bonds the construction of chiral cavities as specific receptor sites.* Pure and Applied Chemistry, 1982. **54**:2093-2102.
205. B. Sellergren, *Molecular Imprinting by noncovalent interactions - Development and Applications in Molecular Recognition*, in *Pure and Applied Biochemistry*. 1988, Lund University: Lund.
206. R. Rajkumar, A. Warsinke, H. Mohwald, F.W. Scheller, and M. Katterle, *Development of fructosyl valine binding polymers by covalent imprinting.* Biosensors and Bioelectronics, 2007. **22**:3318-3325.
207. M.P. Nicholls and P.K.C. Paul, *Structures of carbohydrate-boronic acid complexes determined by NMR and molecular modelling in aqueous alkaline media.* Organic and Biomolecular Chemistry, 2004. **2**:1434-1441.
208. P. Dais and A.S. Perlin, *Intramolecular hydrogen-bonding and solvation contributions to the relative stability of the b-furanose form of Image-fructose in dimethyl sulfoxide.* Carbohydrate Research, 1987. **169,**:159-169.
209. S. Striegler, *Investigation of disaccharide recognition by molecularly imprinted polymers.* Bioseparation, 2001. **10**:307-314.
210. S. Striegler, *Selective carbohydrate recognition by synthetic receptors in aqueous solution.* Current Organic Chemistry, 2003. **7**:81-102.
211. B. Mattiasson and B. Danielsson, *Calorimetric analysis of sugars and sugar derivatives with aid of an enzyme thermistor.* Carbohydrate Research, 1982. **102**:273-282.

7 Appendix

S1

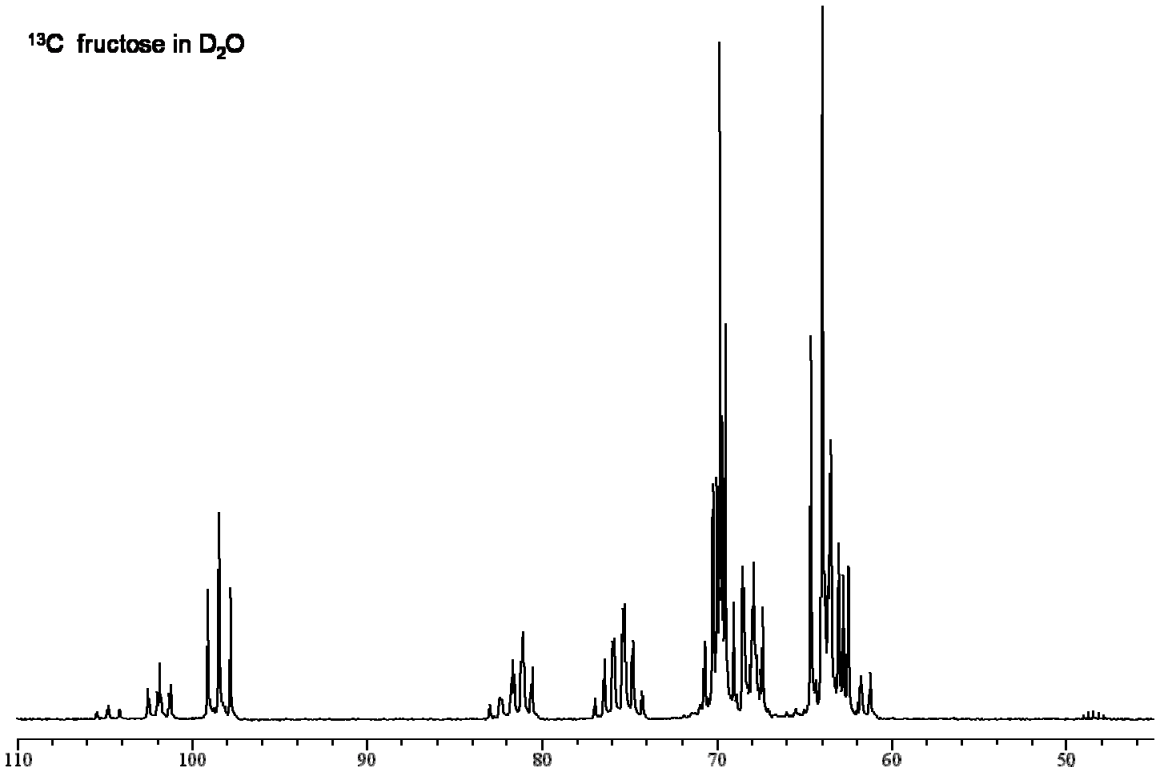

S2

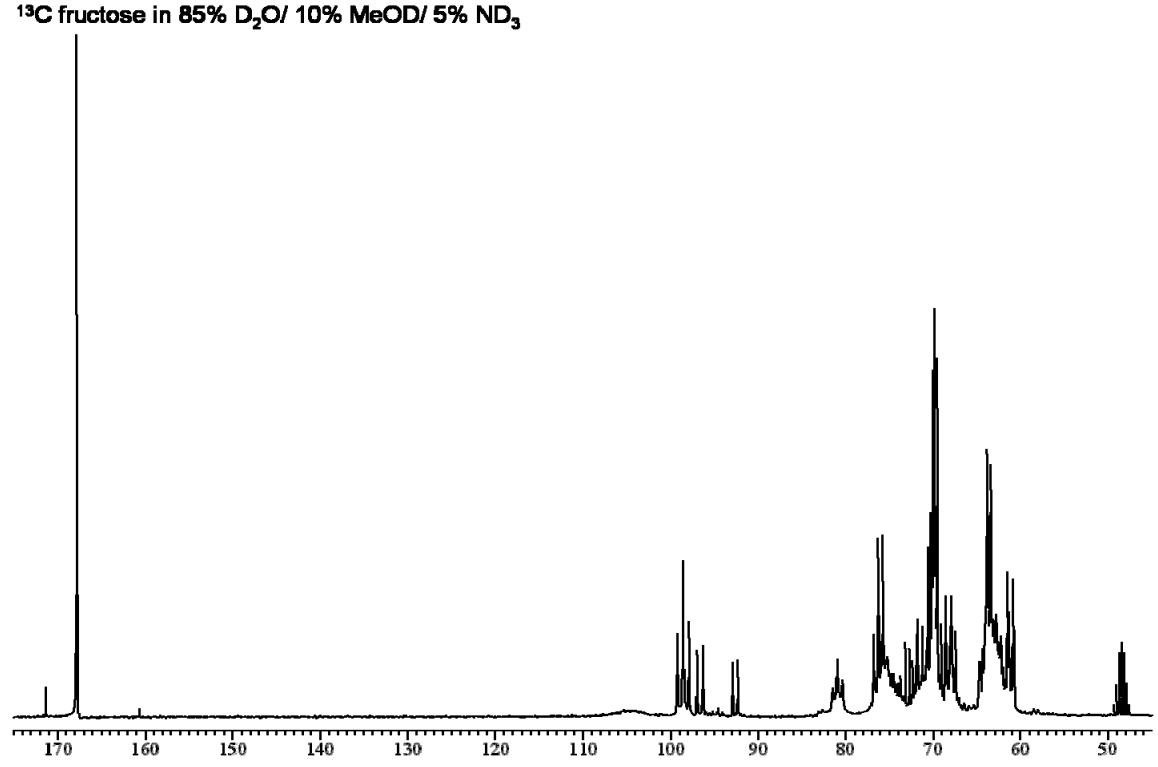

S3

^{13}C glucose in D_2O

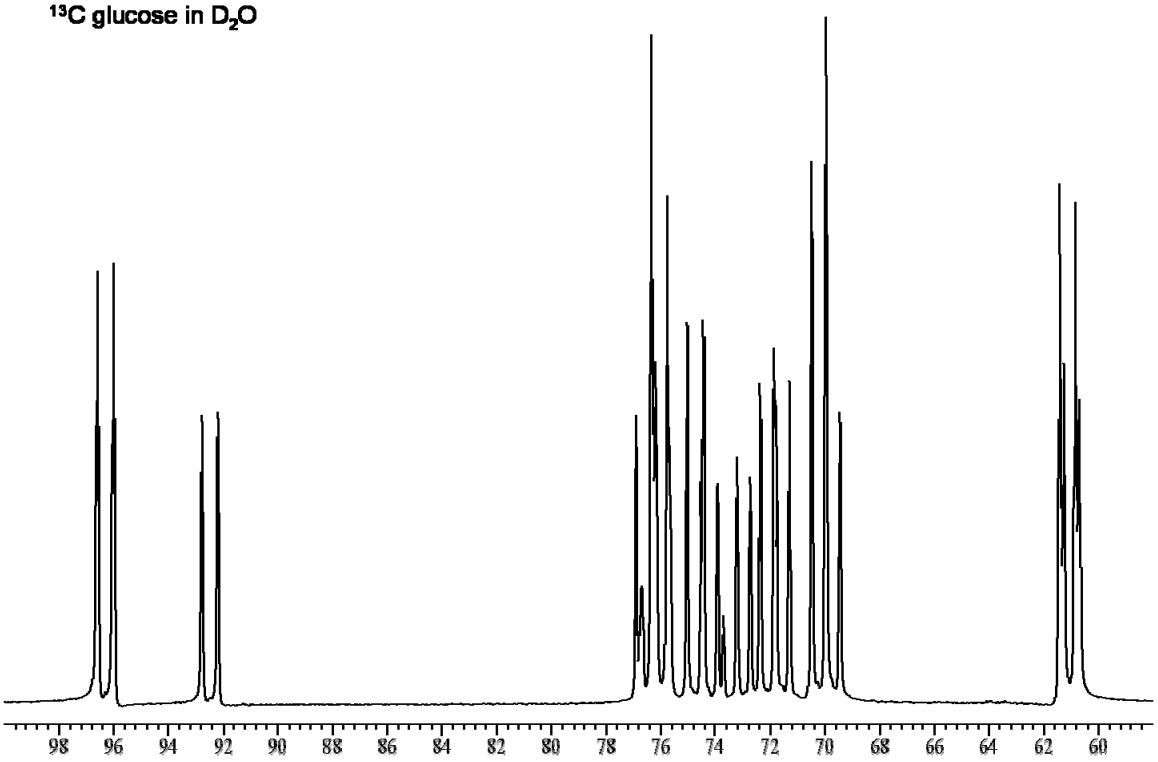

S4

^{13}C glucose in 85% D_2O/ 10% MeOD/ 5% ND_3